USGS
science for a changing world

Net Acid Production, Acid Neutralizing Capacity, and Associated Geophysical, Mineralogical, and Geochemical Characteristics of Animas River Watershed Rocks Near Silverton, Colorado

By Douglas B. Yager, Anne E. McCafferty, Mark R. Stanton, Sharon F. Diehl, Rhonda L. Driscoll, David L. Fey, and Stephen J. Sutley

Open-File Report 2005-1433

U.S. Department of the Interior
U.S. Geological Survey

CONTENTS

Figures

Tables

Plates

ABSRACT

This report presents results from laboratory studies involving the net acid production (NAP), acid neutralizing capacity (ANC), and magnetic mineralogy of thirty-four samples collected in the Upper Animas River watershed near Silverton, Colo., during the summer of 2003. Sampling focused mainly on the volumetrically important, Tertiary-age volcanic and plutonic rocks that are host to base and precious metal mineralization in the study area.

Rocks in the study have all been subjected to a regional propylitic alteration event that modified the primary mineralogy of the host rock, while introducing minerals with an acid neutralizing capacity (ANC) including calcite, chlorite and epidote. Locally, hydrothermal alteration has consumed any ANC and introduced minerals, mainly pyrite, that has a high net acid production (NAP). Laboratory studies included hydrogen pyroxide (H_2O_2) acid digestion and subsequent sodium hydroxide (NaOH) titration to determine NAP, and sulfuric acid H_2SO_4 acid titration experiments to determine ANC on selected samples that generally had low NAP. In addition to these environmental rock property determinations, mineralogical, chemical, and petrographic characteristics of each sample were determined through multiple methods including semi-quantitative X-ray diffractometry (Rietveld method), optical mineralogy, wavelength dispersive X-ray fluorescence, total carbon-carbonate, and 40-element inductively coupled plasma analyses. Magnetic susceptibilities, converted to estimates of volume-percent magnetite were also calculated. Although magnetite is a minor mineral constituent, it is easily measured, and can be positively correlated to measurable percentages of important acid-neutralizing minerals, such as chlorite and calcite and inversely correlated to NAP indicator minerals including pyrite and clay minerals.

Ranks were assigned to the samples based on ANC quantity in kilograms/ton (kg/ton) calcium carbonate equivalent, and ratios of ANC to NAP. Results show the Pyroxene Andesite Member of the Silverton Volcanics has highest ANC with little to no NAP in either the propylitic or weakly sericitically-altered samples. Samples of the propylitically altered Pyroxene Andesite Member also contains the highest mean magnetite abundance (over 8 volume percent) and therefore, may permit its regional mapping using the airborne magnetic and electromagnetic survey data. Samples from the Burns Member of the Silverton Volcanics, in general have a low ANC, high to moderate NAP, and in general, contain little to no magnetite. Samples containing pyrite ($\leq$ 1 weight percent) have NAP that ranges from non-detectable to 39 kg/ton $CaCO_3$. Samples with no detectable calcite often contain abundant chlorite species (clinochlore and chamosite).

Acid titration was performed on a chlorite mineral separate comprised mainly of the minerals clinochlore and chamosite, collected from a Burns Member lava with a high ANC (second highest ANC of all samples studied) and that lacks calcite. Acid titration results indicate that chlorite species have some ANC over a range between pH 4 and pH 2. The calculated ANC of the chlorite mineral separate is 54 kg/ton $CaCO_3$ equivalent. This indicates that samples that lack calcite, where chlorite is also abundant could supply some ANC.

This study provides information that could prove useful to local stakeholders groups and federal land managers involved in mine cleanup efforts. Several samples studied have ANC values that exceed the 20 kg/ton $CaCO_3$ equivalent necessary for consideration

in mine waste remediation. Data collected for the environmental rock properties, NAP and ANC, of Animas River watershed rocks could aid in locating rocks that could be suitable for use in ongoing mine waste remediation efforts.

INTRODUCTION

Land management agencies, in partnership with mine owners, and other local, State and Federal stakeholders in several watersheds located in the western United States are involved in the cleanup of abandoned hard rock metal mines and mine-related features. These cleanup efforts are necessary because many abandoned mine sites have acid generating minerals, predominantly pyrite, that in the presence of oxygen and water, produces sulfuric acid that can be toxic to aquatic life. In addition, acidic water leaches major- and trace-elements from rocks in concentrations that can also be toxic to aquatic life and can adversely effect local watersheds.

Mine site remediation project managers must consider multiple variables in order to achieve the goal of reducing the impact that acid mine drainage has on surface and groundwater (Hutchison, and Ellison, 1992). Mine site configuration in relation to topography, hydrology, local geology including lithology, possible attenuation of metals by underlying substrate be it either surficial deposits or bedrock, geologic structures and hazards, and transportation logistics are but a few examples of those important issues that need careful consideration when designing and implementing a mine site remediation project.

We address a little studied but important geochemical variable-- the acid neutralization capacity (ANC) of local rocks. In addition, we examine the associated magnetic characteristics of these rocks to determine if airborne electromagnetic and magnetic survey data can be used to regionally map rocks that have acid generating or acid neutralizing physical properties. Information on the ANC of rocks in a mined area could prove useful to land managers who are attempting to mitigate the effects of acid mine drainage and who are trying to understand the relative acid generating potential of mine waste piles that contain rocks with varying ANC.

The Animas River watershed near the historic mining town of Silverton, Colorado (Fig. 1), is an excellent area in which to study the ANC of local rocks. A more than 100-year history of mining primarily silver, gold, and base-metals (copper-lead-zinc) has left behind hundreds of abandoned mine-waste piles, mills and associated deposits, fluvial tailings, and mine-adits. Many mining-related features are located on lands managed by the U.S. Forest Service and U.S. Bureau of Land Management and require Federal involvement in any cleanup efforts. The active Animas River Stakeholders Group that is based in Silverton, Colo. is also currently involved in several mine cleanup efforts that could benefit from detailed information on the ANC of local rocks for application in remediation projects. If it is demonstrated that geologic units have significant ANC, then more local source materials could be used in remediation projects, reducing the amount of material that would need to be hauled from long distances. The Silverton, Colo. area is relatively remote, located at 10,000 ft (3,048 m) and is nestled between two high mountain passes, 50 miles from the nearest large town, so utilization of local source materials could help reduce remediation costs associated with hauling.

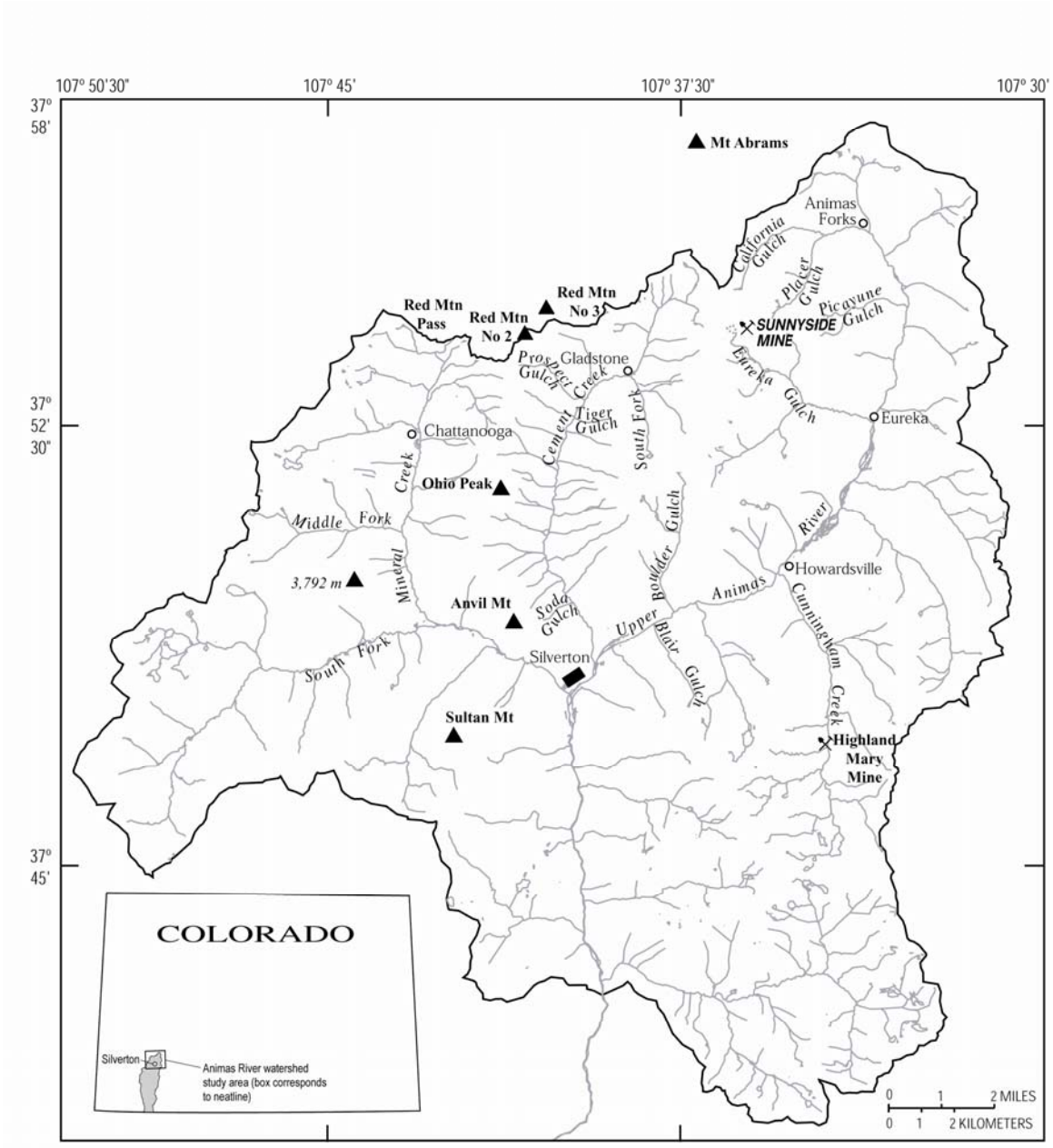

Figure 1. Location map and geographic features referred to in this report.

Complex weathering reactions of chemical constituents of minerals in rocks determine if a sample will produce or consume acid. Reactions at the water-mineral interface involving oxidation, adsorption, desorption, ion exchange, dissolution, and surface area control the processes that ultimately results in the elements that are released into solution or are chemically bound or sequestered (Davis and Kent, 1990). The kinetic rates at which these reactions take place in situ are variable and are thus difficult to reproduce or simulate in a laboratory setting. It is; therefore, important to emphasize that

our laboratory data provide only a relative estimate of a samples readily available neutralizing or acid generating capacity.

Important oxidation weathering reactions that contribute to acid generation in some samples studied include pyrite, the principle acid generating phase (Salmon and Malmström, 2004); chalcopyrite and sphalerite (Salmon and Malmström, 2004); and galena (Blowes and others, 2003) are shown below:

Acid generating minerals present in this study

Pyrite oxidation (FeS_2) (ferric iron reaction path)

$$FeS_2(s) + 14Fe^{3+} + 8H_2O \rightarrow 15Fe^{2+} + 2SO_4^{2-} + 16H^+$$

Chalcopyrite oxidation ($CuFeS_2$) (ferric iron reaction path; trace abundances in some samples)

$$CuFeS_2(s) + 16Fe^{3+} + 8H_2O \rightarrow 17Fe^{2+} + Cu^{2+} + 2SO_4^{2-} + 16H^+$$

Spahalerite oxidation (ZnFeS) (ferric iron reaction path; trace abundances) in some samples)

$$ZnS(s) + 8Fe^{3+} + 4H_2O \rightarrow Zn^{2+} + SO_4^{2-} + 8Fe^{2+} + 8H^+$$

Galena (PbS) (ferric iron reaction path; trace abundances in some samples)

$$PbS(s) + 8Fe^{3+} + 4H_2O \rightarrow + Pb^{2+} + SO_4^{2-} + 8Fe^{2+} + 8H^+$$

Weathering reactions for the high ANC minerals with relatively fast dissolution rates for calcite (Jambor, 2003) and moderate ANC and intermediate dissolution rates for chlorite (Salmon and Malmström, 2004) that are both found in Animas River watershed rocks are shown below.

Acid neutralizing minerals
Calcite ($CaCO_3$)

$$2CaCO_3(s) + 4H^+ \rightarrow 2Ca^{2+} + 2H_2CO_3^-$$

Chlorite ($(MgFeAl)AlSi_3O_{10}(OH)_2$)

$$(Mg_{0.2}Fe^{2+}Fe_{0.2}^{3+}Al)AlSi_3O_{10}(OH)_2(s) + 16H^+ \rightarrow 4.5Mg^{2+} + 0.2Fe^{2+} + 0.2Fe^{3+} + 2Al^{3+} + 3SiO_2(s) + 12H_2O$$

Additional phases locally present in Animas River watershed rocks that were shown in other studies to have some ANC are epidote ($Ca_2(Fe^{3+},Al)_3(SiO_4)_3(OH)$) and hornblende ($Ca_2(Mg,Fe)_4Al(Si_7Al)O_{22}(OH,F)_2$), (Jambor and others, 2002). Other silicate phases

that are thought to have low reactivity and minimal ANC include the sodic feldspars, potassium feldspar, and sericite (Jambor, 2003; Jambor and others, 2002).

GEOLOGIC SETTING

A brief discussion of the geology of the study area is important because it helps to provide context for the various rock types that were studied in our ANC experiments. The western San Juan Mountains record a relatively complete geologic record from Precambrian to Cenozoic time. Within the upper Animas River watershed near Silverton, however; multiple Tertiary volcano-tectonic and intrusive events have obliterated much of the geologic record, but have left thick accumulations of silicic igneous rocks. In general, Animas River watershed study area stratigraphy consists of a Precambrian crystalline basement overlain by Paleozoic, Mesozoic, and Eocene-age sedimentary rocks, and a 1- to 2-km thick, Oligocene- to Miocene-age volcanic cover (Fig. 2), (Yager and Bove, 2002, Yager and Bove, in press).

Mid-Tertiary volcanism

Rocks related to the episode of mid-Tertiary volcanism and later alteration are of principle interest in this study. Tertiary volcanic rocks in the San Juan Mountains blanketed more than 25,000 km^2, forming one of the great epicontinental volcanic piles of intermediate- to silicic- composition volcanic rocks. Onset of mid-Tertiary volcanism records the construction of stratovolcanoes and volcanic shields built up by thick accumulations of andesite to rhyolite flows and breccias that were followed by several eruption cycles of silicic ash flows. The eruption of ash flows led to caldera formation and localized subsidence.

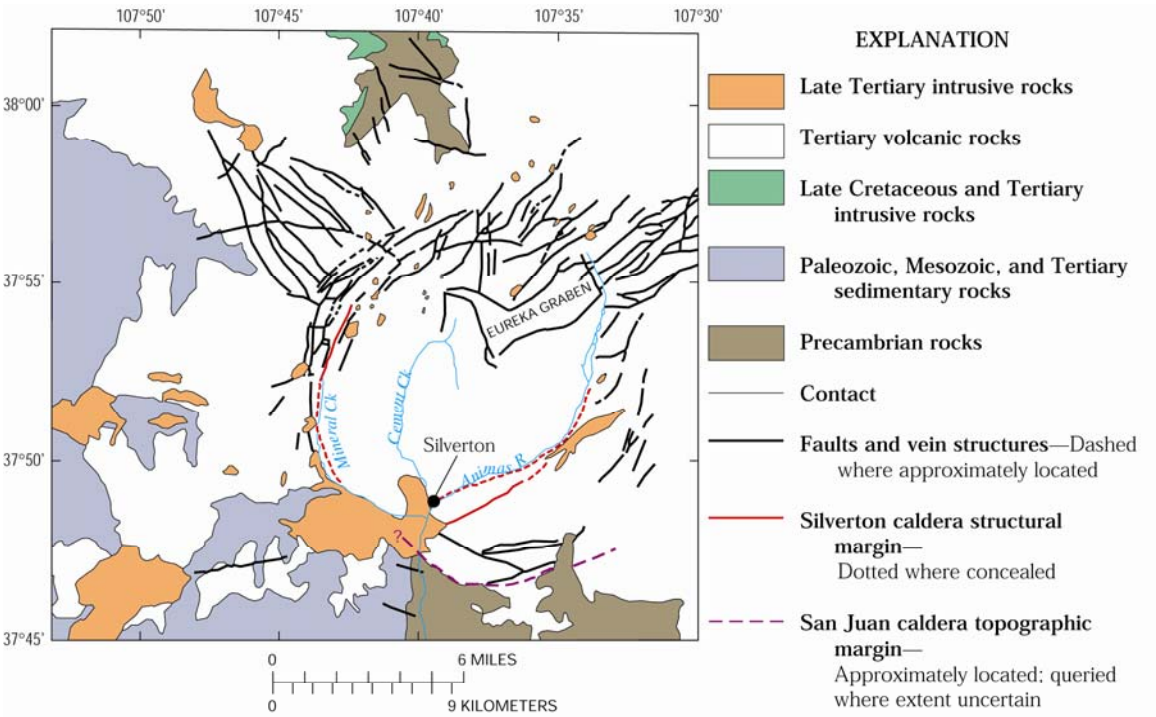

Figure 2. Generalized geology of study area and surrounding regions near Silverton, Colo. Major tributaries to Animas River are shown in addition to major Tertiary volcanotectonic structures related to Silverton and San Juan calderas. Modified from Casadevall and Ohmoto (1977).

Mid-Tertiary volcanism in the San Juan Mountains began between 35 and 30 Ma with the eruption and deposition of voluminous intermediate- composition (52-63 percent SiO_2) lava flows, flow breccias, volcaniclastics, minor mafic tuffs, and abundant mudflows of the San Juan Formation (Lipman and others, 1973; Steven and Lipman, 1976). From 30 to 23 Ma, multiple calderas formed and related volcanic units were deposited throughout the San Juan volcanic field (Lanphere, 1988; Lipman and others, 1997; Bove and others, 2001). Two caldera-forming events took place in the upper Animas River watershed: the 28.2 Ma San Juan-Uncompahgre caldera complex and the younger, nested 27.6 Ma Silverton caldera (Bove and others, 2001). The San Juan caldera in the study area is the southwest half of the roughly dumbbell shaped San Juan-Uncompahgre caldera complex. San Juan caldera eruptives include the intracaldera Eureka Member of the Sapinero Mesa Tuff and outflow Sapinero Mesa Tuff.

San Juan caldera activity culminated with ring fracture volcanism, the products of which constitute the Silverton Volcanics. These rocks, which are primarily intermediate composition lava flows and volcaniclastic sedimentary rocks, fill the caldera depression to a thickness exceeding 1 km and are perhaps the most important rocks in this study area as they could have a relatively high ANC in some places and are host to the majority of mineral deposits mined (Benjar, 1957).

Beginning approximately 1 million years after Silverton caldera formation, numerous stocks, dikes, and other silicic intrusions formed along the Silverton caldera ring fracture zone and are known as the Sultan Mountain stock. The oldest postcaldera granitic stocks (monzonite, monzodiorite, granodiorite, and monzogranite) are about 26.6 Ma and intrude along the southern part of the Silverton caldera ring fracture (Lipman and others, 1976; Ringrose, 1982; Bove and others, 2001).

Mineralization and subsequent erosion events

The Tertiary volcanotectonic activity was followed by multiple silicic igneous intrusion and mineralization events that span more than 20 million years and have resulted in five major alteration types in the study area (Bove and others, this volume). The multiple alteration and coincident mineralization events postdate caldera collapse, taking place between 26 and 10 Ma (Bove and others, 2001). For a detailed discussion of the alteration types, see Bove and others (in press).

Neogene erosion denuded much of the San Juan Mountains volcanic cover. The high potential for erosion developed during this time due to differential displacement of the San Juan Mountains relative to the incipient, adjacent Rio Grande Rift basin to the east and post-mid-Tertiary extensional tectonic activity. Chapin and Cather (1994) estimated Precambrian bedrock offset in adjacent mountain ranges and basins to gauge the amount of late Tertiary relative displacement. Using this technique they determined that an average of 5 km of relative displacement of Precambrian rocks has occurred. They further estimated from basin stratigraphy that 7 - 30 times more sediment was supplied to the Rio Grande Rift basin during the Miocene and Pliocene than in the Pleistocene. Clearly, late Tertiary erosion was important in exposing large surface areas of mineralized terrain and also large areas of igneous bedrock that may have a high ANC. Steven and others (1995) suggested that regional uplift and tilting from 5 to 2 Ma, concurrent with continued active rifting in the Rio Grande Rift to the east, further accelerated erosion and canyon cutting throughout the uplifted area.

Quaternary Glaciation and sedimentation

Pleistocene, Wisconsin age glaciation greatly altered the San Juan landscape (Atwood and Mather, 1932; Gillam, 1998). The San Juan ice sheet was one of the largest (second only to the Yellowstone-Absaroka) to form south of the upper-mid-latitude Laurentide ice sheet (Atwood and Mather, 1932; Leonard and others, 1993). The San Juan ice sheet covered approximately 5,000 km^2, was as much as 1,000 m thick, covered all but the highest peaks, and formed piedmont glaciers that extended to the adjacent foothill areas (Atwood and Mather, 1932).

Unstable slope conditions developed after glacier retreat. Weathering processes in glaciated cirque basins and subalpine to alpine mountain valleys have resulted in accumulation of large volumes of talus, debris cone, and landslide deposits. The mineral constituents present in these surficial deposits may influence their acid generating or neutralizing capacities.

Numerous surficial deposits in the upper Animas River watershed serve as porous and permeable pathways for surface-water infiltration and ground water flow (Blair and others, 2002). From GIS analysis of a geology coverage, (Yager and Bove, 2001), we estimate that 27 percent of the bedrock in the watershed is covered by between 1 and 5 m

or more of Pleistocene to Holocene sedimentary deposits (Yager and Bove, in press). These deposits formed as a result of mass wasting of weathered bedrock outcrops, and accumulated in cirque basins and on slopes and in valleys to form talus, landslides, and colluvium. Alluvial processes have formed multiple generations of stream terraces (Gillam, 1998) and caused deposition of alluvial fans and flood-plain sediments along main drainages and their tributaries (Blair and others, 2002).

ROCK TYPES OF INTEREST FOR POTENTIAL ACID NEUTRALIZATION CAPACITY

Multiple lithologic units throughout the stratigraphic section in or near the study area, from Precambrian basement rocks to Quaternary surficial deposits, have a potentially moderate to high ANC. These rock types are discussed below.[1]

Precambrian Rocks

Precambrian rocks crop out near the periphery of the Animas River watershed study area– principally along the Animas River below Silverton, near Cunningham Creek, near the eastern margin of the watershed, east of the historical Animas Forks townsite, and north of Mount Abrams. Precambrian rocks along the Animas River below Silverton and at the headwaters of Cunningham Creek (sampled in this study) are equivalent to the Irving Formation (Barker, 1969; Luedke and Burbank, 2000). Irving Formation rocks consist of interlayered fine-grained, dark-gray to greenish-gray banded amphibolite with various fine-grained, gray to green, plagioclase-quartz-biotite-bearing gneisses and minor sericite-biotite-chlorite schists (Barker, 1969). Amphibolite is the predominant rock type in the Irving Formation and consists of blue-green hornblende, calcic plagioclase, and epidote; varieties with biotite, chlorite, and quartz are not uncommon (Barker, 1969). In many places, plagioclase-quartz-biotite-bearing gneisses contain one or more of the following phases: chlorite, epidote, microcline, garnet, calcite, magnetite, and pyrite. Regional uplift, tilting to the west, and subsequent retrograde metamorphism (Steven and others, 1969) resulted in formation and concentration of the possible acid-neutralizing mineral assemblage of chlorite-epidote-calcite (Desborough and Driscoll, 1998; Desborough and Yager, 2000).

Paleozoic Sedimentary Rocks

Paleozoic sedimentary units are primarily exposed south and west of Silverton along the Animas River and in the South Fork Mineral Creek subbasin (Luedke and Burbank, 2000; Yager and Bove, in press). Several of the Paleozoic sedimentary units likely have a high ANC due to the presence of limestone interbeds, calcareous units such as mudstone, and the presence of either limestone clasts or calcite-cemented matrix. Calcareous-bearing units include the Upper Devonian Elbert Formation, Mississippian Leadville-Ouray Limestone, Pennsylvanian Molas Formation, Pennsylvanian Hermosa Formation, and the Permian Cultler Formations. The thickest section of Paleozoic strata is preserved along the Animas River below Silverton and in the subbasins that drain South Fork Mineral Creek.

[1] Paleozoic, Mesozoic, and Eocene sedimentary rocks were not investigated for ANC as part of this study.

Mesozoic Sedimentary Rocks

Mesozoic-age rocks are best exposed near the Animas River watershed margins, outside the Tertiary calderas in the headwater subbasins of South Fork Mineral Creek (Luedke and Burbank, 2000; Yager and Bove, in press), As with the Paleozoic section, several units in the Mesozoic sedimentary section contain calcareous-bearing units such as the Triassic Delores Formation, the Jurassic Morrison Formation, and the Jurassic Wanakah Formation.

Tertiary Sedimentary Rocks

Tertiary sedimentary rocks in the Animas River watershed crop out in the western and southern part if the study area, and are composed of the Eocene Telluride Conglomerate. Lower layers within the Telluride Conglomerate contain rounded to subangular cobbles of Mesozoic and Paleozoic red sandstone and limestone and are thus an important unit for its high ANC potential.

Tertiary Igneous Rocks

Rocks of the San Juan Formation represent the oldest Tertiary units sampled and are exposed outward from the Silverton caldera structural margin in the Mineral Creek Basin and near the San Juan caldera margin south of Silverton in the vicinity of Cunningham Creek and Deer Park Creek, among other Animas River subbasins. The San Juan Formation is primarily composed of intermediate composition volcaniclastic sedimentary rocks; however, minor intercalated andesitic lavas are typically porphyritic and consist of plagioclase, clinopyroxene, hornblende, and opaque oxide primary phases. This unit along with all other igneous units studied is altered to a secondary propylitic mineral assemblage (see below).

Subsequent to deposition of the San Juan Formation, ash flows were deposited in response to collapse of both the San Juan and younger nested Silverton calderas and are sources of the Eureka Member of the Sapinero Mesa Tuff and the Crystal Lake Tuff, respectively. The Eureka Member of the Sapenero Mesa Tuff is the intracaldera equivalent of the Sapenero Mesa Tuff, is dacitic to rhyolitic in composition and contains phenocrysts of plagioclase, with lesser amounts of sanidine, biotite, and trace augite. The Crystal Lake Tuff is volumetrically minor in comparison to the Sapenero Mesa Tuff and thus was not sampled.

During San Juan caldera formation, limestone units of the Leadville and Ouray Limestone caved inward toward the central core of the caldera forming megabreccia. One such megabreccia block crops out near the Highland Mary Mine in the Cunningham Creek subbasin.

San Juan caldera activity culminated with ring fracture volcanism, the products of which constitute the Silverton Volcanics. These rocks fill the caldera depression to a thickness exceeding 1 km. The Burns Member of the Silverton Volcanics is characterized mainly by propylitically altered lavas. The Pyroxene Andesite member, which generally overlies the Burns Member, is mainly composed of intermediate composition lava flows with a trend toward more mafic compositions (Yager and Bove, in press), and tends to be somewhat less altered than the Burns Member. The volcaniclastic sedimentary rocks of the Henson Member interfinger with both the Burns and the pyroxene andesite members

(Lipman, 1976). The Henson Member of the Silverton Volcanics (unsampled for this study) is in most places the capping member of this volcanic sequence and is composed mostly of volcaniclastic sedimentary rocks. In general, lavas of the Silverton Volcanics are porphyritic and typically contain phenocrysts of plagioclase, amphibole, pyroxene, opaque oxides, and minor biotite, in a fine-grained to aphanitic groundmass.

Late-stage, 23-to-10 Ma dacitic to rhyolitic intrusions emplaced along the north and northwest structural margin of the Silverton caldera were concomitant with hydrothermal alteration and related mineralization (Bove and others, in press). Dacitic intrusions dated at 23 Ma in the Red Mountain mining district are coarsely porphyritic, containing large (1 cm) phenocrysts of potassium feldspar, plagioclase, quartz, and biotite in a fine-grained groundmass.

Regional Propylitic Alteration

Regional propylitic alteration identified by Burbank (1960) and described further in Bove and others (in press) as a "pre-ore propylitization" event has affected most igneous rocks in the vicinity of the San Juan-Uncompahgre and Silverton caldera complex (Fig. 3). The mineralogy of this assemblage, although variable, consists of quartz, chlorite, epidote, calcite, secondary potassium feldspar, albite, pyrite, and opaque oxides in the presence of unaltered to slightly altered primary feldspar crystals. This alteration type is thought to have formed during the period 28.2 Ma to about 27.6 Ma, as the nearly 1 km sequence of Silverton Volcanics lavas that infilled the San Juan caldera cooled, and in the process of cooling, degassed volatile constituents. Large quantities of carbon dioxide (CO_2), perhaps the primary rock-altering volatile component (among others such as water (H_2O) and sulfur dioxide (SO_2), were released during cooling, altering the original minerals and matrix of the country rock (Burbank, 1960, Bove and others, in press). Rocks that have experienced this type of alteration commonly have a greenish hue in outcrop owing to the presence of chlorite and epidote. Where pyrite is either sparse or absent, the propylitic assemblage can supply some ANC. The subsequent, more intense alteration and mineralization events that were commonly focused along vein structures related to San Juan and Silverton caldera formation in several places overprint the regionally pervasive propylitic alteration assemblage and locally eliminate any ANC of the propylitic assemblage (Fig. 3).

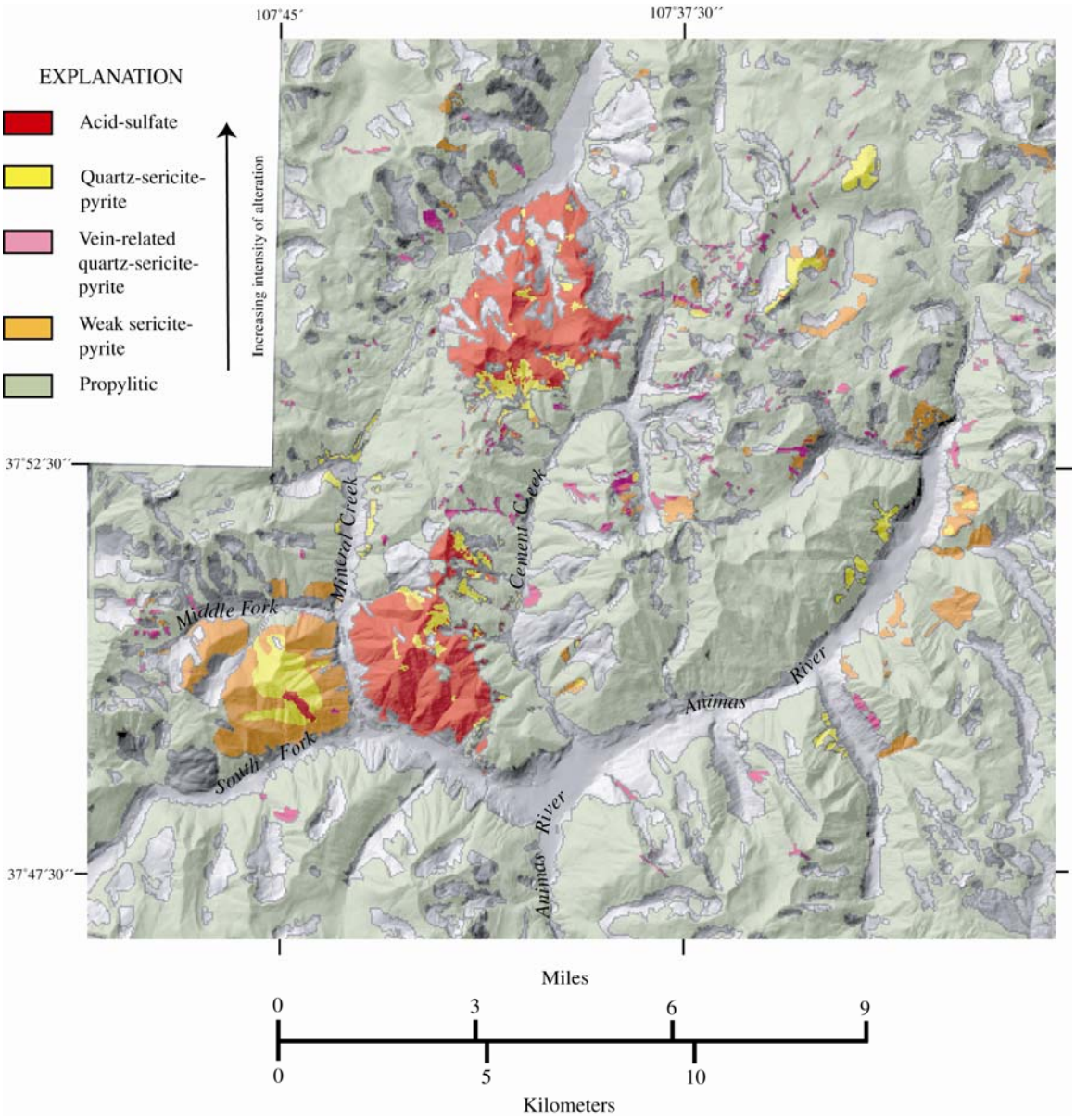

Figure 3. Generalized alteration map of Animas River watershed study area. Data in (Bove and others, in press, Yager and others, in press).

Quaternary Surficial Deposits

Weathering of mineralized bedrock and subsequent deposition of weathered material in downslope surficial deposits will result in acid generation, as water infiltrates and reacts with pyrite and other acid-generating minerals. In contrast, water infiltrating surficial deposits containing abundant propylitic rocks with the mineral assemblage chlorite-epidote-calcite will probably undergo some reduction in acidity (Desborough and Yager, 2000; Yager and others, 2000; Wirt and others, in press).

METHODS

Sample preparation

A suite of 32 composite rock samples was collected in September 2003 for ANC study (table 1). Sample sites were chosen to be representative of the lithologies preserved in several geographic areas (plate 1). Sampling was mainly focused on the most volumetrically important igneous rock types that are host to the majority of mineralization, such as the thick sequence of Silverton Volcanics lavas north of Silverton, Colorado. Additional hand specimens were collected from several of the other Tertiary igneous units, from the Precambrian Irving Formation Gneiss, and from two drill cores collected in September, 2004.

Splits of all samples were first jaw-crushed using steel plates to pebble-size, then pulverized to approximately <200 mesh (70μm) in an agate shatterbox for wavelength dispersive x-ray Fluorescence (WDXRF) analyses (table 2), x-ray diffractometry (XRD) semi-quantitative mineralogy using the Rietveld method (Young, R.A., 1993; Raudsepp and Pani, 2003) (Table 3), total carbon-carbonate analyses (table 4), 40-element inductively coupled plasma analyses (ICP-AES) (Table 5), and for Net Acid Production (Lapakko, 1993). Additional splits were crushed and sieved to less than 2 millimeter (mm) for ANC acid titration experiments. One sample was sieved to between the less than 80 (< 180 μm) and greater than 120 (<125 μm) standard mesh size for a chlorite mineral separation and subsequent acid titration. None of the samples was subjected to grinding during any preparation process. Grinding could lead to surface exposure and water-mineral reactions on layered chlorite surfaces not commonly found in natural weathering processes. Such surfaces may not be exposed during normal weathering processes involving freeze-thaw cycles, rainfall precipitation events, and grain-to-grain abrasion that occurs during fluvial transport.

Magnetic rock properties

One-inch (2.54 cm) diameter cylindrical core plugs approximately 1-inch in length were prepared from all samples. Magnetic susceptibilities were measured from the cores using a Bison Magnetic Susceptibility Bridge[2] and are reported in Table 6.

[2] Use of trade names does not imply endorsement by the U.S. Geological Survey

Table 1. Geologic unit and locality information for samples studied for acid neutralization capacity. Geologic unit abbreviations as follows: pe, Precambrian Irving Formation; Tsj, San Juan Formation; Tig, Sultan Mountain Stock; Tsemb, Picauyune Megabreccia Member of the Sapinero Mesa Tuff; Tse, Eureka Member of the Sapinero Mesa Tuff; Tb, Burns Member of the Silverton Volcanics; Tpa, Pyroxene Andesite Member of the Silverton Volcanics; Td, Tertiary dacite; Qc, Quaternary colluvium.

Field sample number	Unit	Rock type	Longitude	Latitude	Locality Description
HWDY0323	p€	Propylitically altered Gneiss	-107.57503	37.79800	Upper Cunningham Creek
IDY0329	Tsj	Propylitically altered volcaniclastic breccia	-107.72996	37.89609	Black Bear Road, along Mineral Creek
SDY0330	Tsj	Propylitically altered lava	-107.74681	37.84663	Ophir Pass Road
ODY0331	Tsj	Propylitically altered lava	-107.77834	37.85076	Ophir Pass Road summit
SDY0319	Tig	Propylitically altered Sultan Mountain Stock	-107.67500	37.79982	Along Highway 550 south of Silverton
SDY0320	Tig	Propylitically altered Sultan Mountain Stock	-107.72421	37.83556	South of Middle Fork Mineral Creek, north of Silverton
HWDY0322	Tig	Propylitically altered Sultan Mountain Stock	-107.59401	37.83485	Mouth of Cunningham Creek
HDY0315	Tsemb	Propylitically altered Megabreccia	-107.57941	37.93339	East of Animas Forks near Bagley Tunnel
HDY0314	Tse	Propylitically altered tuff	-107.55824	37.91684	North of Picayune Gulch along road
HDY0316	Tse	Propylitically altered Eureka Tuff	-107.59008	37.93068	South of Animas Forks in Placer Gulch
HDY0318	Tse	Propylitically altered Eureka tuff	-107.59047	37.91757	Placer Gulch along road below Gold Prince mine
IRDY0303	Tb	Argillically altered lava	-107.68850	37.89248	Upper Prospect Gulch northeast of Galena Queen Mine
IRDY0403	Tb	Propylitically altered lava	-107.66711	37.88562	Along lower Prospect Gulch Road
SDY0306	Tb	Propylitically altered lava	-107.63692	37.82908	Mouth of Boulder Gulch
SDY0307	Tb	Propylitically altered lava	-107.63792	37.83242	Boulder Gulch north of Silverton
SDY0308	Tb	Propylitically altered lava	-107.63614	37.83685	Boulder Gulch north of Silverton
SDY0309	Tb	Propylitically altered lava	-107.63406	37.84082	Boulder Gulch north of Silverton
SDY0310	Tb	Propylitically altered lava	-107.63168	37.84465	Boulder Gulch north of Silverton
SDY0311	Tb	Propylitically altered lava	-107.63234	37.84745	Upper Boulder Gulch north of Silverton
SDY0324	Tb	Weak sericite-pyrite altered lava	-107.72193	37.85638	Browns Gulch along creek
SDY0325	Tb	Propylitically altered lava	-107.71694	37.85800	0.8 mi east of Highway 550 along Browns Gulch road
DYLPG0412	Tb	Propylitically altered lava	-107.68486	37.89528	Mouth of Prospect Gulch
HDY0313	Tb	Propylitically altered lava	-107.56802	37.88018	Mouth of Eureka Gulch
IRDY0103	Tpa(?)	Quartz-pyrophyllite altered lava	-107.69021	37.89216	Upper Prospect Gulch west of Galena Queen Mine
IRDY0203	Tpa	Propylitically altered lava	-107.69051	37.89214	Upper Prospect Gulch west of sample IRDY0103
SDY0312	Tpa	Propylitically altered lava	-107.63354	37.84946	Upper Boulder Gulch north of Silverton
HDY0317	Tpa	Propylitically altered lava	-107.59704	37.90563	Upper Placer Gulch south of and above Gold Prince mine
SDY0326	Tpa	Propylitically altered lava	-107.71432	37.86005	East of Brooklyn Mine, Browns Gulch
SDY0327	Tpa	Weak sericite-pyrite altered lava	-107.71392	37.86025	Near Brooklyn mine, Browns Gulch
IDY0328	Tpa	Weak sericite-pyrite altered lava	-107.72372	37.89538	Black Bear Road, west of Highway 550
IDY0321	Td	Quartz-sericite altered dacite intrusion	-107.74037	37.87324	Near Chattanooga, west of Highway 550
SDY0305		Silicified vein	-107.64271	37.87124	Sample in gulley upper South Fork Cement Creek
MPGD_51_52.5	Qc	Colluvium	-107.68111	37.89221	Prospect Gulch below Lark Mine

Table 2. Major element oxide analyses (WDXRF).

Field sample number	SiO_2	Al_2O_3	$FeTO_3$	MgO	CaO	Na_2O	K_2O	TiO_2	P_2O_5	MnO	LOI
IRDY0103	66.6	19.3	4.77	<0.10	0.12	0.17	0.10	1.07	0.29	<0.01	6.64
IRDY0203	56.5	15.5	7.61	2.98	6.36	2.17	3.06	0.88	0.37	0.12	3.91
IRDY0303	69.2	16.4	2.85	1.05	0.08	<0.15	3.83	0.75	0.12	0.03	5.39
IRDY0403	60.7	16.1	6.45	2.74	2.96	3.04	4.00	0.80	0.34	0.25	2.30
SDY0305	67.5	13.1	6.02	2.40	0.26	<0.15	3.35	0.82	0.36	0.13	5.51
SDY0306	59.7	15.7	7.29	2.97	3.63	3.07	3.48	0.78	0.31	0.16	2.28
SDY0307	61.9	16.7	6.05	1.93	2.10	0.47	5.36	0.60	0.20	0.48	3.37
SDY0308	61.1	15.7	6.16	1.73	4.31	3.30	3.26	0.78	0.32	0.49	2.23
SDY0309	59.7	14.6	7.96	2.44	7.35	2.32	1.12	0.83	0.35	0.15	2.34
SDY0310	56.5	15.9	9.14	3.34	4.95	1.31	3.41	1.03	0.43	0.43	3.22
SDY0311	57.6	15.9	9.12	3.26	3.86	2.40	2.90	0.97	0.40	0.22	2.88
SDY0312	55.2	16.1	9.13	3.65	5.84	2.44	3.32	1.04	0.43	0.21	1.98
HDY0313	66.6	15.4	3.38	1.03	2.53	2.69	5.45	0.46	0.15	0.31	1.46
HDY0314	67.6	14.7	3.04	1.04	2.06	2.85	4.87	0.43	0.13	0.09	3.04
HDY0315	53.0	15.7	8.78	4.82	4.62	3.45	2.73	1.10	0.42	0.17	4.96
HDY0316	70.2	14.2	2.98	0.77	0.58	1.65	6.32	0.42	0.15	0.10	2.18
HDY0317	57.5	16.3	7.49	1.22	4.67	1.25	3.82	0.93	0.32	0.11	6.24
HDY0318	63.5	17.3	4.48	0.87	2.25	4.25	4.03	0.63	0.23	0.06	1.84
SDY0319	62.7	15.5	5.65	2.13	4.05	3.87	3.94	0.68	0.27	0.11	0.54
SDY0320	71.5	14.7	1.48	0.32	0.88	1.37	6.22	0.28	<0.05	0.05	2.45
IDY0321	79.6	12.1	1.17	0.73	0.05	<0.15	3.88	0.17	<0.05	0.03	2.14
HWDY0322	58.8	15.4	6.98	2.87	5.08	2.56	3.48	0.81	0.37	0.35	2.38
HWDY0323	76.6	11.5	4.03	0.70	0.57	1.00	2.82	0.26	<0.05	0.08	2.36
SDY0324	54.4	16.4	9.43	3.33	6.70	3.10	1.73	1.00	0.48	0.21	2.56
SDY0325	64.3	16.4	4.68	1.16	3.45	3.87	2.24	0.53	0.27	0.24	2.00
SDY0326	58.2	15.5	6.91	2.73	5.87	3.17	2.76	0.82	0.36	0.11	3.12
SDY0327	51.5	16.0	7.93	4.92	5.39	0.56	2.73	1.09	0.40	0.26	8.45
IDY0328	55.6	14.7	7.08	1.52	6.54	2.85	2.00	0.80	0.33	0.25	7.07
IDY0329	61.2	13.9	4.89	0.96	5.12	1.22	3.55	0.59	0.25	0.29	5.79
SDY0330	62.6	16.7	5.52	2.07	4.57	2.98	2.34	0.63	0.29	0.10	1.65
ODY0331	62.1	15.7	5.33	1.58	4.56	3.11	3.19	0.59	0.27	0.13	2.72

WDXRF analyses provided by Joseph E. Taggart, U.S. Geological Survey.

Table 3. Mineralogy determined by X-ray diffractometry (XRD) analysis (values reported in weight percent).

Field sample number	Unit	Calcite	Clinochlore	Epidote	Hematite	Hornblende	Kaolinite	Magnetite
HWDY0323	p€	2	8					
IDY0329	Tsj	8	9					
SDY0330	Tsj		11					7
ODY0331	Tsj	3	12	8				1
SDY0319	Tig		3			16		7
SDY0320	Tig	3	4					
HWDY0322	Tig	< 1	20	14				1.5
HDY0315	Tsemb	6	25					2
HDY0314	Tse	5	6		5			
HDY0316	Tse		6					
HDY0318	Tse	2	9					4
IRDY0303	Tb		2				2 (?)	
IRDY0403	Tb		24					1
SDY0306	Tb		19					5
SDY0307	Tb		18					
SDY0308	Tb		18					
SDY0309	Tb		14	19				< 1
SDY0310	Tb		18	11				
SDY0311	Tb		20	5				1
SDY0324	Tb		20	5		12		4
SDY0325	Tb		12	6				
DYLPG0412	Tb	n/a	n/a	n/a	n/a	n/a	n/a	n/a
HDY0313	Tb		12	7				
IRDY0103	Tsv							
IRDY0203	Tpa (?)	2	8				5	6
SDY0312	Tpa		9		9			11
HDY0317	Tpa	10	13		3			2
SDY0326	Tpa	3	7					8
SDY0327	Tpa	9	15					
IDY0328	Tpa	10	14					
IDY0321	Td				3			
SDY0305	vein		6					

Note: Rietveld XRD analyses provided by Stephen J. Sutley, U.S. Geological Survey. Accuracy and precision using the Rietveld method were shown to vary based on phase abundance. In another study (Raudsepp, and others, 1999) demonstrated that in complex mixtures of varying proportions of skarn minerals that included wollastonite as the major phase, the accuracy ranged from 1.3% to 6% containing wollastonite in mixtures of 30 to 90 weight percent and 6 weight percent respectively.

Table 3 (cont.).

Field sample number	Unit	Mica (sericite)	Plagioclase	Potassium feldspar	Pyrite	Pyrophyllite	Quartz	Sphalerite
HWDY0323	p€	24	7				58	
IDY0329	Tsj	27	15		3		38	
SDY0330	Tsj	11	29	8			33	
ODY0331	Tsj	10	29	11			27	
SDY0319	Tig	3	36	18			17	
SDY0320	Tig	23	13	19			38	
HWDY0322	Tig		23	21	< 1		20	
HDY0315	Tsemb	3	35	14			15	
HDY0314	Tse	12	28	10			33	
HDY0316	Tse	12	15	26	2		38	
HDY0318	Tse	13	39	13	< 1		19	
IRDY0303	Tb	21	2		11			
IRDY0403	Tb	9	29	16			21	
SDY0306	Tb	5	32	22			17	
SDY0307	Tb	33	5	7			37	
SDY0308	Tb		30	22	< 1		28	
SDY0309	Tb		21	11			34	
SDY0310	Tb	7	18	12			32	
SDY0311	Tb	7	26	16			27	
SDY0324	Tb		32	13	1		12	
SDY0325	Tb	11	34	8	< 1		28	
DYLPG0412	Tb	n/a	n/a	n/a	n/a	n/a	n/a	n/a
HDY0313	Tb	7	26	22			25	
IRDY0103	Tsv			< 1	10	60	28	2
IRDY0203	Tpa (?)	7	49	< 1	1		21	
SDY0312	Tpa		39	16			16	
HDY0317	Tpa	32	12				29	
SDY0326	Tpa	3	7					8
SDY0327	Tpa	9	15					
IDY0328	Tpa	10	14					
IDY0321	Td	35					62	
SDY0305	vein	29			12		53	

Note: Sericite is used throughout this report. The term sericite is a field and petrographic term used to describe samples containing micaceaous minerals that are not definitively identified by x-ray diffractometry or by another analytical method. Samples containing sericite in this study are most similar to fine-grained muscovite but could contain illite.

Table 4. Weight percent CO_2, carbon from carbonate, and total carbon analyses.

Field sample number	CO_2 (%)	C (%)	Total carbon (%)
IRDY0103	<0.04	<0.01	0.05
IRDY0203	2.25	0.61	0.65
IRDY0303	<0.04	<0.01	0.05
IRDY0403	<0.04	<0.01	0.05
SDY0305	<0.04	<0.01	0.05
SDY0306	<0.04	<0.01	0.05
SDY0307	0.19	0.05	0.08
SDY0308	0.20	0.06	0.07
SDY0309	<0.04	<0.01	0.05
SDY0310	0.05	0.01	0.05
SDY0311	0.07	0.02	0.05
SDY0312	0.42	0.11	0.13
HDY0313	0.05	0.01	0.05
HDY0314	1.20	0.33	0.34
HDY0315	1.73	0.47	0.49
HDY0316	0.14	0.04	0.07
HDY0317	3.18	0.87	0.86
HDY0318	0.36	0.10	0.12
SDY0319	<0.04	<0.01	0.05
SDY0320	0.59	0.16	0.19
IDY0321	<0.04	<0.01	0.05
HWDY0322	0.17	0.05	0.10
HWDY0323	0.18	0.05	0.10
SDY0324	<0.04	<0.01	0.05
SDY0325	<0.04	<0.01	0.05
SDY0326	1.84	0.50	0.53
SDY0327	3.94	1.08	1.07
IDY0328	4.95	1.35	1.33
IDY0329	3.68	1.00	1.03
SDY0330	<0.04	<0.01	0.05
ODY0331	0.82	0.22	0.31
MPGD_51_52.5	<0.04	<0.01	0.06
DYLPG0412	<0.04	<0.01	0.06

Note: Total Carbon and Carbonate Carbon analyses provided by Zoe Ann Brown, U.S. Geological Survey.

Table 5. Inductively coupled plasma atomic emission spectroscopy analyses (ICP-AES).

Field sample number	Al (%)	Ca (%)	Fe (%)	K (%)	Mg (%)	Na (%)	P (%)	Ti (%)	Ag (ppm)	As (ppm)	Au (ppm)
IRDY0103	6	0.04	3.4	0.077	0.0072	0.057	0.062	0.58	<2	36	<8
IRDY0203	8.6	4.7	5.5	2.7	1.8	1.6	0.17	0.53	<2	<10	<8
IRDY0303	8.2	0.036	2	2.9	0.65	0.033	0.055	0.37	<2	14	<8
IRDY0403	8.4	2.1	4.5	3.2	1.7	2.1	0.16	0.51	<2	<10	<8
SDY0305	7	0.16	4.4	2.7	1.5	0.038	0.17	0.22	2.8	<10	<8
SDY0306	8.1	2.5	5.1	2.8	1.8	2.2	0.15	0.42	<2	<10	<8
SDY0307	8.5	1.4	4.4	4.2	1.2	0.31	0.096	0.14	<2	<10	<8
SDY0308	8.3	3	4.4	2.6	1	2.3	0.15	0.32	<2	<10	<8
SDY0309	7.9	5.2	5.8	0.96	1.5	1.8	0.18	0.43	<2	<10	<8
SDY0310	8.4	3.4	6.4	2.8	2.1	0.94	0.2	0.41	<2	<10	<8
SDY0311	8.3	2.6	6.4	2.4	2	1.7	0.2	0.5	<2	<10	<8
SDY0312	8.5	4.1	6.4	2.7	2.3	1.7	0.21	0.61	<2	<10	<8
HDY0313	7.6	1.7	2.3	4.1	0.56	1.8	0.075	0.16	<2	<10	<8
HDY0314	7.1	1.3	2	3.6	0.62	1.8	0.061	0.17	<2	<10	<8
HDY0315	8.2	3.2	6.2	2.2	3	2.4	0.21	0.72	<2	<10	<8
HDY0316	6.8	0.36	2	4.6	0.44	1	0.07	0.086	<2	27	<8
HDY0317	8.1	3.1	5.1	2.9	0.7	0.83	0.15	0.5	<2	<10	<8
HDY0318	8.5	1.5	3	3	0.51	2.7	0.11	0.39	<2	<10	<8
SDY0319	8	2.8	4	3.2	1.3	2.6	0.13	0.4	<2	<10	<8
SDY0320	6.9	0.54	1	4.4	0.19	0.84	0.022	0.16	<2	<10	<8
IDY0321	5.7	0.011	0.82	2.7	0.42	0.04	0.0086	0.055	<2	<10	<8
HWDY0322	8	3.4	5	2.8	1.7	1.7	0.19	0.47	<2	<10	<8
HWDY0323	5.4	0.33	2.7	2	0.39	0.6	0.019	0.1	<2	<10	<8
SDY0324	8.4	4.4	6.6	1.4	2	2	0.24	0.67	<2	14	<8
SDY0325	8	2.2	3.2	1.7	0.65	2.5	0.12	0.28	<2	<10	<8
SDY0326	8.1	3.9	5	2.2	1.6	2.1	0.18	0.54	<2	14	<8
SDY0327	8.4	3.6	5.6	2.2	3.1	0.39	0.2	0.6	<2	<10	<8
IDY0328	7.5	4.3	5	1.6	0.88	1.9	0.16	0.5	<2	<10	<8
IDY0329	7	3.3	3.4	2.7	0.55	0.76	0.12	0.12	<2	<10	<8
SDY0330	8.3	2.9	3.8	1.8	1.2	1.9	0.13	0.3	<2	<10	<8
ODY0331	7.8	2.9	3.8	2.4	0.91	2	0.12	0.34	<2	<10	<8

Note: ICP-AES analyses provided by Paul H. Briggs, U.S. Geological Survey.

Table 5 (cont.)

Field sample number	Ba (ppm)	Be (ppm)	Bi (ppm)	Cd (ppm)	Ce (ppm)	Co (ppm)	Cr (ppm)	Cu (ppm)	Eu (ppm)	Ga (ppm)	Ho (ppm)
IRDY0103	44	<1	<10	<2	24	16	21	28	<2	21	<4
IRDY0203	886	1	<10	<2	77	21	19	54	<2	23	<4
IRDY0303	1020	2	<10	<2	80	5	9	10	<2	25	<4
IRDY0403	1000	1	<10	<2	86	10	24	14	<2	5	<4
SDY0305	592	2	<10	<2	71	17	18	39	<2	17	<4
SDY0306	994	2	<10	<2	84	20	20	54	<2	13	<4
SDY0307	1400	2	<10	<2	110	18	<1	43	<2	<4	<4
SDY0308	886	1	<10	<2	87	16	10	33	<2	<4	<4
SDY0309	401	1	<10	<2	81	18	9	41	<2	16	<4
SDY0310	749	2	<10	<2	74	29	28	72	<2	<4	<4
SDY0311	730	2	<10	<2	72	29	17	16	<2	8	<4
SDY0312	744	1	<10	<2	74	31	17	84	<2	14	<4
HDY0313	1450	2	<10	<2	76	7	<1	19	<2	<4	<4
HDY0314	907	2	<10	<2	80	7	4	5	<2	14	<4
HDY0315	736	2	<10	<2	76	25	38	49	<2	10	<4
HDY0316	1170	2	<10	<2	76	7	<1	9	<2	11	<4
HDY0317	783	1	<10	<2	61	16	<1	25	<2	21	<4
HDY0318	1630	2	<10	<2	66	7	4	16	<2	20	<4
SDY0319	763	2	<10	<2	84	16	6	16	<2	16	<4
SDY0320	1130	2	<10	<2	105	2	<1	9	<2	14	<4
IDY0321	58	4	<10	<2	24	1	<1	22	<2	21	<4
HWDY0322	760	1	<10	<2	90	20	7	21	<2	<4	<4
HWDY0323	360	2	<10	<2	45	6	<1	6	<2	9	<4
SDY0324	984	1	<10	<2	83	12	<1	155	<2	13	<4
SDY0325	927	1	<10	<2	86	4	<1	68	<2	<4	<4
SDY0326	855	2	<10	<2	76	18	8	53	<2	23	<4
SDY0327	384	1	<10	<2	65	16	147	132	<2	7	<4
IDY0328	493	2	<10	<2	72	22	26	37	<2	<4	<4
IDY0329	1660	1	<10	2	55	12	3	17	<2	<4	<4
SDY0330	742	1	<10	<2	70	11	<1	<1	<2	16	<4
ODY0331	973	1	<10	<2	63	10	1	<1	<2	7	<4

Note: ICP-AES analyses provided by Paul H. Briggs, U.S. Geological Survey.

Table 5 (cont.)

Field sample number	La (ppm)	Li (ppm)	Mn (ppm)	Mo (ppm)	Nb (ppm)	Nd (ppm)	Ni (ppm)	Pb (ppm)	Sc (ppm)	Sn (ppm)	Sr (ppm)
IRDY0103	13	<2	24	4	20	6	12	30	9	<5	618
IRDY0203	40	17	909	6	18	33	14	23	19	5	714
IRDY0303	39	9	208	4	25	31	4	40	12	<5	27
IRDY0403	46	42	1990	4	18	30	18	32	17	<5	609
SDY0305	37	60	1060	11	10	32	14	174	16	6	137
SDY0306	45	38	1220	5	17	33	15	37	15	<5	775
SDY0307	58	40	3740	7	9	40	7	114	11	<5	260
SDY0308	46	41	3840	3	8	33	10	251	14	<5	527
SDY0309	45	46	1190	4	15	34	15	18	18	<5	1320
SDY0310	40	85	3420	4	5	33	23	16	23	<5	431
SDY0311	38	98	1740	4	13	32	22	16	21	<5	846
SDY0312	39	33	1660	5	16	31	21	12	23	<5	823
HDY0313	41	20	2420	4	14	26	3	96	6	<5	422
HDY0314	44	27	645	4	19	28	4	34	7	<5	293
HDY0315	39	66	1390	5	20	30	19	16	24	<5	432
HDY0316	38	11	747	3	14	27	2	22	5	<5	144
HDY0317	32	16	826	4	19	26	7	17	15	<5	324
HDY0318	37	18	436	4	23	22	5	26	9	<5	915
SDY0319	44	7	846	5	23	33	10	27	13	<5	576
SDY0320	54	20	399	3	29	36	<2	32	4	<5	116
IDY0321	16	12	186	7	20	5	<2	44	2	<5	2
HWDY0322	44	30	2750	5	14	37	14	90	15	<5	610
HWDY0323	21	24	566	4	11	24	2	10	13	<5	23
SDY0324	42	16	1670	6	22	35	8	13	26	5	974
SDY0325	44	12	1840	4	23	34	3	28	9	<5	780
SDY0326	39	35	834	5	19	30	12	29	14	5	968
SDY0327	32	68	2080	4	15	25	47	8	24	<5	204
IDY0328	38	14	1950	3	14	27	16	20	15	<5	1520
IDY0329	29	16	2270	3	9	24	4	51	11	<5	319
SDY0330	36	14	747	4	18	28	5	18	11	<5	767
ODY0331	33	13	970	4	19	25	5	20	10	<5	497

Note: ICP-AES analyses provided by Paul H. Briggs, U.S. Geological Survey.

Table 5 (cont.)

Field sample number	Ta	Th	U	V	Y	Yb	Zn
IRDY0103	<20	<4	<100	127	4	<1	5
IRDY0203	<20	9	<100	169	26	3	89
IRDY0303	<20	8	<100	105	13	1	342
IRDY0403	<20	11	<100	133	22	2	164
SDY0305	<20	4	<100	145	12	1	123
SDY0306	<20	14	<100	124	22	2	179
SDY0307	<20	32	<100	90	25	3	338
SDY0308	<20	15	<100	106	23	2	772
SDY0309	<20	11	<100	206	26	3	83
SDY0310	<20	9	<100	210	27	3	266
SDY0311	<20	8	<100	192	25	3	139
SDY0312	<20	9	<100	219	27	3	114
HDY0313	<20	14	<100	46	19	2	215
HDY0314	<20	14	<100	49	18	2	50
HDY0315	<20	6	<100	197	29	3	115
HDY0316	<20	10	<100	35	12	1	55
HDY0317	<20	<4	<100	132	22	2	86
HDY0318	<20	7	<100	74	16	2	63
SDY0319	<20	20	<100	110	24	3	61
SDY0320	<20	18	<100	12	18	2	32
IDY0321	<20	<4	<100	7	<2	<1	8
HWDY0322	<20	12	<100	145	25	3	484
HWDY0323	<20	<4	<100	<2	19	3	30
SDY0324	<20	<4	<100	222	32	3	78
SDY0325	<20	<4	<100	52	23	2	101
SDY0326	<20	8	<100	145	21	2	91
SDY0327	<20	9	<100	220	21	2	266
IDY0328	<20	8	<100	147	20	2	88
IDY0329	<20	<4	<100	70	17	2	1100
SDY0330	<20	<4	<100	77	23	2	86
ODY0331	<20	4	<100	72	21	2	76

Note: ICP-AES analyses provided by Paul H. Briggs, U.S. Geological Survey.

Table 6. Estimates of % magnetite from magnetic susceptibility measurement (k) and x-ray diffraction (XRD) and environmental properties of net acid production (NAP) and acid neutralizing capacity (ANC). Alteration types describe mineral assemblages after Bove and others (?) and include propylitic (prop), sericitic (ser), arg (argillic), and quartz, sericite pyrite (QSP). Samples denoted with a (*) indicate rocks with ilmenite present.

Pyroxene-Andesite Member of the Silverton Volcanics (Tpa)

Sample	Geologic Unit	Alteration	Magnetic Susceptibility k* 10^{-5} (cgs: cm-gm-second)	% Magnetite		Environmental Properties	
				est. from k	XRD	NAP	ANC
HDY0317	Tpa	prop	1440	5.76	2	0.0	65.7
IRDY0203	Tpa	prop	2550	10.2	6	0.0	26.3
SDY0326	Tpa	prop	2120	8.48	8	0.0	9.3
SDY0312	Tpa	prop	2240	8.96	11	7.4	0.6
IDY0328	Tpa	ser	30	0.12	0	0.0	31.7
SDY0327	Tpa	ser	28	0.11	0	0.0	21.7
Burns Member of the Silverton Volcanics : Lava flows (Tb)							
SDY0310*	Tb	prop	67	0.27	0	13.2	98.5
SDY0325	Tb	prop	57	0.23	0	6.9	12.8
IRDY0403*	Tb	prop	164	0.66	1	6.9	6.4
SDY0307	Tb	prop	38	0.15	0	0.4	3.3
SDY0308	Tb	prop	44	0.18	0	0.0	1.2
SDY0309	Tb	prop	300	1.20	1	27.2	0.0
SDY0311	Tb	prop	77	0.31	1	22.6	0.0
HDY0313	Tb	prop	39	0.16	0	35.0	0.0
SDY0306	Tb	prop	820	3.28	5	6.3	2.4
SDY0324	Tb	ser	1460	5.84	4	6.9	1.7
IRDY0303	Tb	arg	15	0.06	0	50.1	0.0
IRDY0103	Tsv	QSP	2	0.01	0	94.8	0.0
Eureka Tuff Member of the Silverton Volcanics: Volcanic Tuffs (Tse and Tsemb)							
HDY0314*	Tse	prop	61	0.24	0	0.0	122.8
HDY0316	Tse	prop	35	0.14	0	10.1	2.1
HDY0318	Tse	prop	1400	5.60	4	39.1	1.4
HDY0315	Tsemb	prop	341	1.36	2	0.0	6.4
San Juan Formation: Volcaniclastic rocks and lava flows (Tsj)							
IDY0329	Tsj	prop	32	0.13	0	0.0	44.4
ODY0331	Tsj	prop	560	2.24	1	0.0	3.9
SDY0330	Tsj	prop	1900	7.60	7	52.4	0.0
Sultan Mountain Stock: Granodiorite (Tig)							
HWDY0322	Tig	prop	670	2.68	1.5	36.0	2.6
SDY0319	Tig	prop	2010	8.04	7	78.6	0.0
SDY320	Tig	ser	23	0.92	0	0.0	14.2
Mineralized Vein (vein) and Dacite Intrusion (Td)							
SDY0305	Vein	QSP	6	0.02	0	79.6	0.0
IDY0321	Td	ser	14	0.06	0	80.9	0.2
Precambrian Rock: Altered Gneiss (PC)							
HWDY0323	p€	prop	31	0.12	0	25.2	1.7

For rocks with magnetite concentrations between 0.1 and 10 percent, volume percentage of magnetite (*Vm*) can be estimated from susceptibility *k* in units of centimeter-gram—second (cgs) with the following equation:

$$Vm = 400\ k$$ (modified from Balsley and Buddington, 1958)

Estimates for volume percent magnetite were determined from the magnetic-susceptibility measurements using this equation and compared with semi-quantitative measurements using x-ray diffractrometry (Table 3).

Net Acid Production Test

The Net Acid Production Test (NAP) was developed as a screening tool to determine the acid generating potential of mine-waste materials (Lapakko, 1993). This method is a static laboratory bench test that utilizes hydrogen pyroxide (H_2O_2) to oxidize sulfide minerals in a sample, creating sulfuric acid that subsequently reacts with other phases present. Because enhanced sulfide oxidation is achieved, this test provides an upper limit for acid generating potential. A modified version of the Lapakko NAP method was used for this study and is described as follows.

This procedure requires incremental addition of 100 ml of 30 percent H_2O_2 to 1.0 gram of-200-mesh (75 μm) rock powder. The sample, along with 50 ml of H_2O_2 is placed in a 250 ml flask and heated to ~94° C for about 1 hour. If all of the H_2O_2 is consumed after 1 hour, the sample is removed from the hot plate, cooled for 5 minutes, and an additional 50 ml of H_2O_2 (100 ml cumulative total) is added, followed by heating to ~ 94° C for an additional 30 minutes. Once this step is complete, the sample is cooled for 15 minutes, 1 ml of 0.016 M Cu-nitrate solution is added, and the sample is boiled for 10 minutes. Again, the sample is cooled and then filtered to remove fine precipitates. The sample is then rinsed with 1 M $CaCl_2$. The initial pH value is recorded after 1 hour or after it is determined that any visible reaction between the sample and the leachate has stopped. The sample is then titrated to a pH of 7.0 with the addition of sodium hydroxide (NaOH). The sample is stirred continuously with a teflon stir bar between pH readings during titration. Final NAP results include the calculated amount of calcite equivalent, in kg/ton, that would be necessary to neutralize the sample to the final pH of 7.00. This calculation is based on the following formula:

Net Acid Production in kg/ton $CaCO_3 = 50 \text{ X } ml_b \text{ X } N_b / \text{ Sample Weight}$
Where ml_b = total volume of NaOH used during titration to pH 7.00,
And N_b = normality of NaOH used

Thus, the higher the NAP value, more calcite would be needed to neutralize a solution containing a sample to a neutral pH of 7.00.

Table 7. Net acid production (NAP) results. Samples highlighted in purple and blue have ≥ 2 and ≤ 1 weight percent pyrite respectively.

Field sample number	Unit	Initial pH	Total Volume NaOH (ml)	Weight (g)	Ending pH	$CaCO_3$ Kg/ton
HWDY0323$_{c,ch}$	$_{P}$€	5.983	5.6	1.032	7.014	25.2
IDY0329$_{c, ch}$	Tsj	<11	n/a	1.009	n/a	n/a
SDY0330 $_{ch}$	Tsj	4.602	11.5	1.020	7.0	52.4
ODY0331 $_{c,ch,ep}$	Tsj	7.524	n/a	1.026	n/a	n/a
HDY0315 $_{c,ch}$	Tsemb	7.949	n/a	1.010	n/a	n/a
HDY0314 $_{c,ch}$	Tse	<10	n/a	1.004	n/a	n/a
HDY0316$_{ch}$	Tse	3.408	2.2	1.011	7.138	10.1
HDY0318$_{c,ch}$	Tse	5.694	8.6	1.022	7.002	39.1
IRDY0303$_{ch}$	Tb	2.304	11.1	1.030	7.137	50.1
IRDY0403 $_{ch}$	Tb	4.513	1.1	1.018	6.891	5.0
SDY0306 $_{ch}$	Tb	5.72	1.4	1.028	7.02	6.3
SDY0307 $_{ch}$	Tb	7.08	0.1	1.090	7.168	0.4
SDY0308$_{ch}$	Tb	7.475	n/a	1.019	n/a	n/a
SDY0309 $_{ch,ep}$	Tb	5.05	5.9	1.009	7	27.2
SDY0310$_{ch,ep}$	Tb	5.638	2.9	1.025	7	13.2
SDY0311 ch,ep	Tb	5.298	5.0	1.027	7.003	22.7
HDY0313 ch,ep	Tb	5.247	8.0	1.063	7	35.0
SDY0324$_{ch,ep}$	Tb	3.539	1.5	1.017	7.101	6.9
SDY0325$_{ch}$	Tb	3.189	1.5	1.004	7.106	6.9
DYLPG0412	Tb	3.886	0.7	1.011	7.206	3.2
IRDY0103	Tpa(?)	2.06	20.9	1.025	6.98	94.8
IRDY0203 $_{c,ch}$	Tpa	9.9	n/a	1.011	n/a	n/a
SDY0312 ch	Tpa	6.533	1.6	1.000	7.005	7.4
HDY0317 c,ch	Tpa	<11	n/a	1.017	n/a	n/a
SDY0326$_{c,ch}$	Tpa	10.918	n/a	1.018	n/a	n/a
SDY0327$_{c, ch}$	Tpa	10.983	n/a	1.020	n/a	n/a
IDY0328$_{c, ch}$	Tpa	<11	n/a	1.016	n/a	n/a
SDY0319 $_{ch}$	Tig	3.907	17.1	1.012	7	78.6
SDY0320 $_{c,ch}$	Tig	8.846	n/a	1.007	n/a	n/a
HWDY0322$_{c,ch,ep}$	Tig	5.733	7.9	1.020	7.007	36.0
IDY0321	Td	3.3	17.5	1.006	7.002	80.9
SDY0305$_{ch}$	(vein)	2.132	17.8	1.040	7.02	79.6

* subscripts “c” “ch” and “ep” denote calcite, clinochlore, and epidote respectively.

Acid Neutralization Capacity Test (acid titration)

The ANC method used in this study is similar to that described in Shaw and others (2002) and initially described by Robertson Geoconsultants, written communication (2000). Sample preparation involves first crushing samples in a jaw-crusher to approximately 2 mm. Jaw-crushed material is sieved to less than 2 mm, and this fraction, including any clay-size material, is collected for ANC investigation. Approximately 30 grams of sample is weighed, placed in a beaker, and an equivalent amount (30 ml) of deionized

water is added to the sample. Nitrogen gas is vigorously bubbled through the deionized water for 1 hour prior to titration to aerate the solution and expel CO_2(g). Formation of carbonic acid via CO_2 hydration, especially at lower initial pH values (approx. =7.0), could affect the dissolution of several minerals. An initial pH is recorded after stirring. Incremental quantities of H_2SO_4 acid are added to achieve titration pH set points at whole unit pH intervals to an end point pH value of 2.00. The sample is stirred with a plastic stirrer when the titrant is delivered and the pH recorded after the pH stabilizes.

The volume of total H_2SO_4 added to achieve pH values of approximately 3 and 2 during acid titration were converted to calcium carbonate equivalent mass units with the following formula, where total acid added in this example is 50 ml, N is the normality of acid used, grams of sample = 50 g, M is moles, formula weight for calcite ($CaCO_3$) is 100 g:

H_2SO_4 (0.05 liters) X 0.1 N H_2SO_4 X = 0.005 Equivalents $CaCO_3$
= 0.005 Moles of $CaCO_3$

$$0.005 \text{ M } CaCO_3 \times \frac{100 \text{ g } CaCO_3}{1 \text{ M } CaCO_3} = 0.50 \text{ grams of } CaCO_3$$

$$\frac{0.50 \text{ g } CaCO_3}{50 \text{ g sample}} \times \frac{1000 \text{ g}}{1 \text{ kg}} \times \frac{1000 \text{ kg } CaCO_3}{1 \text{ ton}} \times \frac{1 \text{ kg } CaCO_3}{1000 \text{ g}} = 10 \text{ kg/ton } CaCO_3$$

Note that some samples contain only chlorite and not calcite, nonetheless; the volume of acid is converted to calcium carbonate equivalent mass units.

RESULTS

Magnetic Rock Properties

Volume percent magnetite calculated via the magnetic susceptibility are, on average, higher (0.7% more for the propylitically altered rocks and 0.2 % for the sericitically altered rocks) than estimates from the XRD method. Given these relatively small average differences, we conclude that estimating magnetite content from magnetic susceptibility provides a reasonable and quick measure of the magnetite content of rocks within the study area.

Table 8. Acid neutralizing capacity calculated in terms of calcium carbonate equivalent (kilograms/ton) to reach pH values of 3 and 2 respectively, during 0.1 N H_2SO_4 titration. NAP values shown for comparison.

Field sample number	Unit	$CaCO_3$ equivalent units calculated in kilograms per ton for titration to pH ~ 3	$CaCO_3$ equivalent units calculated in kilograms per ton for titration to pH ~ 2	NAP
HWDY0323	pЄ	1.4	1.7	25.2
IDY0329	Tsj	14.5	44.4	none
ODY0331	Tsj	1.9	3.9	none
HDY0315	Tsemb	5.3	6.4	none
HDY0314	Tse	87.3	122.8	none
HDY0316	Tse	1.3	2.1	10.1
HDY0318	Tse	0.9	1.4	39.1
IRDY0403	Tb	n/a	6.4	5.0
SDY0306	Tb	1.0	2.4	6.3
SDY0307	Tb	n/a	3.3	0.4
SDY0308	Tb	0.7	1.2	none
SDY0310	Tb	65.5	98.5	13.2
SDY0324	Tb	0.4	1.7	6.9
SDY0325	Tb	9.2	12.8	6.9
DYLPG0412	Tb	0.4	0.7	no NAP completed
IRDY0203	Tpa (?)	18.5	26.3	None
SDY0312	Tpa	n/a	0.6	7.4
HDY0317	Tpa	13.3	65.7	none
SDY0326	Tpa	3.7	9.3	none
SDY0327	Tpa	21.6	21.7	none
IDY0328	Tpa	29.8	31.7	none
SDY0320	Tig	5.5	14.2	none
HWDY0322	Tig	1.3	2.6	36.0
IDY0321	Td	n/a	0.2	80.9
MPGD_51_52.5	Qc	n/a	0.4	no NAP completed

Net Acid Production

Prior to ANC acid titration, NAP was determined using the method described in Lapakko and Lawrence (1993). The NAP results are reported in table 7. Basic statistics of these results are shown in figure 4. The NAP value is reported in kg/ton $CaCO_3$ equivalent, and can be interpreted as the amount of $CaCO_3$ that is required to neutralize a sample to pH 7. Therefore, the higher NAP values indicate a higher acid generating potential. Low or non-detectable NAP values are suggestive that a sample may have ANC. In general, of the 34 total samples analyzed NAP values range from not detectable (13 samples) to 95 kg/ton $CaCO_3$ equivalent (Table 7). The mean NAP value is 32 kg/ton $CaCO_3$ equivalent. We discuss NAP in relation to the abundance of sulfide mineral species in the following sections.

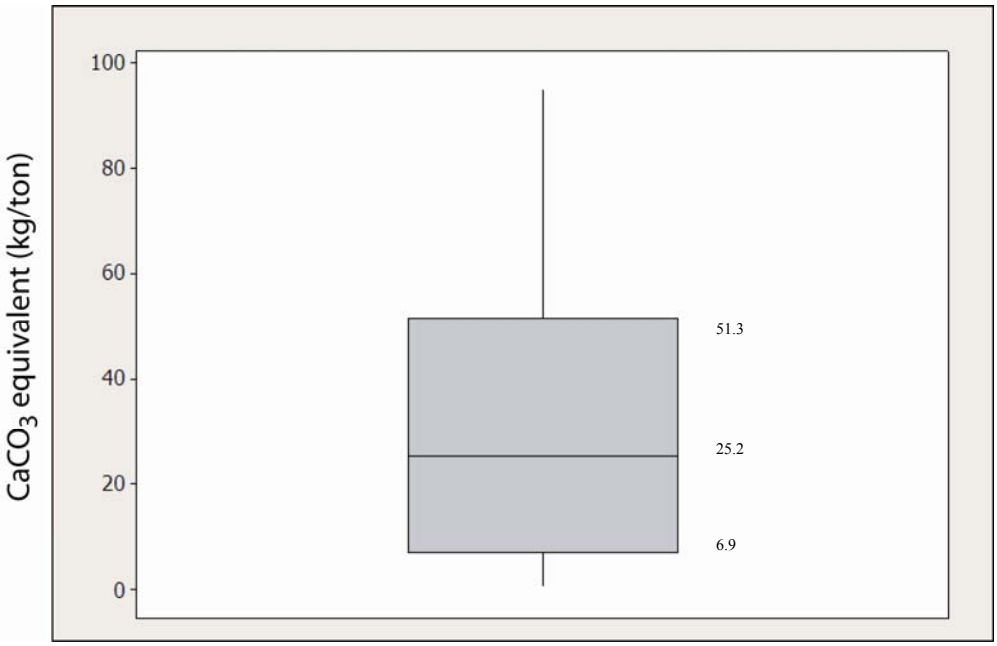

N	N*	Mean	SE Mean	StDev	Minimum	Q1	Median	Q3	Maximum
21	13	32.4	6.5	29.7	0.4	6.9	25.2	51.3	94.8

Figure 4. Box plot and basic statistics for NAP results. N (number of samples), N* (number of samples where no NAP detected), SE Mean (sample standard error of the mean), StDev (sample standard deviation), Q1 (1st quartile), Q3 (3rd quartile). Box represents the 2nd and 3rd quartiles; whiskers represent outliers in the 1st and 4th quartiles.

Sulfide-bearing samples

Pyrite is observed in several propylitically altered samples (Table 3). Those samples containing pyrite concentrations between 2 and 12 weight percent and that also lack calcite have NAP values that range from 10 to 95 kg/ton $CaCO_3$ equivalent and have the highest average NAP value of 59 kg/ton $CaCO_3$ (HDY0316, IRDY0303, SDY0305, IRDY0103). Three samples that contain pyrite (2 to 3 weight percent) in addition to abundant calcite (8 to 10 weight percent), however; have no detectable NAP. The large quantity of calcite is apparently neutralizing any NAP generated during H_2O_2 reaction.

Samples containing sparse pyrite (≤ 1 weight percent) have NAP that ranges from non-detectable to 39 kg/ton $CaCO_3$. Samples with no detectable NAP (IRDY0203, SDY0308, SDY0326) contain the possible acid neutralizing phase clinochlore, and with the exception of SDY0308, also contain the acid neutralizing phase calcite. Similar to those samples mentioned above with greater pyrite abundances and that also contain abundant calcite, the calcite is apparently neutralizing any acid generated during H_2O_2 reaction. The lowest NAP determination of 13 kg/ton $CaCO_3$ and relatively high ANC in this group of sparse pyrite-bearing samples was observed in a sample that lacks calcite (see ANC discussion of sample SDY0310 below).

Additional acid-generating sulfide phases detected by SEM but initially not observed in the field or by XRD analysis include silver-bearing pyrite(?) and chalcopyrite (SDY0309), pyrite rimmed by iron oxide (HDY0313), and chalcopyrite (SDY0310). The

presence of sulfide minerals in these samples helps to explain the moderate NAP determinations that range between 13 and 35. SEM analyses revealed that sulfide grains are usually small (1 – 5 μm) and though not uncommon, are present below the ~1 to 5 weight percent X-ray diffractometry detection threshold.

Non-sulfide-bearing samples (?)

Anomalously high NAP results were obtained for at least one sample (SDY0311) that contains no detectable sulfide minerals based on both X-ray diffraction and SEM analyses. Similar anomalously high NAP results that lack detectable sulfides based on X-ray diffraction data were obtained for three additional samples (SDY0319, SDY0330, HWDY0323); however, SEM analyses is pending that may reveal the presence of sulfide phases.

Several possible scenarios could be involved to help explain relatively high NAP determinations for samples that lack sulfide phases. The most likely scenarios involves the presence of sparse (< 1 weight percent sulfide) that is not detectable based on XRD analyses, or hydrolysis reactions of ferric iron and water. Hydrolysis reactions involving ferric iron cause the water molecule to be split while also generating hydrogen ions. The Lapakko method is designed as a non-conservative technique to estimate NAP as sulfur species are targeted for complete dissolution during boiling in H_2O_2. Thus, in this vigorous dissolution process, ferric iron could be liberated from a number of iron-bearing mineral species such as clinochlore, hematite, and hornblende.

An example of the type of hydrolysis reaction that involves ferric iron is as follows:

$$4\ Fe^{3+} + 12\ H_2O \rightarrow 4\ Fe(OH)_3\ ^{-} + 12\ H^{+}$$

Another possibility is the dissolution of finely disseminated sulfate salts that have a high surface area, readily dissolve, and thus have a high NAP. The presence of sulfate salts, while frequently abundant on surface coatings in mine waste, were not observed in rocks studied.

Acid Neutralization Capacity

The ANC acid titration method used in this study (Shaw and others 2002, Robertson Geoconsultants, written comm. 2000) provides an estimate of the ANC of rock and mineral particles. ANC was calculated in terms of kg/ton $CaCO_3$ equivalent and assumes that all of the ANC is attributable to calcite. We know that this is not the case in our study as many samples contain clinochlore, some lack calcite and yet have identifiable ANC.

ANC for 25 samples is reported in table 8. A sample map (Plate 1) indicates the ANC rank. Basic statistics of these results are shown in fig. 5. NAP determinations were initially used to indicate those samples that were likely candidates for further ANC study. A prerequisite for completing acid titration on a sample is that it had a low NAP value (< 10 kg/ton $CaCO_3$); however, 4 samples were included for ANC investigation that had NAP determinations > 10 kg/ton $CaCO_3$ and were investigated for ANC due to the

presence of clinochlore (ubiquitous in our samples) and or calcite. ANC was calculated for $CaCO_3$ equivalent values at titration end points pH 3 and pH 2. The pH titration end points for determination of ANC are based primarily on neutralizing capacity ranges of the minerals calcite clinochlore, and epidote. Calcite has a neutralizing effect at any acidic pH. Clinochlore; however, dissolves more slowly than calcite (Jambor and Blowes, 1998) and was shown to have some ANC effect in acidic solutions of pH of ~ 4.0.

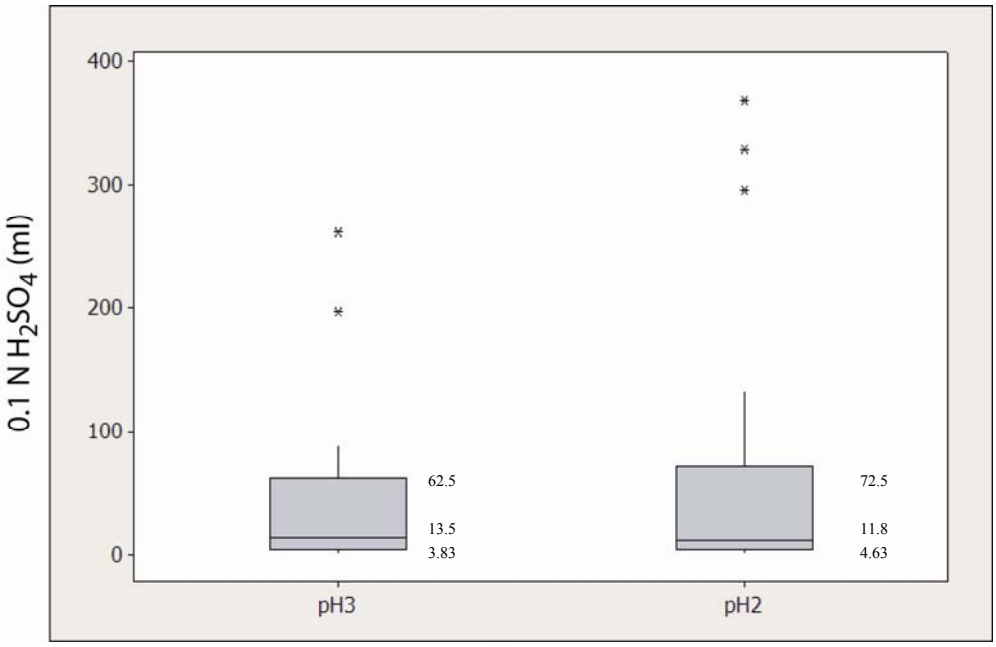

	N	N*	Mean	SE Mean	StDev	Minimum	Q1	Median	Q3	Maximum
pH3	20	5	44.0	15.5	69.5	1.1	3.83	13.5	62.5	262.0
pH2	25	0	63.1	21.4	106.9	0.6	4.63	11.8	72.0	368.6

Figure 5. Box plot and basic statistics for total acid added to achieve pH 3 and pH 2 during acid titration. N* (number of samples where no NAP detected), SE Mean (sample standard error of the mean), StDev (sample standard deviation), Q1 (1st quartile), Q3 (3rd quartile). Box represents the 2nd and 3rd quartiles; whiskers represent outliers in the 1st and 4th quartiles.

In addition, previous studies have shown that chlorite (clinochlore and chamosite, both species of the chlorite group of minerals were detected in SEM and XRD analysis of Animas rocks in this study) have some ANC (Kwong and Furgeson, 1997, Jambor and others, 2002). The chlorite group also tends to be more important in terms of ANC when compared to other silicate phases including sodic plagioclase, alkali- feldspar, and muscovite (Jambor and others, 2002). Therefore, the ANC was investigated in a pH range that would help to evaluate the role that clinochlore might play in neutralizing more acidic solutions where calcite has either dissolved, or is not present.

The ANC for 25 samples studied ranges from 0.4 to 87 kg/ton $CaCO_3$ equivalent at a titration set point of pH 3. ANC ranges from 0.4 to 123 for pH 2 (Table 8, Fig. 6). The mean values for total H_2SO_4 added are 44.0 ml and 63.1 ml at pH 3 and pH 2 respectively (Fig. 5). Maximum acid added is 262 ml at pH 3 and 387 ml at pH 2 (Fig. 5).

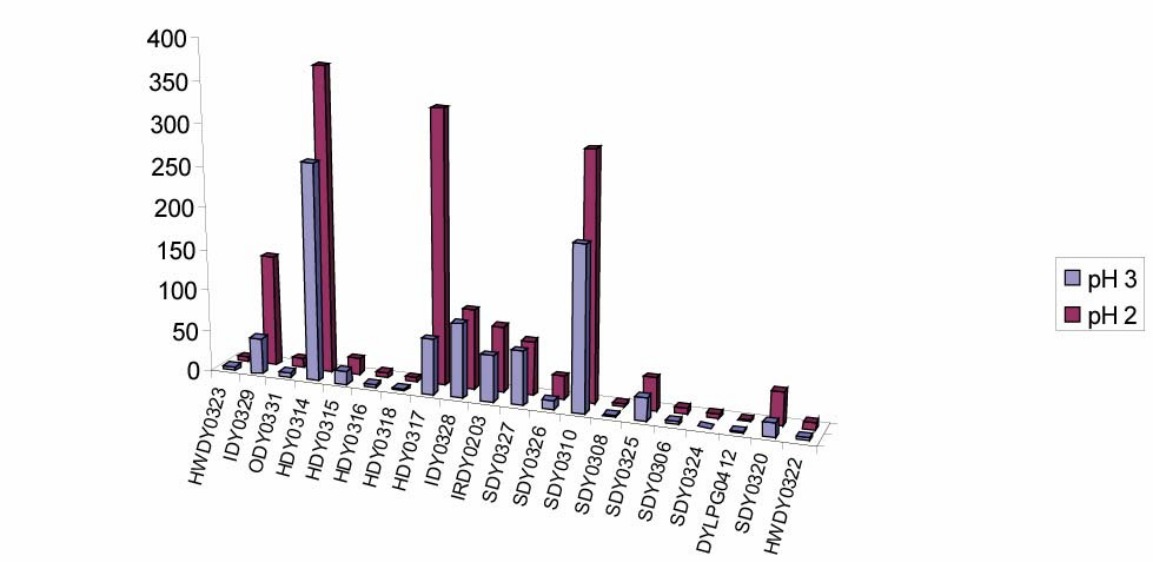

Figure 6. Graph comparing total amount of acid added at titration setpoints of pH 3 (light blue) and pH 2 (magenta).

Anomalously high acid titration determinations are observed in three samples. Three samples at pH 2 have anomalously high total acid added and are outside of the 4th quartile data range (samples SDY0310, HDY0314, HDY0317); two of these samples fall outside the 4th quartile data range at pH 3(SDY0310, HDY0314) (Fig. 5). Acid titrations were done using a 0.1N H_2SO_4, solution with the exception of one mineral separate (SDY0310) that used a 0.01N H_2SO_4 solution.

The ANC of the main rock types sampled are grouped based on Geologic Formation and are discussed from stratigraphically oldest to youngest in the following sections. Note that when a mineral species is mentioned as present or absent, this is based generally on X-ray diffraction analyses; samples where minerals were determined by SEM analyses are duly noted. Refer to Plate XX for sample locations.

ANC of Major Rock Types

Precambrian Irving Formation

Precambrian Irving Formation gneiss was collected in upper Cunningham Creek (HWDY0323) where it crops out beneath the Tertiary Volcanic sequence. It contains the acid neutralizing minerals calcite (2 weight percent) and chlorite (8 weight percent) but lacks detectable sulfides. Other mineral phases include quartz, albite, and muscovite. The total H_2SO_4 added during acid titration is 4.24 ml and 5.03 ml at pH values of 3 and 2 respectively. When statistically compared to all samples, the total volume of acid added at pH 2 and pH 3 are each within the second quartile of the data range (Fig. 5).

The shape of the titration curve is suggestive of some ANC where at pH 7, the slope begins to flatten and continues this trend to pH 5 indicating a resistance to change in pH or neutralizing capacity (Fig. 7). The slope remains gently sloping to pH 2. Despite having some ANC, the Irving Formation sample tested has a low (< 1) ratio of ANC to NAP.

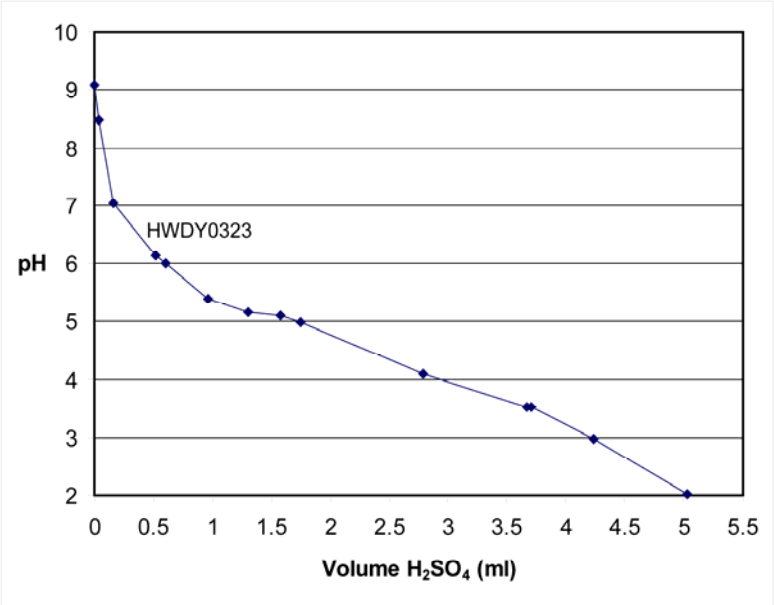

Figure 7. Acid titration curve for Precambrian Irving Formation.

San Juan Formation

San Juan Formation lava flow (ODY0331) and volcaniclastic breccia (IDY0329) outcrops west of the Silverton caldera contain significant calcite.

The lava flow contains 3 weight percent calcite and the vocaniclastic breccia contains 8 weight percent calcite. Both samples have a moderate abundance of clinochlore ranging between 9 and 12 weight percent, with the lava flow having the highest percentage. Additional mineral phases include quartz, plagioclase, secondary microcline, epidote, sericite, and magnetite in the lava flow, whereas the volcaniclastic breccia contains comparable phases but lacks potassium feldspar and epidote. The total H_2SO_4 added during acid titration to achieve pH 2 for the volcaniclastic breccia and the lava flow is 133 ml and 12 ml representing the 4^{th} quartile and near the median of the data range respectively (Fig. 5).

While the overall total acid added is nearly 10 times greater for the volcaniclastic breccia compared to the lava, the general shapes of the titration curves are similar (Fig. 8). Inflection points and flattening of each curve is observed just below pH 7 indicating that initially, neutralization is likely due to calcite. In addition, the titration curve slopes shallow further between pH 4 to pH 2 suggesting a relatively high ability to resist changes in pH. No NAP was detected in either sample; therefore, any available ANC will likely not be inhibited by acid generation due to sulfide oxidation.

Eureka and Picayune Megabreccia Members of Sapinero Mesa Tuff

Eureka Member of the Sapinero Mesa Tuff (Tse) outcrop samples (HDY0314, HDY0316, HDY0318) along with Picayune Megabreccia Member of the Sapinero Mesa Tuff (HDY0315) were collected northeast of Silverton near Picayune Gulch, Animas Forks townsite, and in Placer Gulch. Those samples HDY0314 and HDY0315 having the highest abundance of calcite (5 to 6 weight percent) have variable clinochlore abundances that range between 6 and 25 weight percent respectively. Calcite is also observed in HDY0318 (2 weight percent) along with trace pyrite (< 1 weight percent). HDY0316 lacks calcite, but contains clinochlore. Additional mineral phases preserved include quartz, plagioclase, potassium feldspar, sericite, ± hematite, and intergrown magnetite and ilmenite.

The largest amount of acid added for not only the unit Tse but for all samples studied is HDY0314 that required 368 ml of H_2SO_4 to achieve pH 2. This is equal to 123 kg/ton $CaCO_3$ equivalent and with no detectable NAP, ranks as the sample with the highest relative ANC of those studied. Two additional Tse samples (HDY0316, HDY0318) required 6.32 and 4.27 ml of H_2SO_4 to achieve pH 2. Trace abundance of pyrite in HDY0318 appears to be counteracted by the presence of 2 weight percent calcite, whereas HDY0316 lacks calcite and has the highest silica content (70.1 Weight percent on a non volatile free basis) (Fig. 9) that perhaps make it more indurated and less easily weathered when compared to the other two Tse samples.

Picayune Megabreccia Member of the Sapinero Mesa Tuff (Tsemb) (HDY0315) has the second highest ANC of the San Juan caldera-related rocks studied; although, this unit is composed of pre-existing rocks that caved into the San Juan caldera near its margin during caldera collapse. Many of the caldera wall rock fragments that are part of the Picayune Megabreccia Member rock matrix are likely equivalent in age and compositions to rocks of the San Juan Formation collected west of Mineral Creek and are now commingled in an ash flow tuff matrix. This sample required 19 ml of H_2SO_4 to reach pH 2 and similar to HDY0314 above, had no detectable NAP and thus ranks 10th in terms of its ANC. This is equivalent to 6 kg/ton $CaCO_3$ equivalent.

Comparison of the acid titration curves for Eureka Member units shows the distinct differences in ANC. The sample with the highest ANC, HDY0314 exhibits a slight flattening of the acid titration curve starting at pH 6 followed by an abrupt plateau at pH 4; the plateau continues to pH 3 where the curve becomes only slightly steeper to pH 2 (Fig. 10A). Titration curve comparison of Tse units that have relatively low ANC are shown in Figure 10B. The titration curve for Picayune Megabreccia of the Sapinero Mesa Tuff (HDY0315) indicates an initial steep drop between pH ~ 9 to pH 7, where the slope slightly flattens. Curve plateaus are seen at pH 6, and 4 with the greatest neutralizing capacity observed between pH 4 and 3. At pH 3; however, the slope steepens, indicating the neutralizing capacity of participating minerals was being eliminated by the H_2SO_4 titrant.

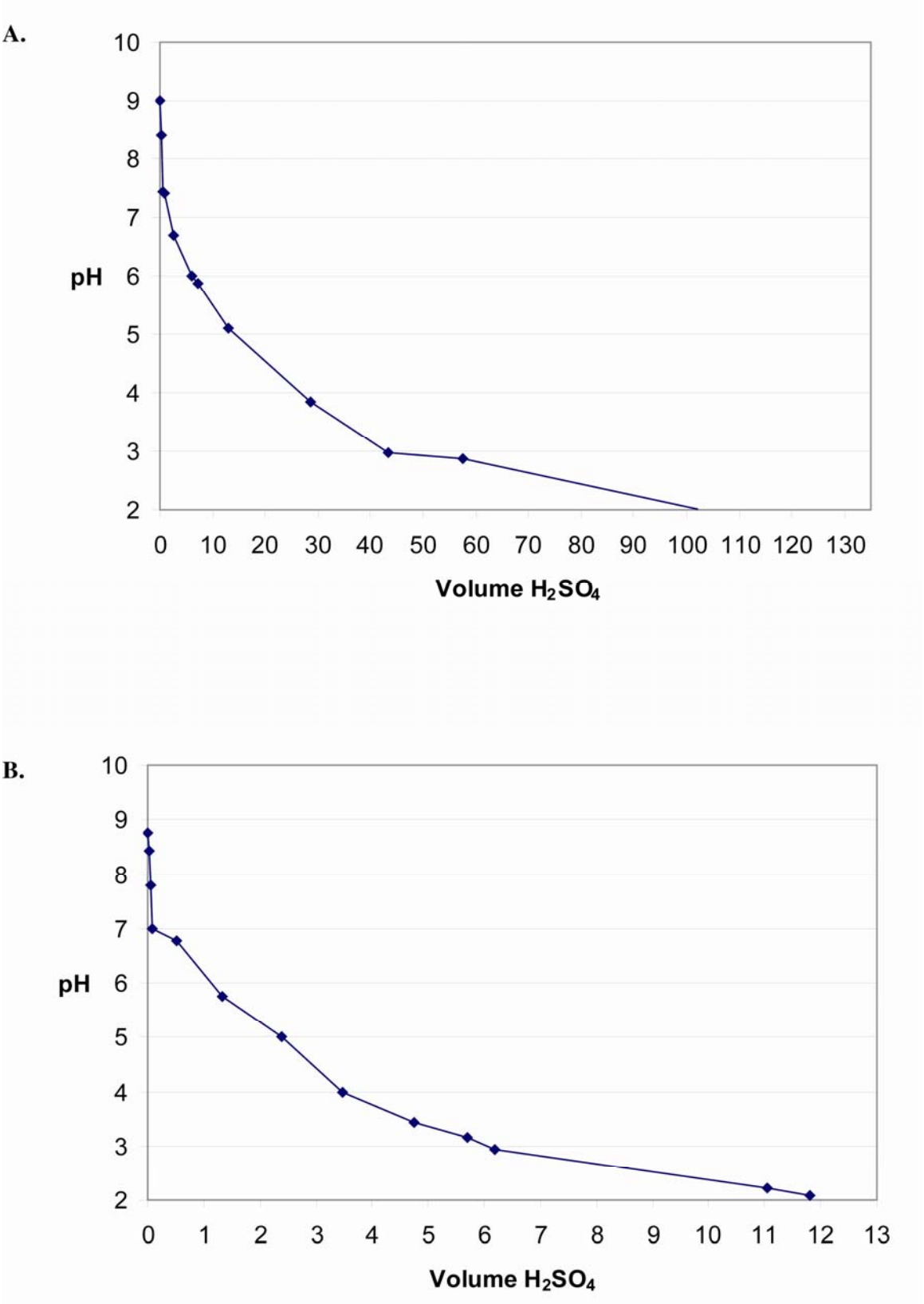

Figure 8. Acid titration curves for San Juan Formation. Lahar breccia (A), Intermediate composition lava (B).

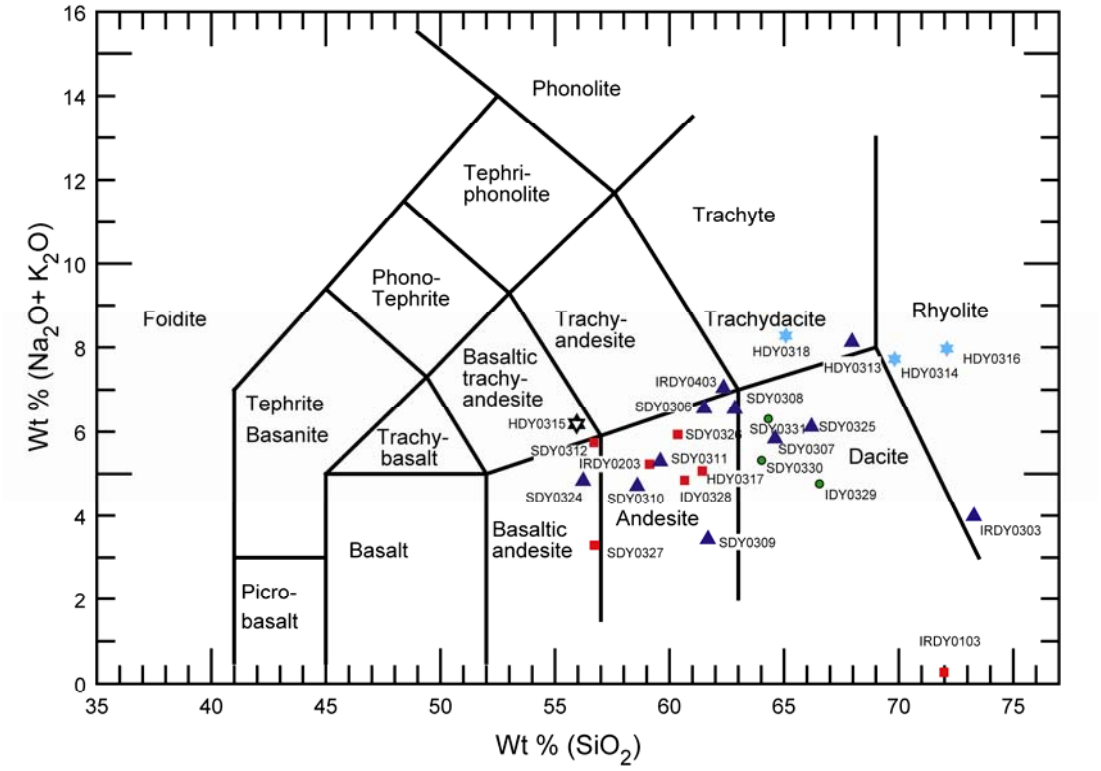

Figure 9. Total alkali versus silica rock classification (LeBas and others, 1986). Green dots, San Juan Formation; blue triangles, Burns Member of the Silverton Volcanics; red squares, Pyroxene Andesite Member of the Silverton Volcanics; blue stars, Eureka Member of the Sapinero Mesa Tuff; open star, Picauyune Megabreccia Member of the Sapinero Mesa Tuff.

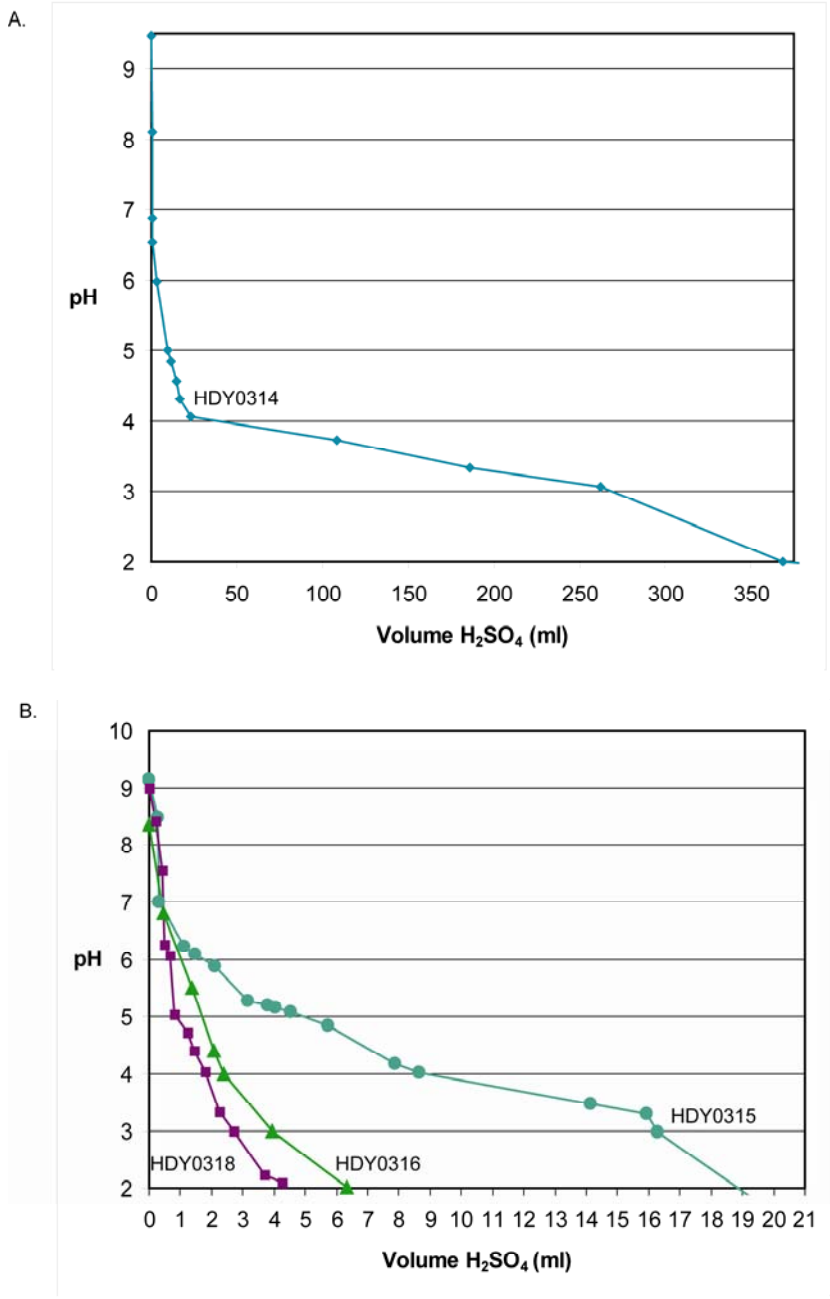

Figure 10. Acid titration curves for (A) Eureka Member of Sapinero Mesa Tuff requiring relatively large total volume of H_2SO_4 (B) Eureka Member of Sapinero Mesa Tuff (samples HDY0318 and HDY0316) and Picauyune Megabreccia of Sapinero Mesa Tuff (sample HDY0315) requiring addition of relatively small total volume of H_2SO_4.

The two additional Eureka Member of Sapinero Mesa Tuff samples exhibit similar titration curve shapes a high ANC when compared with their Tse counterpart HDY0314.

Sample HDY0316 exhibits no distinct titration curve plateaus, although; the curve gradually flattens with addition of H_2SO_4 titrant to pH 2, indicating some neutralizing capacity. A subtle plateau is observed at pH 5 for HDY0318; the curve gradually flattens from this plateau to pH 2.

Sultan Mountain Stock

Sultan Mountain stock (Tig) was sampled at three locations where it is preserved along the western and southern margins of the Silverton caldera. The locations sampled include a road cut exposure south of Silverton along highway 550 (SDY0319), an outcrop at the mouth of Cunningham Creek (HWDY0322), and a float block north of Silverton (SDY0320). Sample SDY0319 was excluded from ANC study due to a high NAP value of 79 kg/ton $CaCO_3$ equivalent. Both samples studied for ANC contain calcite. SDY0320 has the highest calcite abundance (3 weight percent), whereas the outcrop near the mouth of Cunningham Creek has < 1 weight percent calcite. Pyrite (< 1 weight percent) is present in HDY0322. Additional mineral phases include quartz, albite, potassium feldspar, ± epidote, and intergrown magnetite and ilmenite.

Moderate ANC along with no detectable NAP is observed in SDY0320; 40 ml of H_2SO_4 were required to achieve pH 2 (Fig. 11A). This is equivalent to 14 kg/ton $CaCO_3$ equivalent and ranks 8th in terms of ANC. In contrast, HWDY0322 required much less acid (7.7 ml H_2SO_4) to reach pH 2, which is consistent with the lower calcite abundance and with the trace amount of pyrite.

The acid titration curve for SDY0320 shows a steep but gradual decrease in slope between pH 6.6 and 4 and is followed by an abrupt plateau at pH 4 (Fig. 11B). The shallow slope is maintained between pH 4 to pH 2 indicating some neutralizing capacity over this pH range. In contrast the titration curve for SDY0320 is initially steep and gradually flattens to a plateau at pH 5. The curve does not exhibit a significant decrease in slope until pH 3.5 where it remains relatively shallow to pH 2.

Silverton Volcanics

Arguably the most important unit for our ANC study is the Silverton Volcanics. These rocks are important because as host to the majority of base- and precious-metal deposits, they are adjacent to vein mineralization and are thus invariably commingled with mine waste and mill tailings. They also are the most voluminous volcanic rock type and comprise a nearly 1 km thick by 8 km wide volcanic fill within the area affected by collapse of the San Juan and Silverton calderas (Yager and Bove, 2002). Consequently, it is important to understand the ANC of these rocks and the importance that they might have in attenuating metals and acidity in weathering processes of the mountain bedrocks and of mine waste piles. The Silverton Volcanics is composed of the Burns Member (Tb) that occurs lower in stratigraphic section, whereas the Pyroxene Andesite Member is commonly found higher in stratigraphic section. ANC for both Members are discussed separately below. The Henson Member, which also occurs stratigraphically high in the Silverton Volcanics section, is composed mainly of intermediate composition volcaniclastic sedimentary rocks and was not sampled.

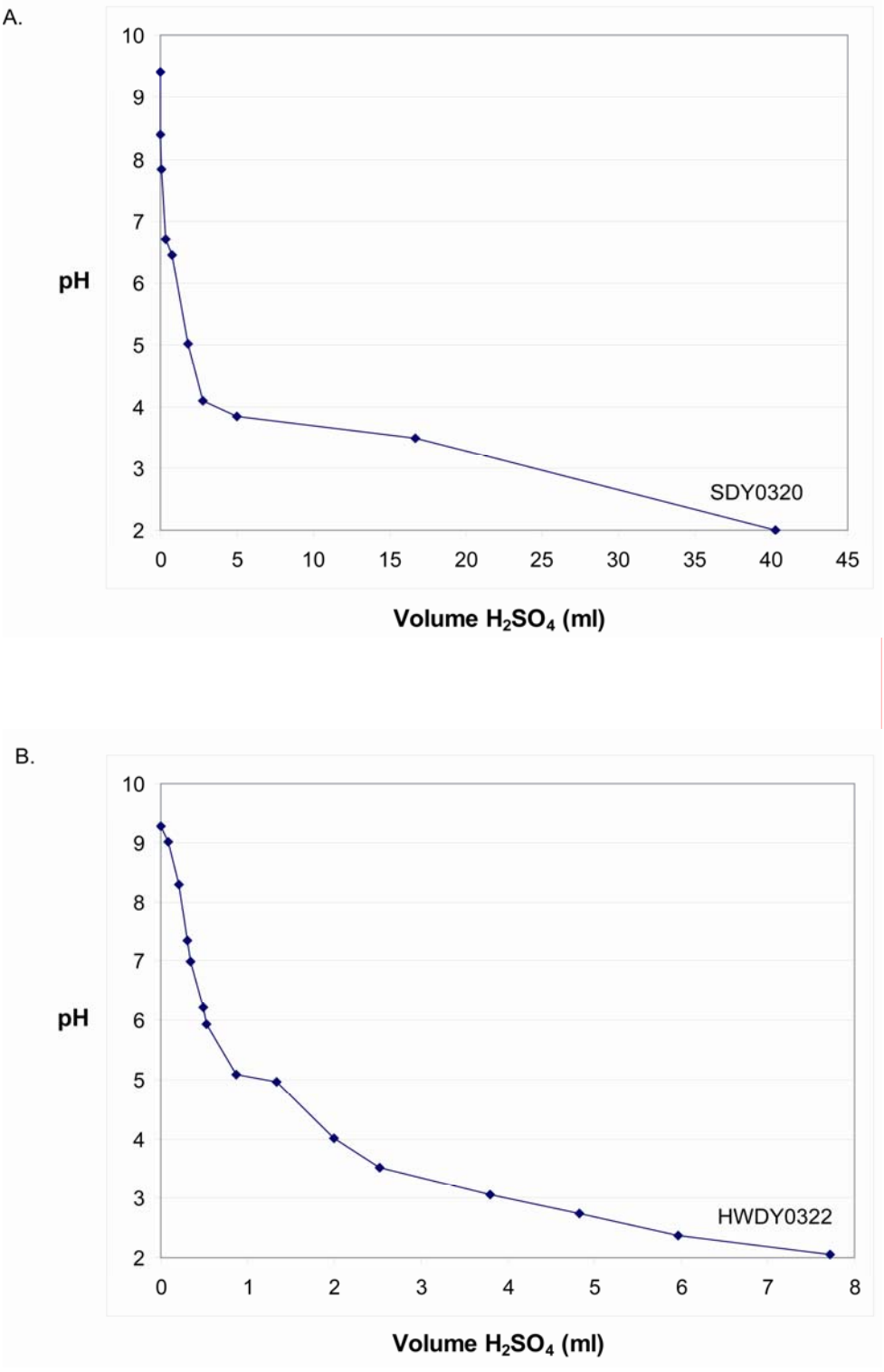

Figure 11. Acid titration curves for Sultan Mountain Stock requiring relatively large total volume of H_2SO_4 (A) float block, and (B) outcrop sample requiring relatively small total volume H_2SO_4.

Burns Member

Burns Member volcanics were collected within the core of the San Juan and Silverton calderas. A traverse in Boulder Gulch enabled the collection of Burns Member lava flows sequentially up stratigraphic section into the overlying Pyroxene Andesite Member (SDY0306, SDY0307, SDY0308, SDY0309, SDY0310, SDY0311) Plate 1. Additional Burns Member rocks were collected from outcrops in Browns Gulch (SDY0324, SDY0325), in Prospect Gulch (DYLPG0412, IRDY0303, IRDY0403), and at the mouth of Eureka Gulch (HDY0313) Plate 1. These rocks are mainly dacitic to andesitic (intermediate) in composition; one rhyolite (IRDY0303) and one basaltic andesite (SDY0324) were also sampled (Fig. 9). Minerals present consist of varying percentages of the propylitic assemblage clinochlore, ± epidote, quartz, intergrown magnetite and ilmenite, sericite (reported as "mica or muscovite" in XRD analyses, secondary potassium feldspar, and trace amounts of ± pyrite, ± chalcopyrite, ± galena (Fig. 12). Remnants of the primary igneous phases plagioclase, ± apatite, and ± rutile were also identified in some samples. Calcite is rare to absent in these lava flows.

When Burns Member (Tb) samples are compared as a group, the total H_2SO_4 added to achieve a pH 2 ranged from a low of 0.7 ml in a drill hole core sampled from bedrock 155 ft. below the surface at the base of Prospect Gulch (DYLPG0412) to a high of 99 ml in a sample from Boulder Gulch located north of Silverton (Fig. 13). All samples with the exception of (SDY0308) had some detectable NAP, likely caused by the presence of pyrite in at least 4 samples (SDY0308, SDY0324, SDY0325, SDY0310). Sample SDY0310; however, ranks 1st in ANC among Tb samples (98 kg/ton $CaCO_3$ equivalent) and 2nd among all samples studied (Fig. 14A). The ANC is likely also readily available due to a high ANC to NAP ratio of 7 (Table 9) as a ratio of acid neutralizing to acid generating potential of greater than 1.3 has been considered acceptable for samples being considered in mine waste remediation projects (Lister, 1994).

A chlorite mineral separate was attempted on SDY0310 using a Frantz magnetic separator. The resultant magnetic fraction contained a mixture of the phases (listed in decreasing order of abundance determined by XRD) chamosite, clinochlore, albite, potassium feldspar and quartz. The chlorite species chamosite and clinochlore were the only silicate phases present that had significant ANC in previous studies. The mineral separate was subjected to acid titration in a 0.01 N H_2SO_4 solution to determine whether the high ANC of this sample that lacks carbonate, could possibly be attributed to chlorite. The resultant titration curve (Fig. 14B) indicates a strong plateau between pH 4 to pH 2, indicate some neutralizing capacity over this pH range that was determined to be 54 kg/ton $CaCO_3$ equivalent. This considers the more dilute acid used and a factor of 6 lower initial sample mass.

A.

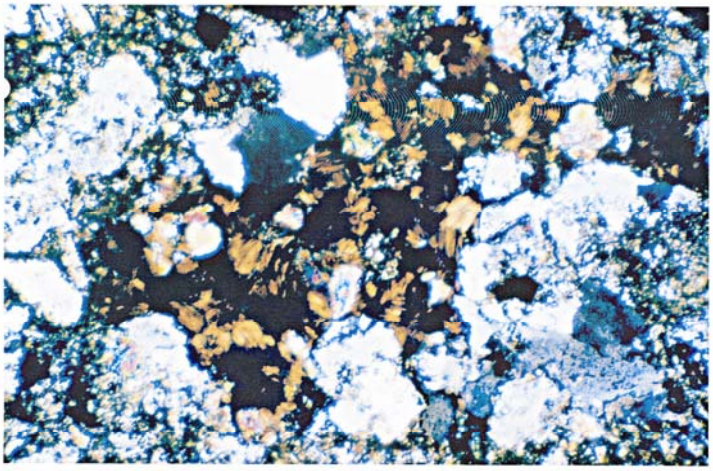

B.

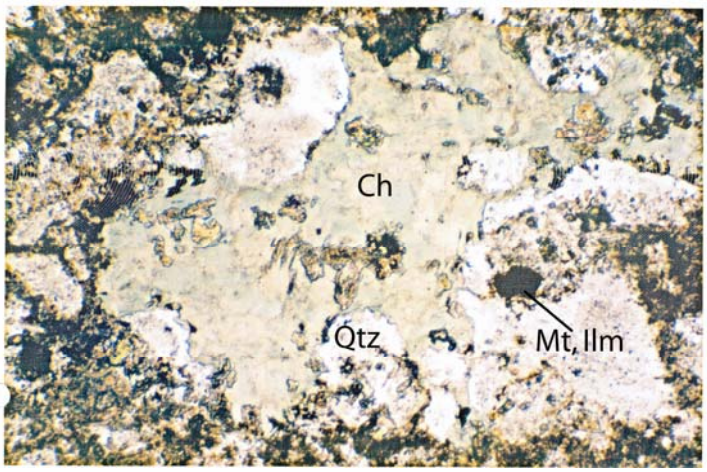

Figure 12. Photomicrograph in cross nicols, A, and in plain light B of Propylitically altered Burns Member of the Silverton Volcanics lava. A is cross polarized Ch, chlorite; Qtz, quartz; Mt, Ilm, intergrown magnetite and ilmenite. Fine grained matrix is composed of secondary potassium feldspar, sericite, plagioclase, and quartz. Greenish hue (plane light) is due to abundant chlorite.

Pyroxene Andesite Member

Outcrops of Pyroxene Andesite member were sampled in the upper parts of the following subbasins: Prospect Gulch (IRDY0203), Boulder Gulch (SDY0312), Placer Gulch (HDY0317), Browns Gulch near the Brooklyn mine, and along the Black Bear Road west of highway 550 (IDY0328) Plate 1. Pyroxene Andesite Member lava flows are composed of the propylitic mineral assemblage of clinochlore, calcite, quartz, ± trace clinopyroxene, intergrown magnetite and ilmenite, sericite (reported as "mica or muscovite" in XRD analyses, secondary potassium feldspar, and trace amounts of ± pyrite. Primary plagioclase is preserved in most samples.

Pyroxene Andesite member rocks differ mineralogically when compared to Burns Member units that were sampled in this study. Pyroxene Andesite member commonly lacks epidote, but contains abundant calcite (3 to 10 weight percent) and commonly contains hematite (Fig. 15).

Table 9. Acid neutralizing capacity, ANC to NAP ratio, and acid neutralizing capacity ranking. Samples highlighted in purple and blue have ≥ 2 and ≤ 1 weight percent pyrite respectively. Samples are grouped by geologic unit, and are ranked in order of descending ANC within a geologic unit.

Field sample number	Unit	Weight (g)	Initial pH	Total Volume 0.1 N H_2SO_4 (ml) to reach pH ~ 3.00	Total Volume 0.1 N H_2SO_4 (ml) to reach pH ~ 2.00	$CaCO_3$ Kg/ton ~ pH 3.00	$CaCO_3$ Kg/ton ~ pH 2.00	ANC/NAP Ratio pH 3	ANC/NAP Ratio pH 2	ANC Rank pH2
HWDY0323$_{c,ch}$	$_{p}$€	30.07	9.09	4.24	5.03	1.41	1.67	0.06	0.07	22
IDY0329$_{c,\ ch}$	Tsj	30.00	9.00	43.50	133.28	14.49	44.43	*	*	4
ODY0331$_{c,ch,ep}$	Tsj	30.00	8.77	5.71	11.79	1.90	3.93	*	*	11
HDY0314 $_{c,ch}$	Tse	30.00	9.47	261.97	368.56	87.32	122.85	*	*	1
HDY0315 $_{c,ch}$	Tsemb	30.00	9.14	15.92	19.38	5.31	6.45	*	*	10
HDY0316$_{ch}$	Tse	30.05	8.35	3.94	6.32	1.31	2.10	0.13	0.21	20
HDY0318$_{c,ch}$	Tse	30.06	9.00	2.72	4.27	0.90	1.42	0.02	0.04	23
HDY0317 $_{c,ch}$	Tpa	50.06	**9.50**	66.82	328.92	13.35	65.70	*	*	3
IDY0328$_{c,\ ch}$	Tpa	30.03	8.46	89.44	95.12	29.78	31.67	*	*	5
IRDY0203 $_{c,ch}$	Tpa(?)	30.02	**8.50**	55.42	78.86	18.46	26.27	*	*	6
SDY0327$_{c,\ ch}$	Tpa	30.01	8.34	64.80	65.16	21.59	21.71	*	*	7
SDY0326$_{c,ch}$	Tpa	30.03	9.43	11.11	27.84	3.70	9.27	*	*	9
SDY0312 $_{c}$	Tpa	30.06	9.08	n/a	1.97	n/a	0.6	n/a	0.08	21
SDY0310$_{ch,ep}$	Tb	30.05	**8.50**	197.00	296.07	65.55	98.50	4.98	7.49	2
SDY0308$_{ch}$	Tb	30.00	9.43	2.20	3.63	0.735	1.21	*	*	12
SDY0307 $_{ch}$	Tb	30.07	9.22	n/a	10.01	n/a	3.33	n/a	7.81	13
IRDY0403 $_{ch}$	Tb	30.07	**8.40**	n/a	19.41	n/a	6.45	n/a	0.94	14
SDY0325$_{ch}$	Tb	30.06	9.63	27.80	38.63	9.25	12.85	1.33	1.85	15
SDY0306 $_{ch}$	Tb	30.02	8.87	4.67	7.14	0.99	2.37	0.16	0.37	16
SDY0324$_{ch}$	Tb	30.04	6.39	1.14	4.98	0.38	1.66	0.06	0.24	17
DYLPG0412	Tb	30.07	6.23	1.25	2.12	0.41	0.71	0.13	0.22	24
SDY0320 $_{c,ch}$	Tig	30.02	9.40	16.67	40.27	5.55	14.21	*	*	8
HWDY0322$_{c,ch,ep}$	Tig	30.04	9.27	3.79	7.72	1.26	2.57	0.03	0.07	18
IDY0321	Td	30.00	7.29	n/a	0.655	n/a	0.20	n/a	0.00	19
MPGD_51_52.5	Qc	30.02	2.84	n/a	1.24	n/a	0.41	n/a	n/a	n./a

subscripts "c" "ch" and "ep" denote calcite, clinochlore, and epidote respectively. XRD is not determined for samples DYLPG0412 and MPGD_51_52.5. Weight is initial mass of sample; an equal volume (ml)of deionized water was added to a sample; initial pH is that recorded at start of titration; $CaCO_3$ is calculated from total H_2SO_4 acid added at pH titration set points of ~ 3 and ~ 2;initial pH in bold indicates estimated value. Note that the total acid added to achieve pH ~ 3 and ~ 2, were within 0.5 pH units or closer to these respective titration set points in most samples. ANC/NAP ratio is based on the ANC reported in this table in CaCO3 equivalent divided by the NAP CaCO3 equivalent in table XX. Analyses that are not available are indicated by "n/a". An "*" indicates that there was no NAP detected. ANC rank was determined on (1) total amount of H_2SO_4 acid added to achieve titration endpoint of ~ 2 and (2) NAP values, where samples with no detectable NAP or high (> 1.3) ANC/NPA ratios being also ranked higher than those with ANC/NAP ratios below 1.3 as suggested in Lister (1994).

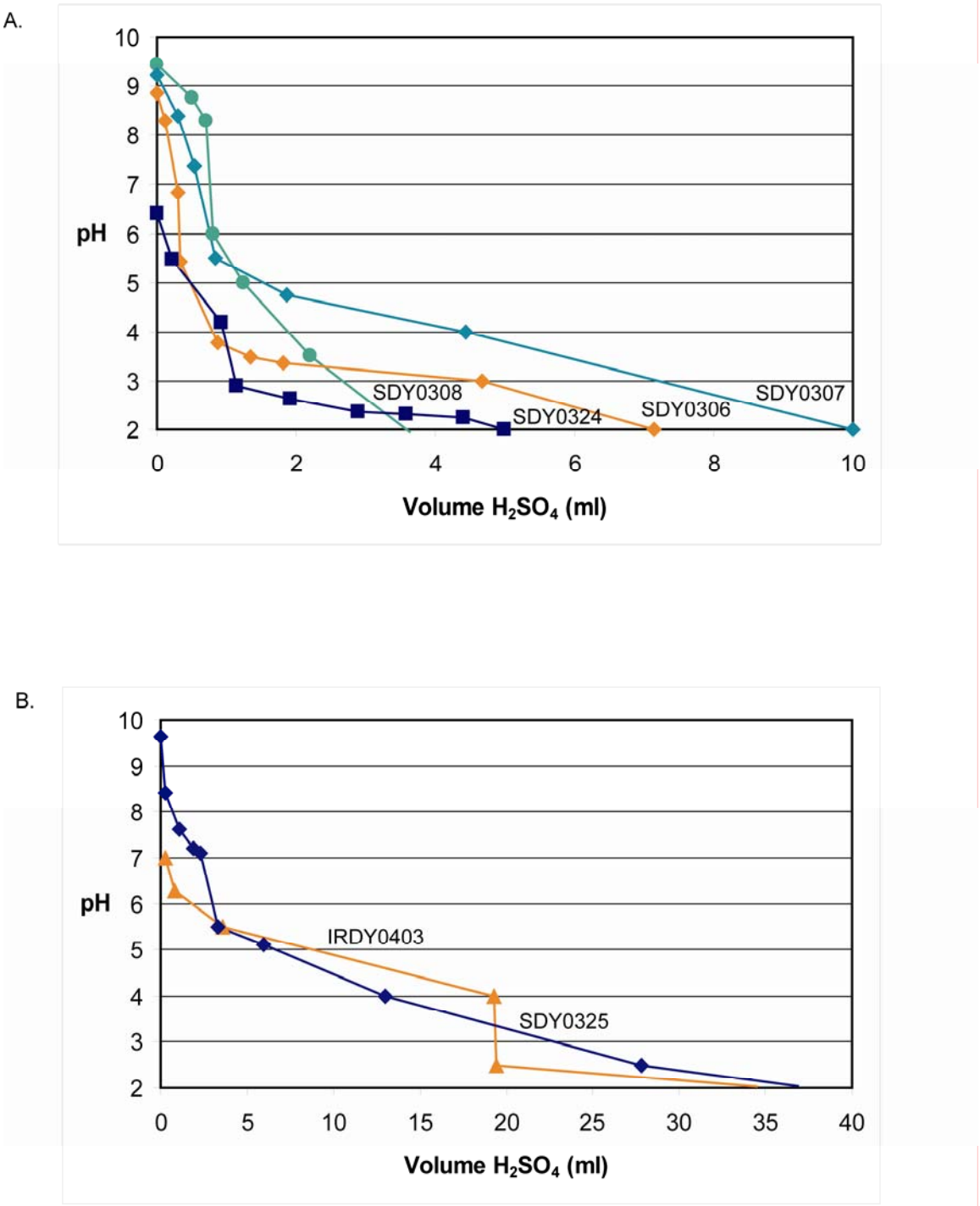

Figure 13. Acid titration curves for Burns Member of the Silverton Volcanics. Relatively small amount of total H_2SO_4 acid added for titration (A); moderate amount of total H_2SO_4 acid added (B). All samples are intermediate composition lavas that are propylitically altered.

A.

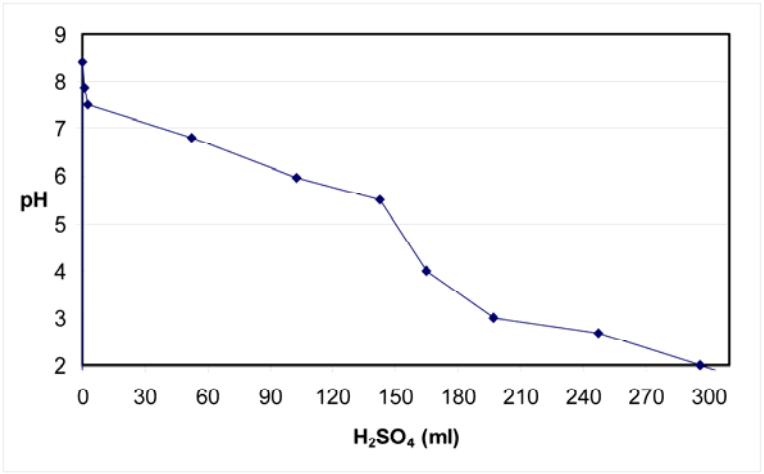

B.

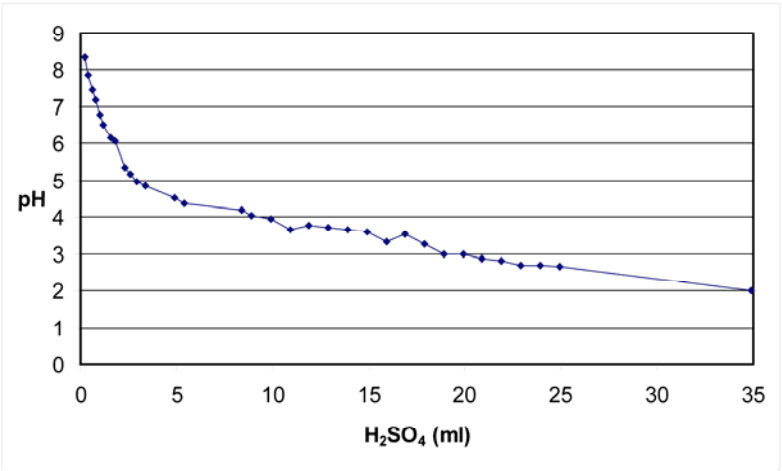

Figure 14. Acid titration curve for propyllitically altered Burns Member of the Silverton Volcanics lava (sample SDY0310). Whole rock hand sample (A), mineral separate (B). Whole rock sample titrated with 0.1 N H_2SO_4, mineral separate titrated with 0.01 N H_2SO_4. Mineral separate contains a mixture of clinochlore, chamosite, quartz, albite, and secondary potassium feldspar based on X-ray diffraction analysis. No calcite was detected in either whole rock or mineral separate.

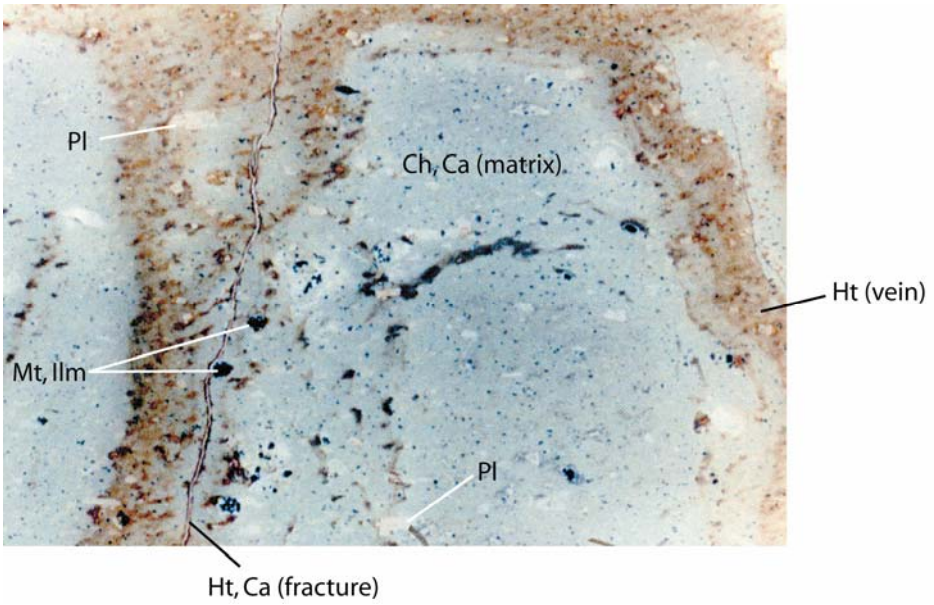

Figure 15. Scanned thin section (2 cm X 4 cm) of Pyroxene Andesite Member lava (HDY0317). Ch, chlorite; Ca, calcite; Pl, remnant plagioclase; Ht, hematite; Mt, Ilm, intergrown magnetite ilmenite. Greenish hue due to abundant chlorite; reddish brown hue due to hematite.

ANC of Pyroxene Member lava flows range from a low of 2.0 ml (SDY0312) H_2SO_4 added to achieve a pH of ~2 (Fig. 16) to a high of 329 ml H_2SO_4 (HDY0317) (Fig. 17). HDY0317 has an ANP of 66 kg/ton $CaCO_3$ equivalent and no detectable NAP that ranks 3rd highest in ANC among all samples and 1st for Pyroxene Andesite Member rocks. Other Pyroxene Andesite member rocks (IDY0328, IRDY0203, SDY0327, SD0326) rank 5th, 6th, 7th, and 9th respectively compared with all other samples. Thus, when considering the ANC along with the commonly low- to non-detectable NAP, the Pyroxene Andesite Member is one of the most important units with relatively high ANC.

Dacite Intrusion

A dacite intrusion was sampled near Chatanooga, west of Highway 550 (IDY0321), (Plate 1). The outcrop sampled is quartz-sericite-altered and contains large remnants of 1-2 cm potassium feldspar phenocryts. The primary mineralogy has been totally altered to an assemblage of quartz, sericite, and hematite. Any effective ANC has been largely obliterated due hydrothermal alteration. This is reflected in the high NAP (81 kg/ton $CaCO_3$ equivalent) and the low (0.65 ml H_2SO_4) total amount of acid required for titration (Fig. 18, Table 9). This sample is illustrative of the lack of ANC and high NAP of rocks that have suffered more intense hydrothermal alteration when compared to less intensely altered propylitically altered units (Fig. 19).

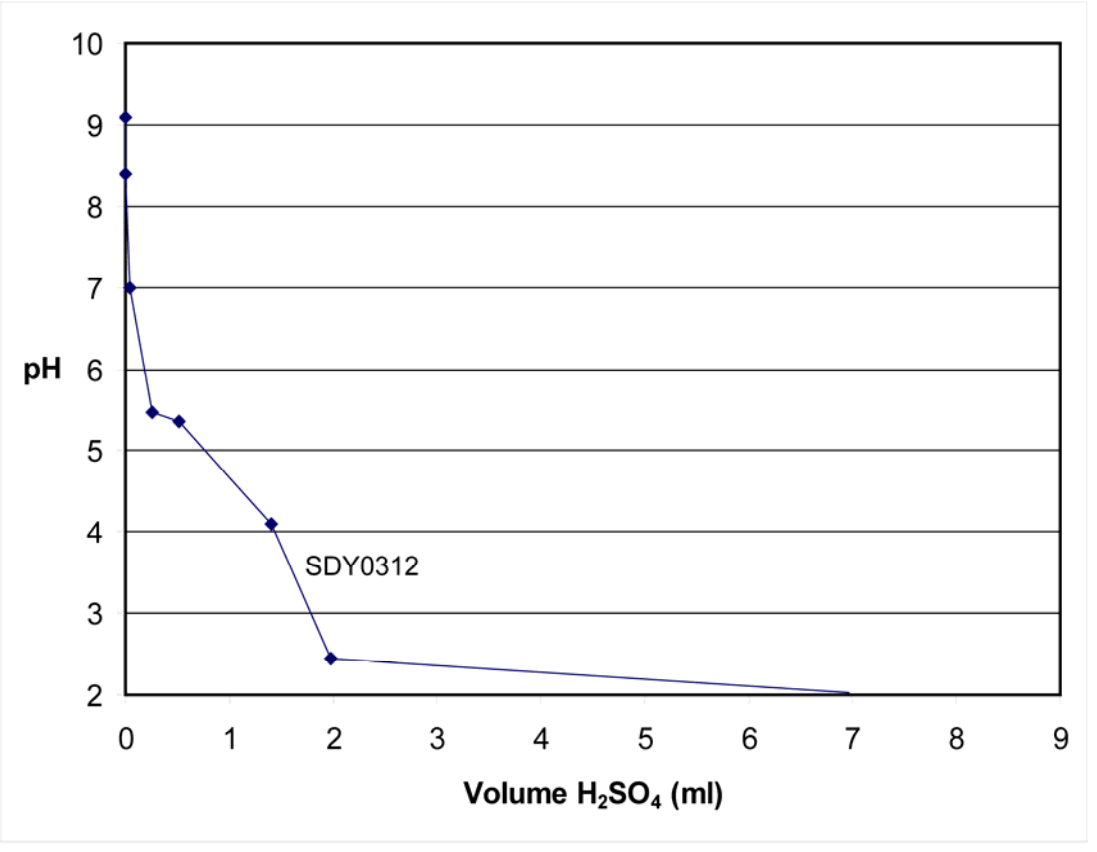

Figure 16. Acid titration curve for Pyroxene Andesite Member of the Silverton Volcanics requiring small amount of total H_2SO_4 acid added for titration.

A.

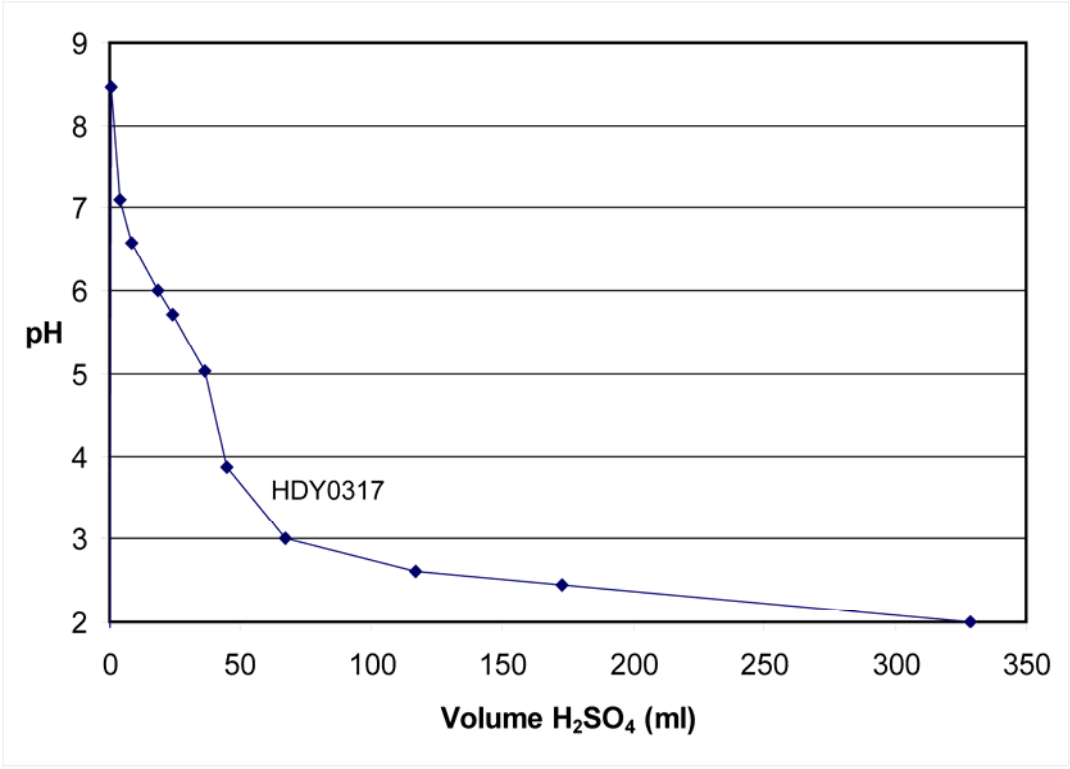

B.

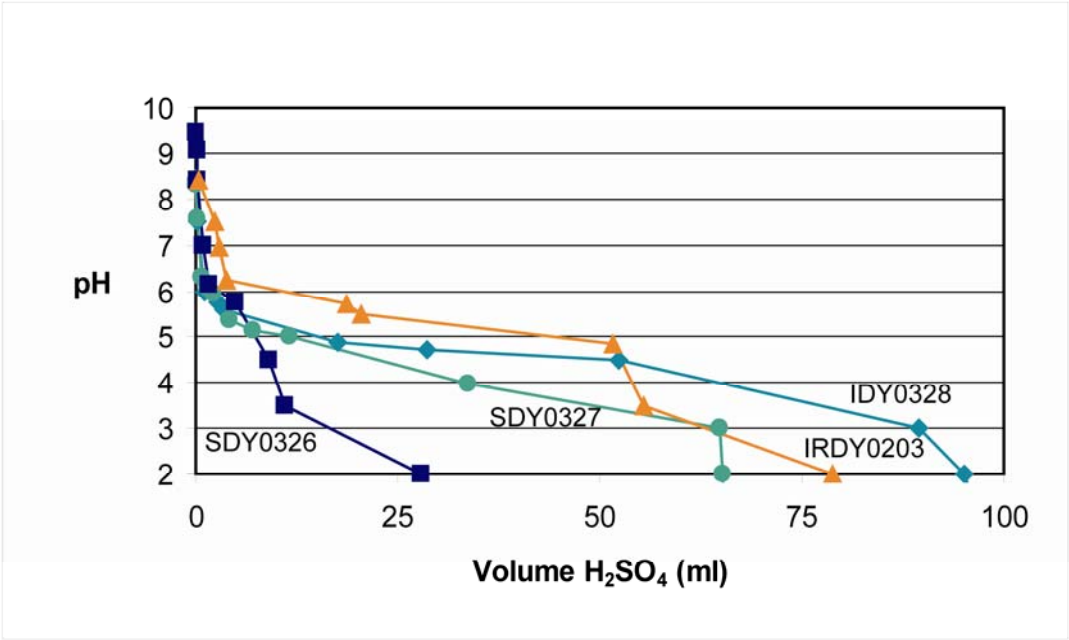

Figure 17. Acid titration curves for Pyroxene Andesite Member of the Silverton Volcanics. Relatively large amount of total H_2SO_4 acid added for titration (A); moderate amount of total H_2SO_4 acid added (B). All samples are intermediate composition lavas that are propylitically altered.

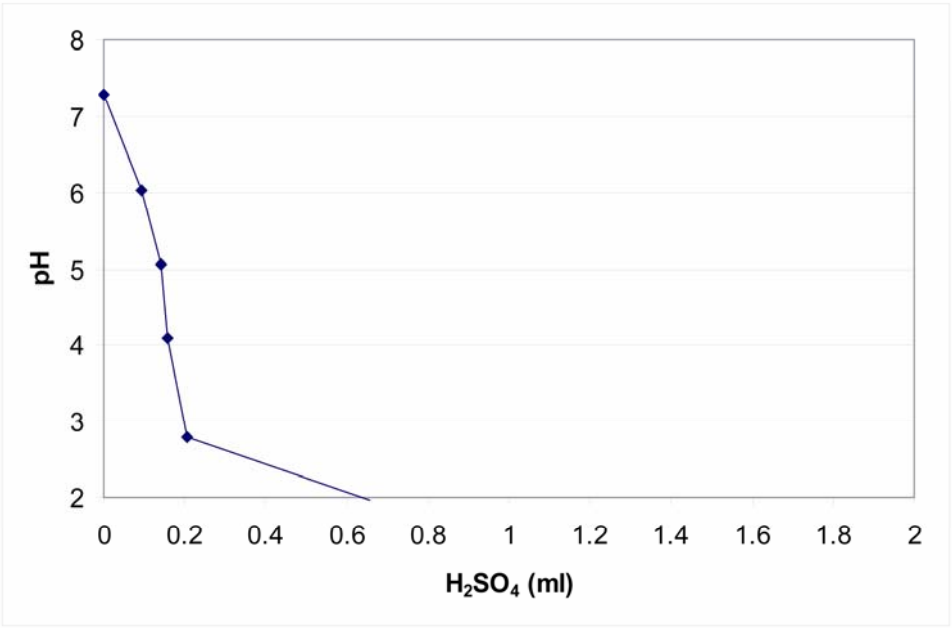

Figure 18. Acid titration curve for quartz-sericite altered dacite intrusion (IDY0321).

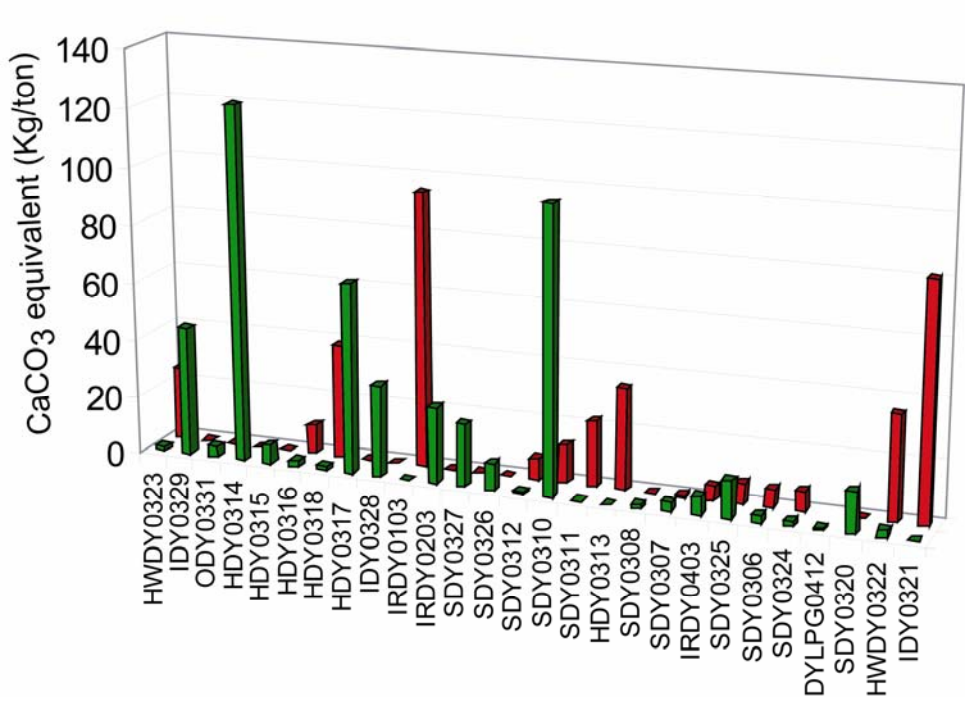

Figure 19. Net acid production (red) and acid neutralizing capacity (green) in kilograms/ton $CaCO_3$ equivalent for samples that were analyzed using both methods.

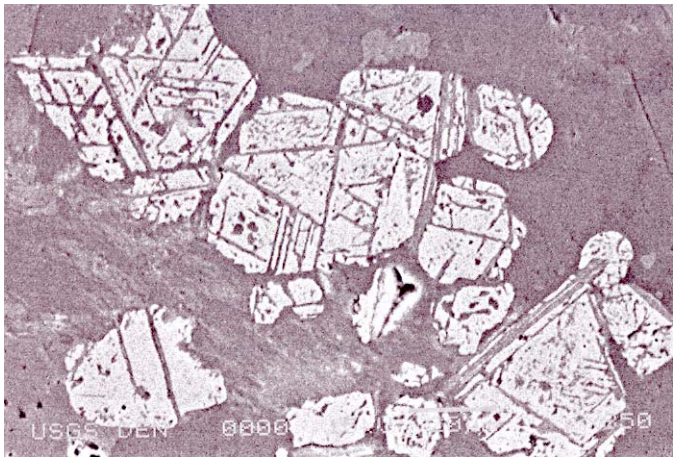

Figure 20. SEM backscatter electron image of Ilmenite (dark bands) intergrown along octahedral lattice planes of magnetite (bright). Largest grain is ~60 μm.

Magnetic Properties of major rock types

A goal of this project is to determine if geophysical properties including magnetic susceptibility can be used to map, at a watershed scale, those rocks with a possible high NAP or ANC.

Magnetite is a common accessory mineral in igneous rocks and is ubiquitous in the volcanic and plutonic rocks in the Animas River watershed study area. Magnetic properties are dependant on the amounts of ferrimagnetic minerals present, which are primarily iron titananium-oxide minerals, of which magnetite (Fe_3O_4) is the most common. Two ferrimagnetic minerals are present in the rocks collected for this study and include magnetite and ilmenite. Magnetite is most common and detected in 14 out of 24 samples. Ilmenite is presents in amounts below XRD detection limits, but was detected in microscopic analysis in minor amounts (less than 1 weight percent) in several samples. Magnetite-ilmenite intergrowths are common where ilmenite is observed to have crystallized along the octahedral lattice planes within magnetite (Fig. 20). Magnetic susceptibility is a measure of the degree for which a substance can be magnetized and for most rock types, is proportional to the volume percent of ferromagnetic minerals, principally magnetite. Since ilmenite occurs in small quantities and its susceptibility is roughly 100 times less than the susceptibility of magnetite (Dobrin and Savit, 1988), we can be confident that the magnetic susceptibility measured in the cores for this study is overwhelmingly influenced by the mineral magnetite.

Magnetic susceptibilities were measured to (1) estimate the volume-percent magnetite for the representative geologic units and (2) explore the relationship between magnetite content and important NAP and ANC rock properties.

Magnetic and Environmental Properties

This section compares magnetite content to important environmental rock properties. The samples in Table 6 are organized to illustrate and develop an understanding of how magnetite content varies with geologic unit, alteration type, degree of alteration, mineral assemblages and associated NAP and ANC.

Magnetite Content as a Function of Sericitic and Propylitic Alteration

Typically, in igneous rocks that have undergone hydrothermal alteration that have reached sericitic levels, primary magnetite will commonly be destroyed. With one exception, this is the case for samples investigated for this study. Magnetite content for propylitically altered samples is more than three times that of the weak- to strong-sericitically altered rocks. Most samples in this study where sericitized, are only weakly sericitized as propylitic assemblage minerals are still preserved while sericite abundance has increased. Average magnetite content in the propylitically altered rocks is 3 volume percent, in contrast to an average value of less than 1 volume percent for the sericitically-altered samples (Fig. 21).

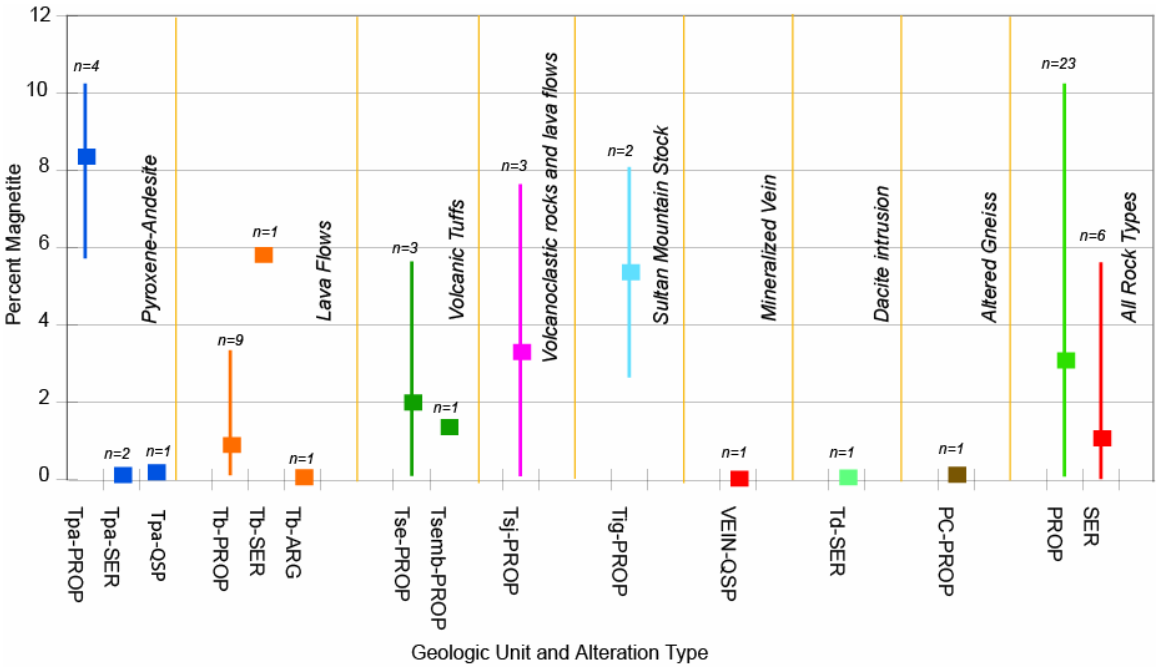

Figure 21. Volume-percent magnetite for samples collected in the Upper Animas watershed study area. With the exception of one rock lithology (Tb-SER), rocks that have been propylitically altered contain higher amounts of magnetite than rocks that have undergone sericitic alteration (SER and QSP). Geologic unit abbreviations from Table 1.

Alteration typically causes conversion of magnetite to nonmagnetic, more highly oxidized and hydrated iron-oxide minerals such as limonite. In cases where redox conditions are reducing, magnetite can be destroyed as its iron is reduced. The resulting ferrous iron is combined with sulfur to form pyrite. Overall, the resulting geophysical effect of the alteration processes is a reduction in magnetite content and a corresponding lowering of magnetic susceptibility.

In some cases, magnetite can be produced with increased degree of alteration. This may be the case for some Burns Member volcanic rocks, although there are too few samples to determine if this is typical. For the one sample of weakly sericiticized Burns Member, there is a significant increase in magnetite in comparison with the propylitically

altered counterparts. SDY0324 is the most highly altered sample of the Burns Member lava flows collected and contains nearly 6 volume percent magnetite. In contrast, the less intenselely-altered propylitic Burns Member rocks have only 0.5 volume percent average magnetite abundance. One argillically altered sample (sample IRDY0303) is devoid of magnetite. More samples of weak-sericitically altered Burns Member lavas are needed to test the hypothesis that magnetite increases with increased alteration in this unit.

Magnetite, Clay Content, Acid Generating, and Acid Consuming Minerals

Alteration commonly results in substantial modification to the primary mineral phases of the original affected rock or protolith. In this section, we compare estimates for magnetite, ordered from highest to lowest values, to corresponding amounts of propylitic

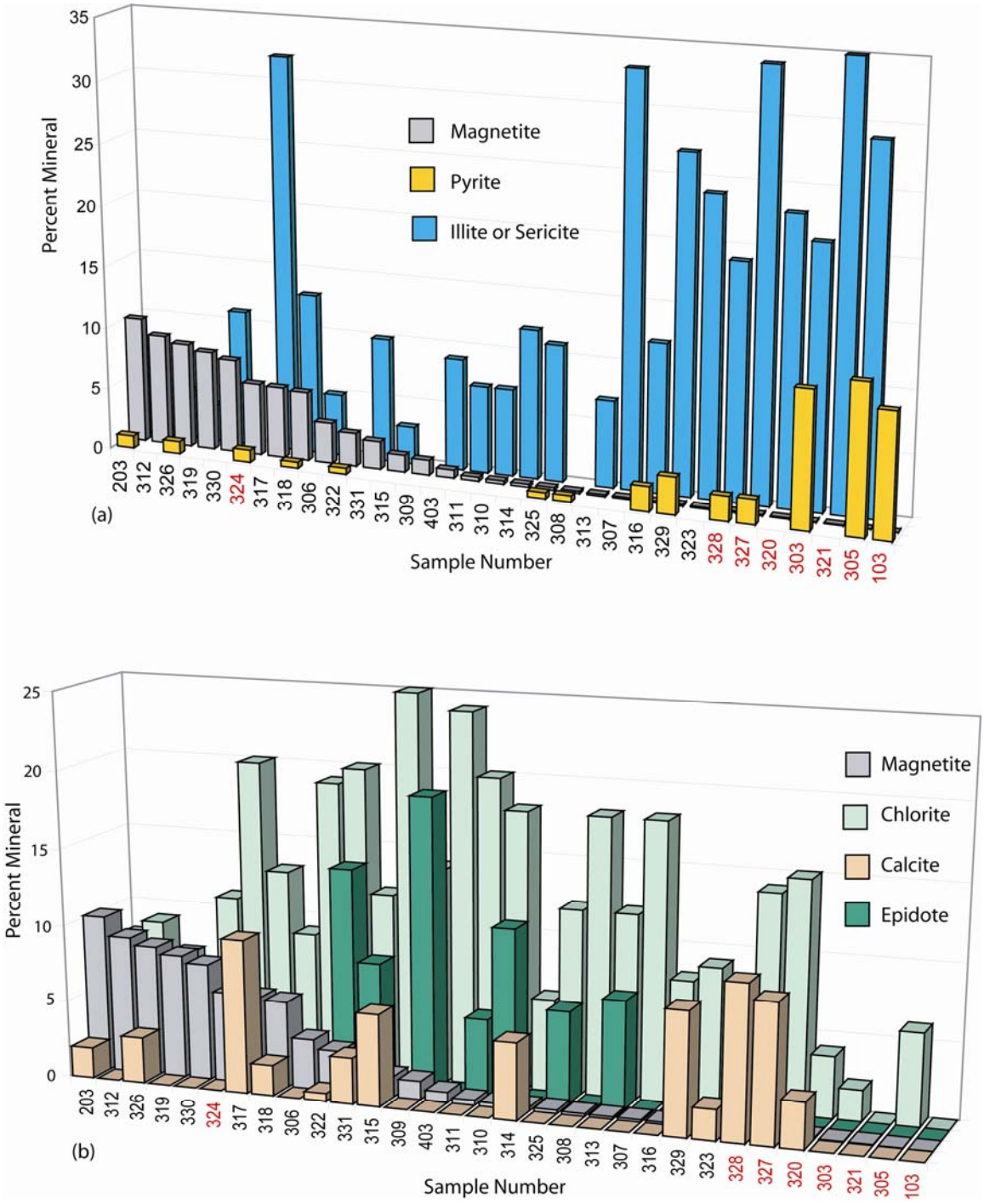

Figure 22. (a) Magnetite content, clay minerals of sericite or sericite, and acid-producing mineral pyrite. (b) Magnetite and minerals that provide acid neutralizing. Samples that contain sericitic, argillic, or quartz, sericite, pyrite mineral assemblages are in red. Sample numbers are represented by the last three characters for samples in Table 1.

and sericitic mineral assemblages to evaluate how magnetic mineralogy varies with variation in alteration.

Pyrite is the primary mineral that is responsible for generating acidity and usually the main cause for high NAP. Clay content is another gauge for degree of alteration. In general, higher clay contents indicate a higher the degree of alteration. Mica was measured via XRD and is used here as a measure for clay minerals, either in the form of sericite or the commonly used term sericite that describes potassium clays that are similar in composition to muscovite. Clay content was compared to magnetite and pyrite content to determine the relationship between degree of alteration and magnetic properties.

Magnetite content is inversely proportional to amounts of pyrite and clay minerals in most of the geologic units studied (Fig. 22). Rocks with high concentrations of magnetite are typically devoid of pyrite, although exceptions exist in two samples of propylitically altered pyroxene andesite (IRDY0203 and SDY0326) and one sample of sericitically-altered Burns volcanic rock (SDY0324). In general, however, clay and pyrite content increases with decreasing magnetite content.

Higher ANC is found primarily within the propylitically altered rocks. Bove and others (in press) define two major mineral assemblages within the propylitic lithologies that include rocks dominated by calcite, epidote, and chlorite (CEC); and a second group of rocks dominated by a mineral assemblage comprised of calcite, sericite, and chlorite (CIC). Calcite, chlorite, and epidote are the main minerals responsible for providing acid consumption. Figure 22 shows these important mineral assemblages with corresponding magnetite content for all samples.

The correlation between minerals with some ANC and magnetite abundance is less strong than that of the correlation between magnetite and pyrite abundance, but some generalization can be made. Three of the four samples with highest amounts of magnetite (greater than approximately 8 volume percent) are from the Pyroxene Andesite Member of the Silverton Volcanics. All the magnetite-rich samples are propylitically altered, contain less than 10 weight percent chlorite, zero to 3 weight percent calcite, and no epidote. These samples would be classified under the CIC propylitic assemblage.

Rocks with moderately high to low amounts of magnetite (less than 8 to approximately 0.1 volume percent) all have chlorite present (8 to 25 weight percent, with an average of 14 weight percent), are typically propylitically altered, and a contain calcite in the range of 0 to 10 weight percent, with an average of 5.8 weight percent. Most of the samples within this range also contain epidote and would be classified under the CEC mineral assemblage.

Rocks with little to no magnetite (less than 0.1 volume percent), are typically sericitically to QSP altered, have no calcite, and little to no chlorite (0 to 6 weight percent).

Magnetic Rock Properties and Mineralogy of Geologic Units

Although too few samples are available to determine statistical significance, with the exception of the Burns and Pyroxene Andesite Members of the Silverton Volcanics, the rocks collected for this study were considered representative of the overall geologic unit. Consequently, we assume that the magnetic and the environmental rock properties (defined as NAP and ANC for this study) measured are generally representative for a

given geologic unit. In this context, the section that follows explains how magnetite varies with minerals important to NAP and ANC in each geologic unit studied.

Pyroxene-Andesite Member of the Silverton Volcanics

Seven samples of the Pyroxene Andesite Member of the Silverton Vocanics were collected for this study and are divided into three groups for discussion purposes. Groups are defined on the basis of magnetite content, from highest to lowest values (Fig. 23). The first group consists of the three most magnetite-rich samples (IRDY203, SDY0312, and SDY0326). These samples are characterized by high percentages of magnetite (8-10 volume percent), low clay content (0 to 5 weight percent), and low amounts of pyrite (0 to 0.5 weight percent). NAP for the three samples range from none (IRDY0203 and SDY0326) to moderately low (SDY0312). In terms of ANC-related mineralogy, the samples of magnetite-rich pyroxene andesite are associated with little calcite (0 to 3 weight percent), and moderate amounts of chlorite (7 to 9 weight percent). ANC for the three samples ranges from none (SDY0312) to moderate (IRDY0203).

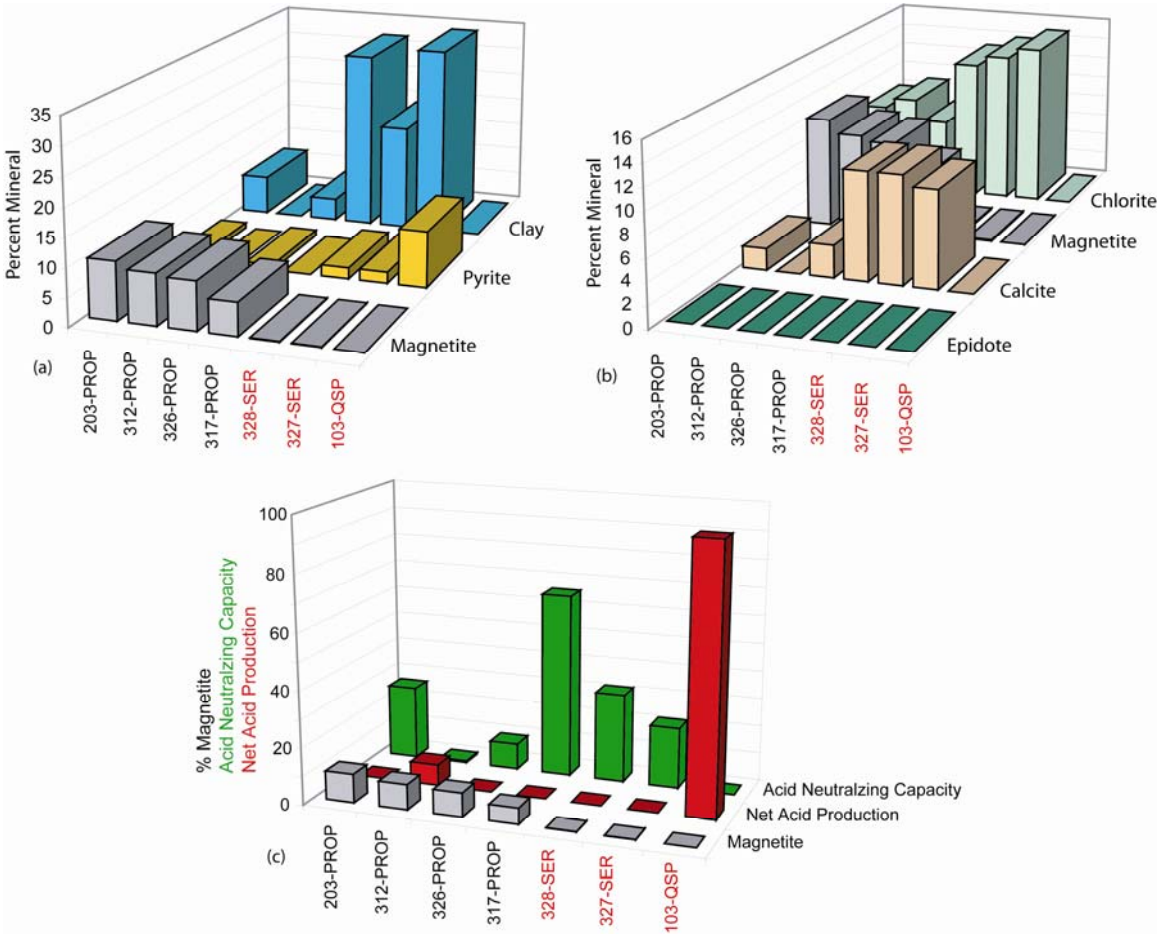

Figure 23. (a) Magnetite and minerals related to acid generation and alteration, (b) magnetite and acid consuming minerals, and (c) magnetite, acid neutralizing capacity, and net acid production for Tertiary pyroxene andesite samples. Sample numbers are represented by the last three characters for samples in Table 1.

.

Group 2 in the pyroxene andesite consists of samples HDY0317, IDY0328, and SDY0327. This group includes one propylitic and two sericitic samples. Magnetite content for the propylitic sample (HDY0317) is somewhat reduced from the Group 1 samples (5.7 volume percent) but is much higher than the magnetite content of the weakly sericitically-altered samples (IDY0328 and SDY0327), which have little to no magnetite. Aside from the magnetic mineralogy, the three samples in group 2 share mineralogical and environmental rock properties. All three are high in clay content (20 to 30 weight percent), calcite (9-10 weight percent), and chlorite (13-15 weight percent). All have no NAP and moderate to high ANC. Interestingly, in comparison with all the other geologic units sampled, only the weakly sericitically-altered Pyroxene Andesite member shows an increase in ANC with an increase in degree of sericitization.

Group 3 among the Pyroxene Andesite Member samples consists of the QSP altered sample (IRDY0103). This sample is devoid of magnetite, clay, calcite, and chlorite. It has no ANC and high NAP.

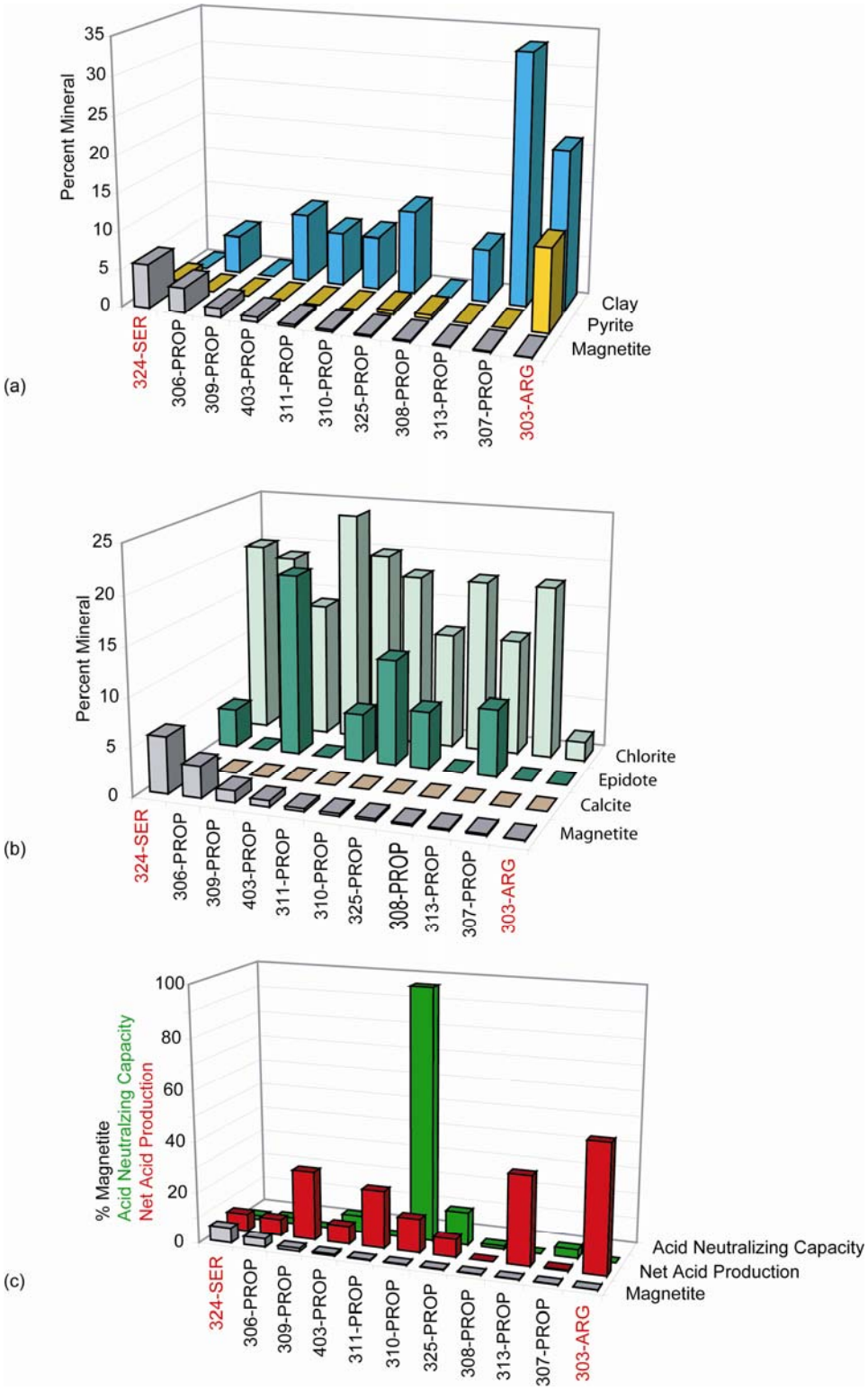

Figure 24. (a) Magnetite and minerals related to acid generation and alteration, (b) magnetite and acid consuming minerals, and (c) magnetite, acid neutralizing capacity, and net acid production for Burns Member lava flow samples. Sample numbers are represented by the last three characters for samples in Table 1.

Burns Member of the Silverton Volcanics

The Burns member has a considerable range of magnetic and environmental rock properties. Although direct correlations between magnetic and environmental properties are not readily apparent, some general observations can be made. Eleven samples of Burns Member lava flows were collected from several locations across the watershed study area. This sample group has a disparate range of acid neutralizing capacity, ranging from a low of 0 to an extreme high of 98 kg/ton $CaCO_3$ equivalent (Fig. 24). We divide the Burns samples into two groups; one based on samples with significant amounts of magnetite and one group of samples with little to no magnetite. The first group includes the four Burns samples with highest percentages of magnetite (SDY0324, SDY0306, SDY0309, and IRDY0403). The sample with the most magnetite (SDY0324) is sericitcally altered, in contrast to the other three samples, which are propylitically altered (Fig. 24). Sample SDY0324 has nearly 6 volume percent magnetite. The magnetic mineralogy of this sample is in contrast to all other weakly sericitized lithologies in our study. There is more magnetite in the sericitically-altered rocks than the propylitically altered rocks. For all the geologic units sampled, only the Burns Member yielded more magnetite with higher degrees of alteration (figure 24a).

In general, samples in group 1 have a low percentage of clays, greater than 10 weight percent chlorite, no calcite, and some epidote. Average NAP is moderate (14), average ANC is low (2.1), and average magnetite content high (2.5 volume percent). This suggests that the magnetic mineralogy of this unit has some potential to be used to rule out Burns Member volcanic rocks with high ANC. In other words, we would expect that magnetite-rich areas within the Burns rocks could have correspondingly low ANC and moderate to high NAP.

Group 2 within the Burns samples have little to no magnetite (SDY0311, SDY0310, SDY0325, SDY0308, HDY0313, SDY0307, and IRDY0303). In general, clay and pyrite content increase and chlorite decreases with decreasing amounts of magnetite. No calcite is present in any of the samples. Four of the seven samples (SDY0311, SDY0310, SDY0325, and HDY0313) with little to no magnetite have some epidote (Fig. 24) indicating a higher degree of propylitic alteration (Bove and others, in press).

Group 2 has a wide range of environmental properties and little correlation with magnetite content, although high net acid production tends to occur in association with Burns samples with the least amount of magnetite (Fig. 24c).

.

Eureka Member of the Sapenero Mesa Tuff

The three samples collected of the Eureka tuff (HDY0318, HDY0314, and HDY0316) are propylitically altered and contain a range of magnetite from nearly none to over 5 volume percent (Fig. 25). A sample of the Picayune megabreccia member is also included in this group (HDY0315). Sample HDY0318 contains the most magnetite of the Eureka tuff samples and is also highest in NAP. This sample also contains approximately 0.5 weight percent pyrite and 2 weight percent calcite, although it has no appreciable ANC.

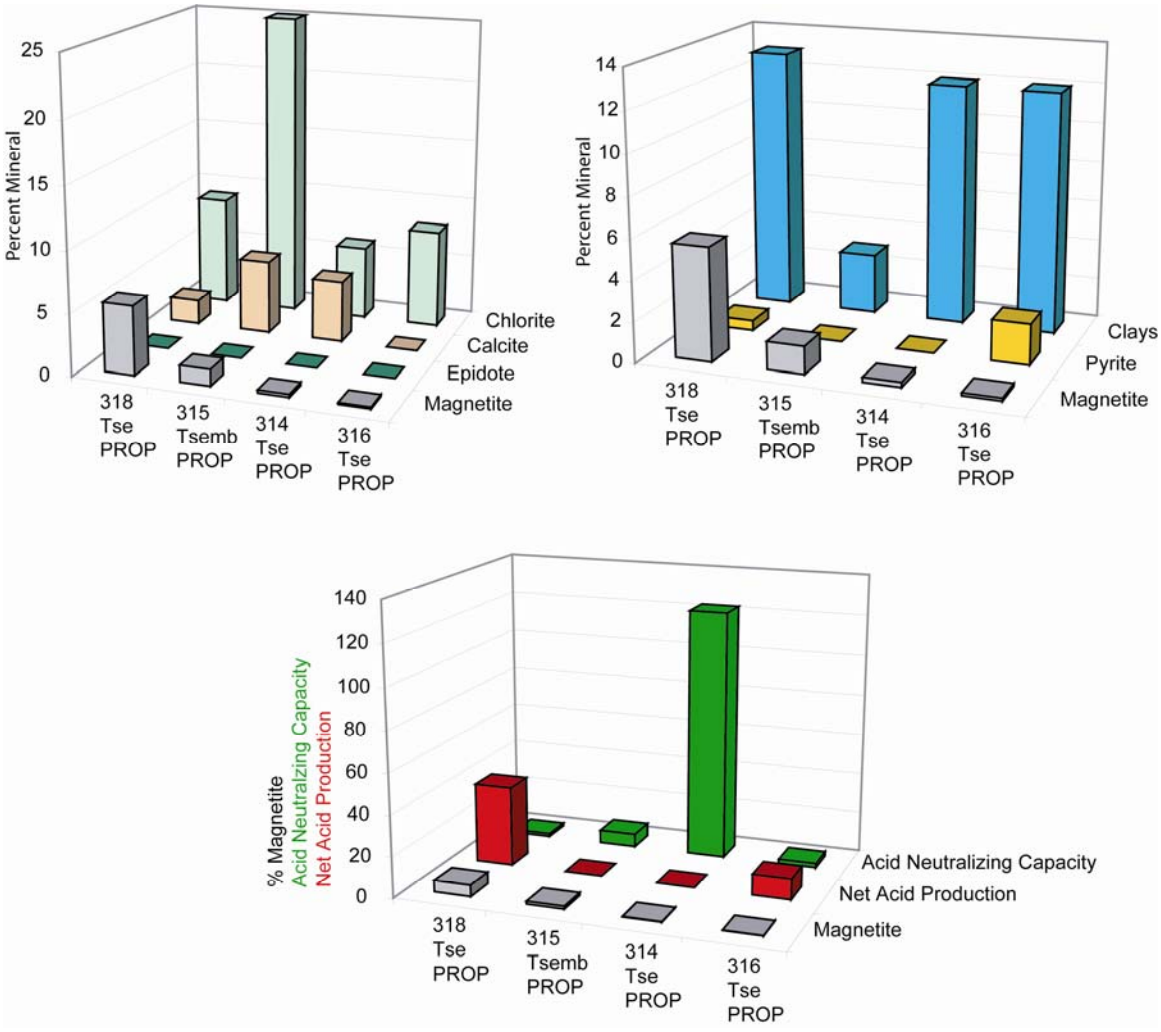

Figure 25. (a) Magnetite and minerals related to acid generation and alteration; (b) magnetite and acid consuming minerals; and (c) magnetite, acid neutralizing capacity, and net acid production for Eureka and Picauyune Megabreccia Members of the Sapinero Mesa Tuff. Sample numbers are represented by the last three characters for samples in Table 1.

San Juan Formation

Three samples of propylitically altered San Juan Formation volcanic rocks were sampled and show a range of magnetite from zero to over 6 volume percent. Generally calcite, pyrite, and clay content increase with decreasing amounts of magnetite. Environmental properties are inversely correlated with magnetite content. The sample with the most magnetite has highest NAP. Sample IDY0329 has little to no magnetite and has high ANC (Fig. 26).

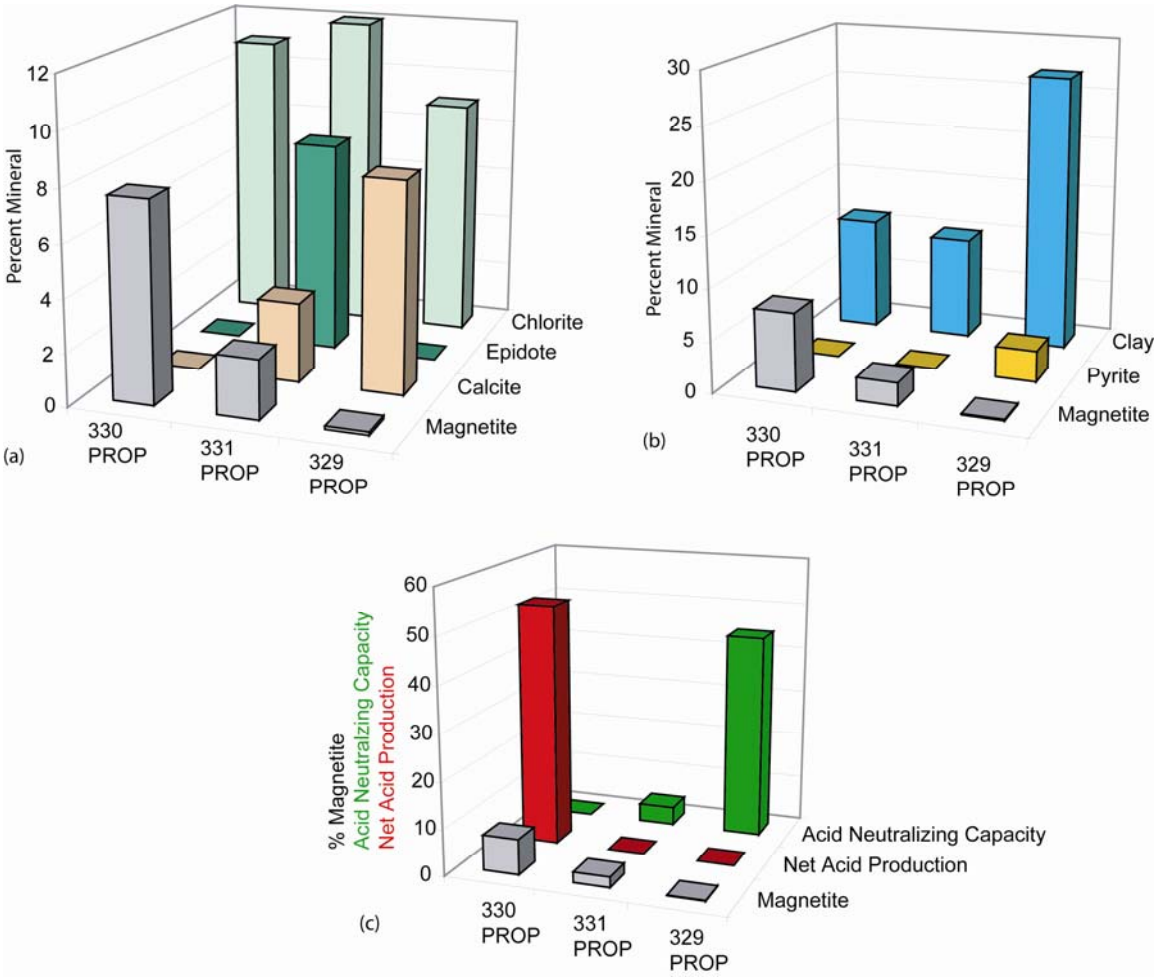

Figure 26. (a) Magnetite and minerals related to acid generation and alteration; (b) magnetite and acid consuming minerals; and (c) magnetite, acid neutralizing capacity, and net acid production for San Juan Formation samples. Sample numbers are represented by the last three characters for samples in Table 1.

Sultan Mountain Stock

Two samples of propylitically-altered and one sample of weakly sericitized Sultan Mountain Stock were sampled. Magnetite content is abundant in the propylitically-altered samples (SDY0319 and HWDY0322) and shows a pronounced decrease with increased alteration (sample SDY0320) (Fig. 27). NAP is greatest in the sample with the most magnetite and is least in the sample with no NAP. ANC is highest in the sample with the least amount of magnetite.

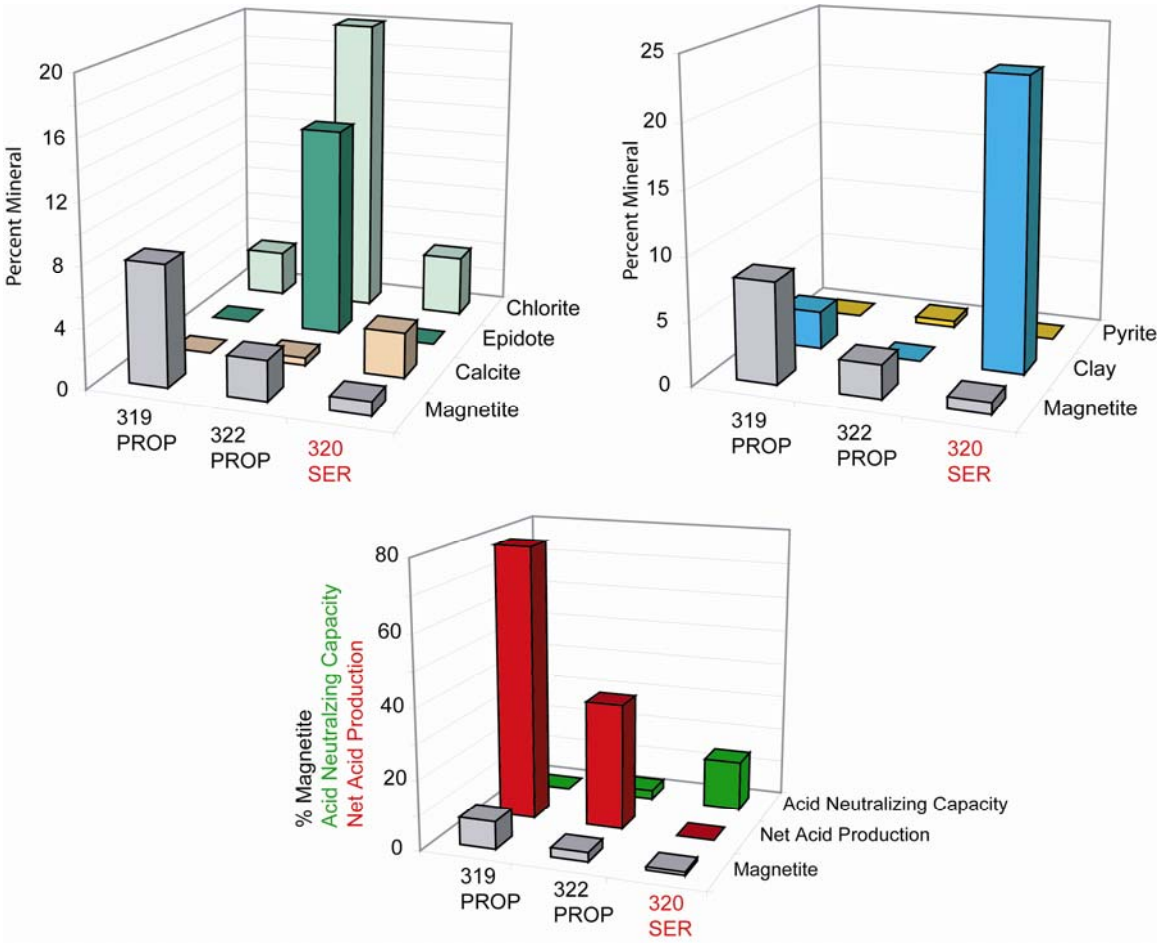

Figure 27. (a) Magnetite and minerals related to acid generation and alteration; (b) magnetite and acid consuming minerals; and (c) magnetite, acid neutralizing capacity, and net acid production for Sultan Mountain Stock. Sample numbers are represented by the last three characters for samples in Table 1.

Mineralized Vein, Dacite Intrusion, and Precambrian Irving Formation

Geologic units with only one sample include mineralized vein, dacite intrusion, and Precambrian Irving Formation gneiss. All three samples have high NAP, little to no ANP, and no magnetite (Fig. 28). Without additional sampling of this unit, it is not possible to discuss how magnetite content may vary with degree of alteration and mineralogy.

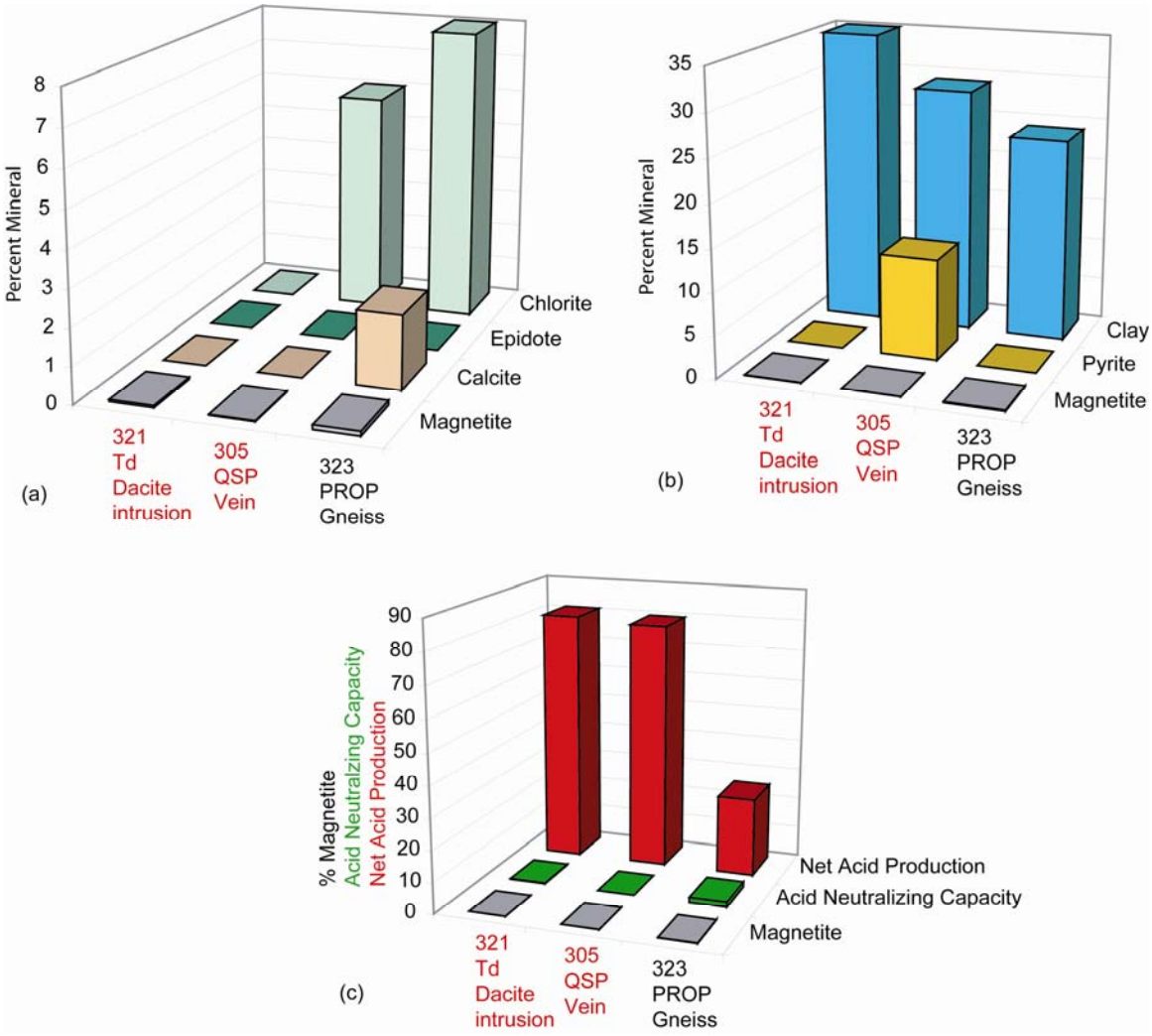

Figure 28. (a) Magnetite and minerals related to acid generation and alteration; (b) magnetite and acid consuming minerals; and (c) magnetite, acid neutralizing capacity, and net acid production for Tertiary dacite intrusion, mineralized vein, and Precambrian gneiss. Sample numbers are represented by the last three characters for samples in Table 1.

Summary of magnetic minerals, NAP, and ANC

Table 10 provides a summary of the magnetic mineralogy as compared to the environmental properties of acid neutralizing capacity and net acid production.

Table 10. Summary of environmental properties, alteration degree, and expected magnetite content for sampled lithologies; Tpa: Pyroxene Andesite Member of the Silverton Volcanics; Tsj: San Juan Formation; Tb: Burns Member of the Silverton Volcanics; Tig: Sultan Mountain Stock; Tse: Eureka and Picuyune Megabreccia Members of the Sapinero Mesa Tuff; PC: Precambrian Irving Formation gneiss; Vein: Mineralized vein; Td: dacite intrusion.

ENVIRONMENTAL PROPERTIES	ALTERATION					
	PROPYLITIC		SERICITIC		QSP	
	Magnetite Content		Magnetite Content		Magnetite Content	
	High	Little to None	High	Little to None	High	Little to None
HIGH ANC	Tpa	Tsj Tb	Tb	Tpa Tig	--	--
HIGH NAP	Tig Tse Tsj	PC Tb	--	--	--	Vein Td Tpa

DISCUSSION

Non-equilibria reactions involving calcite

ANC in our laboratory studies are determined by numerous physical and chemical weathering reaction variables; most of these variables are also involved in neutralizing and acid generating reactions that occur in nature. One variable involves calcite disequilibria reactions. Calcite, with its rapid reaction rate is among the first minerals to dissolve, and will continue to do so until eliminated. Silicate phases that are less reactive than calcite and that commonly dissolve at lower pH will dissolve, in some cases, after calcite has been consumed. This is useful information in the long-term management of mine waste because non-carbonate silicate minerals could continue to supply some ANC after calcite dissolution (Sherlock and others, 1995).

It is important to note that during our acid titration experiments, calcite was not fully consumed. Evidence for these non-equilibrium conditions were observed in samples that had been leached for 24 hours in 0.1N HCl, and continued to exhibit weak CO_2 effervescence due to continued dissolution of calcite. We cannot rule out, especially in samples with high calcite abundances, that carbonate species continued to react

throughout the entire acidic pH range even as less reactive silicate phases dissolved, thus complicating interpretation of some titration curves.

In those samples that have a high ANC and that effectively lack carbonate (e.g., SDY0310), CO_2 carbonate analyses (Table 4) were used in combination with XRD, SEM, and petrographic analyses to confirm the lack of calcite. Where all techniques were found to be consistent with the lack of calcite, then it was determined that a high ANC could be attributed to a phase or phases other than calcite. These results are consistent with previous interpretations of relatively high ANC samples with sparse to absent calcite, but that contain chlorite (Desborough and Yager, 2000). Due to the potential importance of chlorite in this and previous ANC studies, the maximum calcite equivalent ANC attributed to dissolution of chlorite was also calculated based on its abundance determined by XRD (Table 11).

Another indication of the relative importance of chlorite is observed when samples that lack calcite, and contain chlorite (based on XRD) are plotted against total acid added during acid titration between pH 5 – pH 2 (Fig. 29). Chlorite dissolution and ANC will likely to be important over this pH range. A weak correlation is observed when samples containing the highest abundances of calcite are removed from the regression analyses that confound interpretation of the relative importance of other non-carbonate phases.

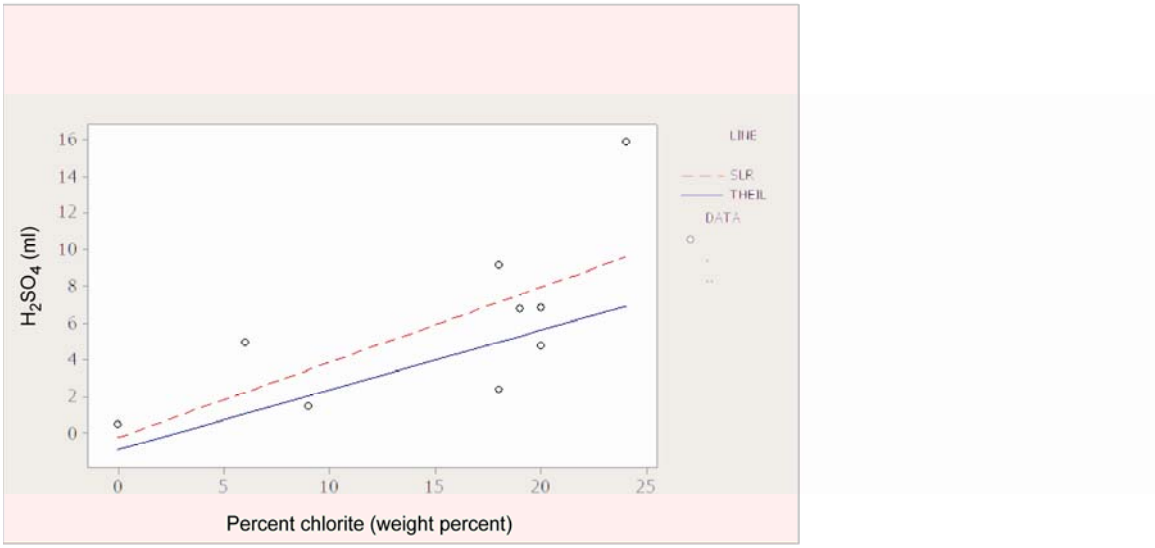

Figure 29. Kendall's tau regression for Animas River watershed samples that lack detectable calcite based on X-ray diffraction analyses and that contain chlorite. Dependent variable (y-axis) is amount of H_2SO_4 acid added during titration between pH of 5 and pH 2. Independent variable (x-axis is weight percent chlorite) determined by X-ray diffraction. Correlation values: Kendall's tau A = 0.55, Kendall's tau B = 0.57. P value = 0.04, N = 9.

Textural as well as mineralogical differences between samples are important in determining ANC. An example of the textural influences on ANC is indicated in sample HDY0314, which contains calcite, but was found to have an excess of ANC from species other than calcite (Table 11). This apparent ANC deficit could be attributed to numerous

factors involving the distribution of calcite in veins, replaced phenocryts, and in the rock matrix. Also, intergrown mixtures of minerals, e.g., calcite and possible clinochlore in collapsed pumice fiamme and in the matrix (Fig. 30), are in part likely responsible for some ANC. Those minerals that are prone to react and thus readily available to supply ANC are those exposed in void spaces where surface area and potential for acidic water-rock interaction is high (Fig. 31). Each outcrop sampled within a geologic unit will sometimes show variability in ANC that is due to textural and mineralogic characteristics or variables such as original composition of the protolith (original host rock prior to propylitization), local degree of alteration, relative abundance and grain size of alteration

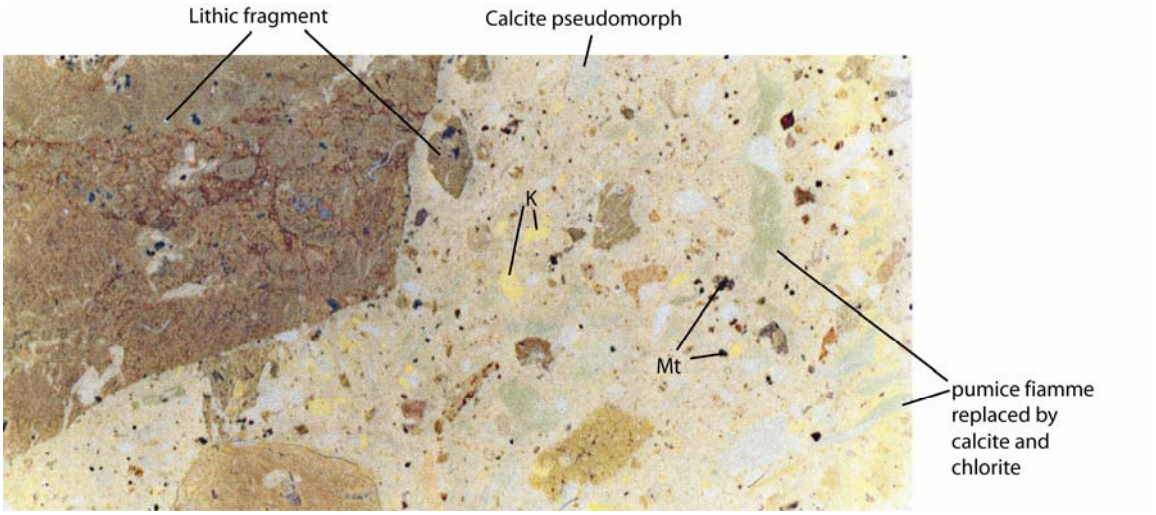

Figure 30. Eureka Member of the Sapinero Mesa Tuff (HDY0314).
Pumice fiamme have been replaced by mixtures of calcite and chlorite. Calcite has also replaced primary phenocrysts, and is distributed in veins (not shown). Lithic fragments incorporated during eruption of the tuff from preexisting units have a brownish hue. K, potassium feldspar; Mt, magnetite.

assemblage minerals with ANC, percent porosity, and surface area. All of these factors combine to produce the relative ANC rank discussed below.

Magnetic rock properties are also strongly dependent on principally the volume percent magnetite. In all samples investigated thus far in SEM and in petrographic studies, our samples contain intergrown mixtures of magnetite and the mineral ilmenite (Fig. 20). If ilmenite is present in large abundances, then ilmenite will have an overall effect of reducing the magnetic rock properties.

Observation of ANC Rank, mineralogy and magnetic properties

Pyroxene Andesite Member of the Silverton Volcanics

A discussion of ANC ranking that follows pertains only to those samples that were subjected to acid titration. ANC rank was determined based on (1) the total amount of acid added to achieve pH 2 during acid titration, and (2) the ANC/NAP ratio; the highest

ANC rank is assigned a number one, followed in descending order by samples with lower rank (Plate 1. Table 9).

The Pyroxene Andesite Member of the Silverton Volcanics generally has little to no NAP, and has the highest mean ANC (26 kg/ton $CaCO_3$ equivalent, n=6); however, 4 of the samples analyzed had an average ANC of 36 kg/ton $CaCO_3$ equivalent (Table 9), with 5 samples being in the top ten in terms of ANC rank. Only one Pyroxene Andesite Member sample had detectable NAP. Thus, it is unlikely that these samples would generate acid that could interfere with acid consumption. This unit generally contains calcite, chlorite, and some pyrite but usually lacks epidote.

A deficit of $CaCO_3$ equivalent ANC is seen in Pyroxene Andesite Member samples when the calculated ANC value based on carbonate concentrations is compared with observed ANC for total acid added to pH 2 (Table 11). This is an indication that calcite may be distributed throughout the rock in such a manner that its reactivity and availability for participation in ANC reactions during acid titration may be limited. Also, trace amounts of iron or manganese in the calcite lattice could impede the reactivity of calcite; although, this has not yet been determined in microbeam analyses. The samples HDY0317 and SDY0312 that have the smallest deficit with respect to the observed and calculated ANC would imply that calcite in these samples is in the most readily available form to react and completely dissolve.

While collecting samples for this study, several areas contained Pyroxene Andesite Member outcrops that were not mapped during previous studies. Outcrops were identified near the Brooklyn Mine and along the Black Bear Road near the intersection with Highway 550. This unit is relatively distinctive in the field with its dark (nearly black matrix) aphanitic texture (lacks coarse crystals) abundant hematite bands, and

Table 11. Calcite attributed to weight percent carbonate (Table 4), ANC determined for acid titration to pH 2, excess ANC due phases or factors other than calcite, and maximumANC for chlorite, assuming one mole of chlorite reacts to consume 16 H+ as shown in Salmon and Malmström (2004). A positive value for the column "excess ANC from other than calcite" indicates that another phase other than calcite or some chemical process may be responsible for the additional total ANC.

Field sample number	Unit	ANC from carbonate calcite	$CaCO_3$ Kg/ton ~ pH 2.00	Excess ANC from other than calcite	Maximum ANC from chlorite (Kg/ton $CaCO_3$ Equivalent)
HWDY0323	$_{p}$Є	4	1.67	-2	14
IDY0329	Tsj	83	44	-39	16
ODY0331	Tsj	18	4	-14	22
HDY0314	Tse	27	123	95	11
HDY0315	Tsemb	39	6	-33	45
HDY0316	Tse	3	2	-1	11
HDY0318	Tse	8	1	-7	16
HDY0317	Tpa	72	66	-7	23
IDY0328	Tpa	112	32	-81	25
IRDY0203	Tpa(?)	51	26	-25	14
SDY0327	Tpa	90	22	-68	27
SDY0326	Tpa	42	9	-32	13
SDY0312	Tpa	9	1	-9	16
SDY0310	Tb	1	98	98	32
SDY0308	Tb	5	1	-4	32
SDY0307	Tb	4	3	-1	32
IRDY0403	Tb	0	6	6	43
SDY0325	Tb	0	13	13	22
SDY0306	Tb	0	2	2	43
SDY0324	Tb	0	2	2	36
DYLPG0412	Tb	0	1	1	0
SDY0320	Tig	13	14	0	7
HWDY0322	Tig	4	3	-2	36
IDY0321	Td	0	0.2	0	0
MPGD_51_52.5	Qc	0	0.4	0.4	0

absence of epidote. Interestingly, the presence of epidote in the propylitic assemblage is an indicator of a higher intensity of alteration (Bove and others, in press).

The Pyroxene Andesite Member, is on average, the most magnetic unit; 4 propylitically altered Pyroxene Andesite Member samples contain the highest mean volume percent magnetite (Fig. 23, Table 6). In contrast, magnetite has apparently been reduced in two samples affected by more intense alteration. The presence of phases calcite and chlorite important for their ANC, generally higher magnetite concentrations, and overall lack of epidote suggests that the Pyroxene Andesite Member lava flows that occur high in the Silverton Volcanics stratigraphic section escaped more intense

propylitic alteration. The magnetic geophysical signature of this high ANC unit may permit its regional mapping using the airborne magnetic and electromagnetic survey data.

Burns Member of the Silverton Volcanics

ANC for nine samples collected from the Burns Member of the Silverton Volcanics averaged 16 kg/ton $CaCO_3$ equivalent. However, when the sample with the highest ANC among this unit (SDY0310) is excluded, the average ANC is 4 kg/ton $CaCO_3$ equivalent. This is well below the ANC threshold of 20 kg/ton $CaCO_3$ equivalent for materials being considered in mine waste remediation projects (Jambor and others, 2002). Further, 5 of 9 samples have ANC/NAP ratios below 1.3 that would also exclude there use in mine waste remediation projects (Lister, 1994).

In contrast to Pyroxene Andesite Member lavas, the Burns Member volcanic rocks commonly lack calcite, and have low magnetite contents. In addition, several Burns Member samples contain epidote that indicates a generally more intense degree of propylitic alteration (Bove and others, in press) that removed primary- and or inhibited secondary-magnetite growth.

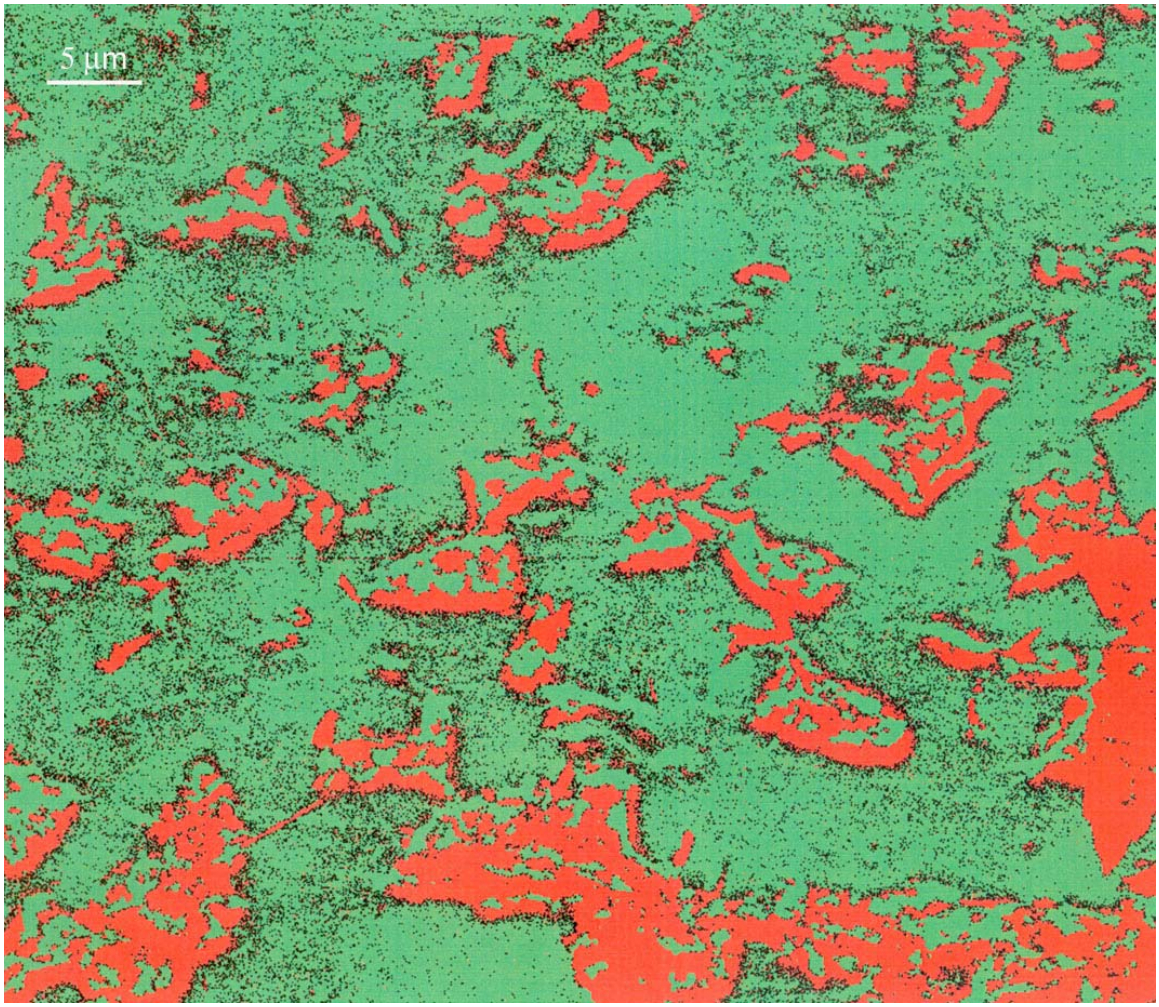

Figure 31. SEM backscatter image of sample HDY0314. Green areas are high relief; red areas are voids. A calculated maximum estimate of percent void space is 22 percent.

Other geologic units

Additional units that warrant additional sampling due to one or more samples having a high ANC, but that were not sampled sufficiently to make generalizations about the units overall ANC include the San Juan Formation and the Eureka Member of the Sapinero Mesa Tuff.

The San Juan Formation includes one sample that is ranked 4th in ANC among all samples studied (IDY0329), contains abundant calcite, and chlorite, and has a high magnetic signature (Tables 6, 9). The authors have sampled other San Juan Formation outcrops (not analyzed in this study) that are exposed in tributary basins above Middle Fork Mineral Creek that contain abundant calcite and chlorite and likely have a high ANC.

The Eureka Member of the Sapinero Mesa Tuff includes only 4 samples (this study) and incorporates a sample that has the highest ANC (HDY0314) among all samples studied. Clearly, further sampling could aid in identifying the aerial extent of the high ANC outcrops within the Eureka tuff and would help confirm the high ANC of this potentially important unit. The Eureka Member with the highest ANC rank also has a high magnetic signature that could aid in mapping those outcrops that have a potentially high ANC.

The Precambrian Irving Formation in Cunningham Creek (HWDY0323) is known to contain abundant calcite, therefore, it is unclear why this sample did not produce a higher ANC rank. While HWDY0323 lacks pyrite (XRD) it also has a relatively high NAP. Therefore, additional samples could be useful in interpreting this potentially important ANC unit as the Animas River below Silverton traverses various members of the Precambrian section that could supply some ANC.

Most samples of the Sultan Mountain stock were collected in areas represented by a magnetic high . Field observations near the North Star mine waste pile southwest of Siilverton (William Simon, Animas River Stakeholders Group President, personal communication, 2004) indicate re-vegetation is successful on waste rock composed mainly of Sultan Mountain stock. This waste pile occurs in an area of a magnetic low, indicating that a phase of the Sultan Mountain stock (not sampled) could supply more ANC than that observed in our study.

Conclusions

Regional propylitic alteration in the Animas River watershed near Silverton has introduced a mineral assemblage with varying degrees of NAP and ANC (Figures 32, 33) and magnetic properties. Where more intense alteration assemblages overprint the propylitic assemblage, this tends to remove magnetite, and thus reduce magnetic susceptibility while eliminating minerals with ANC, although important exceptions may exist in the Tertiary Burns lava flow rocks. NAP also increases when sulfide minerals are introduced. In general, our NAP and ANC studies confirm that where rocks are propylitically altered, the units have higher ANC, but where sericite has been introduced along with pyrite, then the ANC is diminished and NAP enhanced. Subtle variations in

degree of alteration are observed where sericite has been introduced yet the relatively high proportion of ANC minerals calcite, epidote, and chlorite have not been preserved during a weak-sericitic alteration event. These rocks generally have a higher ANC and magnetite abundances as well as lower NAP. Not surprisingly, samples that exhibit argillic and quartz-sericite-pyrite alteration have the highest NAP with pyrite being common in these assemblages; magnetite has often been eliminated.

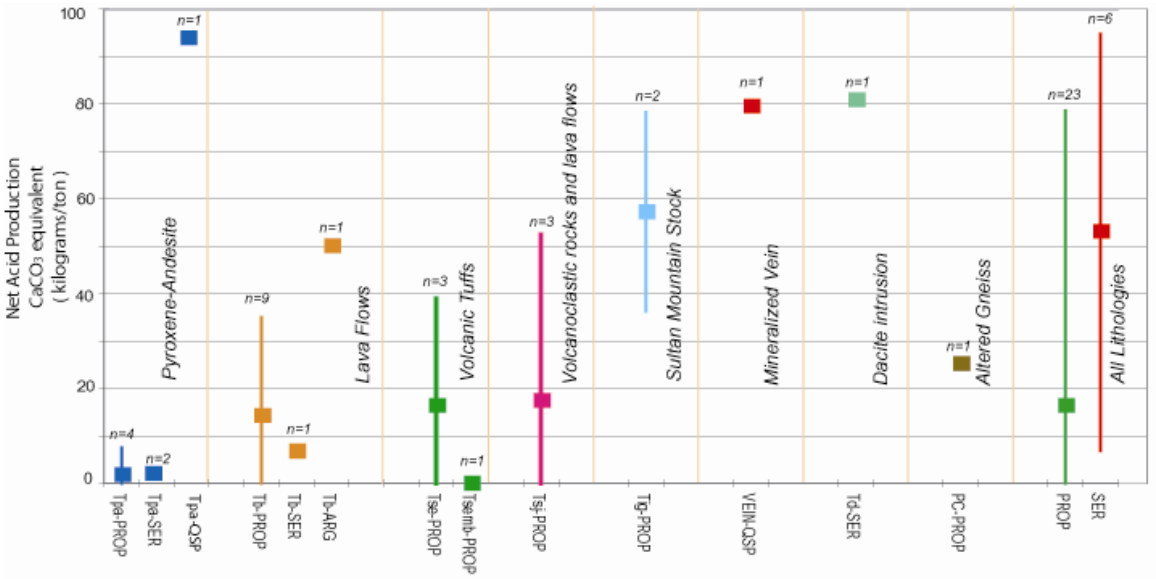

Figure 32. Net acid production (NAP) by lithologic unit for samples collected in the Upper Animas watershed. Higher values of NAP indicate that rock's mineralogy has a higher potential to generate acidic waters. On average, the sericitically-altered rocks (SER and QSP) lithologies have higher NAP than the propylitically-altered rocks (PROP).

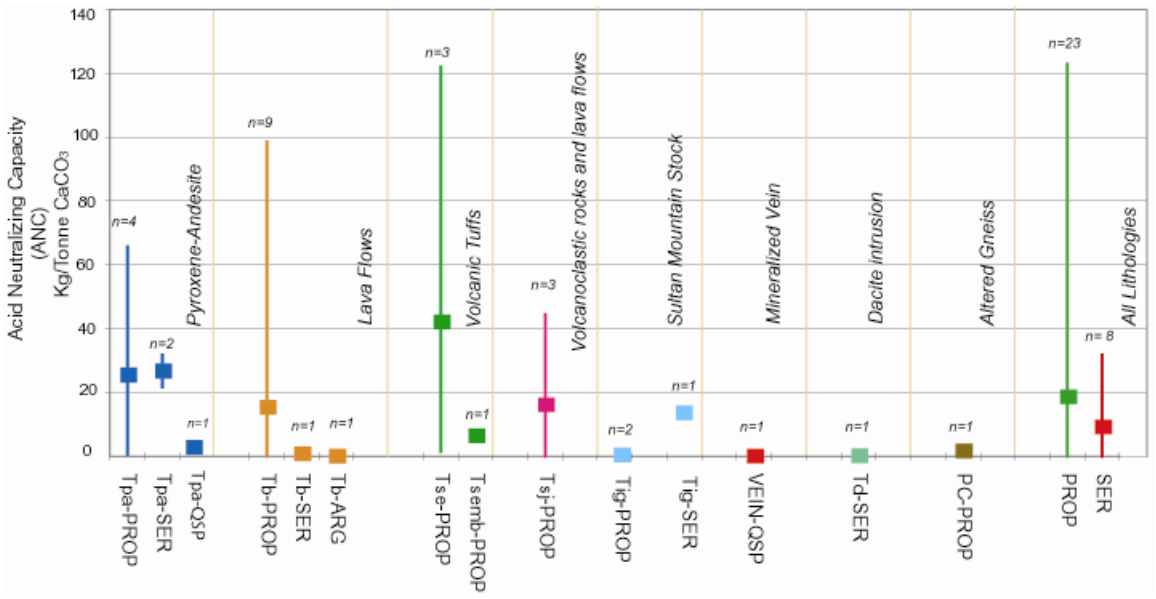

Figure 33. Acid neutralizing capacity (ANC) by lithologic unit for samples collected in the Upper Animas watershed. Rocks with higher values of ANC have higher potential to neutralize acidic waters. With one exception, (unit Tpa), rocks that are propolytically-altered (PROP) have higher average ANC than thier sericitically (SER or QSP), argillically (ARG), or altered counterparts.

While the presence of calcite is important in quickly neutralizing acidic water, our study indicates that even though a sample may lack detectable calcite, these samples can supply some ANC when other aluminosilicate phases are present, primarily chlorite. Although not directly comparable with the reactivity and calcium carbonate equivalent as calcite, the chlorite species chamosite, clinochlore are apparently locally important in supplying some ANC; this is consistent with findings in other studies. A chlorite mineral separate and subsequent acid titration experiment clearly indicates that chamosite, and clinochlore supplied some ANC during acid titration, especially between pH 4 to pH 2. The slower reaction times involving chlorite and perhaps epidote dissolution in some samples could continue to supply ANC at lower pH ranges (below pH 4) after calcite has completely dissolved and thus could supply a longer-term source of ANC if used in mine waste remediation projects.

There is a continuum in mineralogy represented in the propylitic alteration assemblage that affects the entire study area and ultimately controls environmental rock properties. Our studies show that even though a propylitically-altered outcrop might have abundant (as much as 32 weight percent) sericite, and appear to be relatively altered and or weathered in outcrop, these types of samples can have a relatively high ANC when calcite and chlorite are present. Thus, while field mapping is an important component in identifying samples with possible ANC, further detailed lab analysis is essential in determining with some certainty that a sample has a high ANC.

The highest ANC of all geologic units studied is the Pyroxene Andesite Member of the Silverton Volcanics. This is a volumetrically important unit, is host along with the

Burns Member to much of the base- and precious-metal mineralization in the study area. Generally high magnetite contents and attendant relatively high magnetic susceptibilities permit the unit to be regionally mapped with airborne magnetic survey data. Additional mineralogic characteristics of this unit are its lack of epidote, and ubiquitous presence of chlorite and calcite. Perhaps as important as a high ANC, Pyroxene Andesite Member rocks where propylitically altered to weakly sericicitized, in most cases lack NAP. As a result, all available ANC will not be inhibited by NAP generated by sulfide oxidation.

Burns Member rocks, which commonly occur stratigraphically below the Pyroxene Andesite Member volcanics have generally been subjected to slightly higher degrees of propylitization as indicated by the presence of epidote in several samples (Bove and others, in press). This, along with a general dearth of magnetite and calcite, and the presence of pyrite in several samples, imparts a low ANC and relatively high NAP. However, an anomalous Burns Member lava has the second highest ANC, contains abundant chlorite, yet lacks calcite indicating that locally, Burns Member rocks can have a relatively high ANC that is related to the mineralogical variability in the propylitic assemblage. As with other geologic units, the highest NAP determinations were observed in more intensely altered samples.

Other geologic units that warrant additional study due to too few samples analyzed for ANC include the Eureka Member of the Sapinero Mesa Tuff, the San Juan Formation, and the Sultan Mountain Stock.

A volcaniclastic breccia collected in the San Juan Formation has the 4th highest ANC of all samples studied, contains abundant calcite, and yet has a low magnetite content and corresponding low magnetic susceptibility. The San Juan Formation commonly has a high magnetic signature, therefore, use of the airborne magnetic survey data to identify areas of this unit that have a low magnetic signature may help to identify additional outcrops with possible high ANC.

The outcrop with the highest ANC studied was collected from the Eureka Member of the Sapinero Mesa Tuff. Microscopic analysis revealed that many physical factors are in part controlling the high ANC. Calcite and chlorite are distributed throughout the sample in many textural forms. Calculated void space was also high imparting a high potential for mineral-rock dissolution. While the presence of minerals with a high ANC is important, this sample indicates that textural characteristics of how the high ANC minerals may be distributed may be important in supplying ANC.

One sample of Sultan Mountain stock has a relatively high ANC and lower magnetite abundance when compared with additional Sultan Mountain Stock samples. Other Sultan Mountain Stock samples have lower silica contents compared to the relatively high ANC sample and have both higher magnetite contents and magnetic susceptibilities, therefore, similar to the San Juan Formation, use of the airborne magnetic survey data to identify areas of this unit that have a low magnetic signature may help to identify additional outcrops with a possible high ANC.

Future Study Directions

Some items are related to the geophysical component of this study but many are related to further defining the acid neutralizing and acid generating capacities of lithologies that require additional samples and analysis to provide a statistically representative dataset for interpretation. These proposed efforts would build upon and strengthen the knowledge gained through this study resulting in a more thorough understanding of how the physical magnetic and electromagnetic properties are related to the environmental properties (ANC and NAP) of the plutonic and volcanic rocks within the Animas River watershed near Silverton.

We recommend that any additional samples collected should be analyzed using the same approaches and laboratory protocols as were used for this study in order to provide consistency.

The following is divided into two major categories; (1) field and laboratory efforts that would involve field sampling and laboratory analysis and (2) efforts that would involve analysis of existing geophysical map data mainly through computer analysis and modeling.

Sample Strategies and Laboratory Studies

- Sample and analyze more sericitically altered Burns Member of the Silverton Volcanics to test the hypothesis that higher degrees of alteration (and hence acid generating potential) are associated with magnetite enrichment.
- Sample and analyze the Henson Member of the Silverton Volcanics; a unit that was not sampled for this study.
- Sample and analyze additional sericitized and propylitically altered Eureka and Picauyune Megabreccia Member of the Sapinero Mesa Tuff.
- Sample and analyze Sultan Mountain Stock in areas that have a lower magnetic signature than those samples analyzed in this study
- Conduct laboratory measurements of the electrical resistivity of samples collected for this study and any new samples.
- Conduct chemical analyses of leachates on a select number of samples to determine the chemical elements present due to dissolution of mineral phases at various pH units. This will help define which ANC mineral is contributing to neutralizing acidity produced by pyrite and at varying pH.
- Conduct quantitative electron microbeam analyses of chlorite species among other aluminosilicate phases are necessary to determine stoichiometry and major element ratios. These data may aid in predicting ease of dissolution or reactivity that could supply a readily available source of ANC.
- Conduct laser ablation ICP-MS analysis of carbonates that may prove useful in identifying trace constituents that could impede reaction rates.

Map Scale Efforts and Analysis

- Digitize and incorporate available (published) mapping of the Tertiary pyroxene-andesite and Tertiary Henson rock outcrops into existing digital geologic compilation (Yager and Bove, 2002; Yager and Bove, in press). Although these units are incompletely mapped for the entire study area and volcano-stratigraphic issues remain, the mapped areas that are available will provide control in

developing sampling strategies and airborne geophysical data analysis and interpretation.

- Further evaluate and define whether geologic units with high ANC and high NAP have characteristic airborne magnetic and electromagnetic anomaly signatures using helicopter geophysical survey data collected in 1997 (Smith and others, in press). Use these results along with the alteration mapping of Bove and others (in press) to construct a map identifying areas with high NAP and ANC.

Acknowledgments

We thank Robert R. McDougal for assistance in the field. Del and Laura Smith (Silverton residents) for providing field logistical support that aided our sampling efforts. We appreciate the professional guidance on NAP and ANC methods from Kathy Smith, Stan Church, and George Desborough. Reviews by George Desborough and Philip Hageman improved a preliminary version of this report. Kay Zillich, U.S. Forest Service Hydrologist, and Stephanie O'Dell, San Juan Forest Abandoned Mine Lands Coordinator, under a U.S. Forest Service-U.S. Geological Survey interagency agreement number 04-IA-11021300-017, supported our research.

Disclaimers

Any use of trade names is for descriptive purposes only and does not imply endorsement by the U.S. Government. This report has not been reviewed for geologic nomenclature.

References Cited

Atwood, W.W., and Mather, K.F., 1932, Physiography and Quaternary geology of the San Juan Mountains, Colorado: U.S. Geological Survey Professional Paper 166, 176 p.

Balsley, J.R., and Buddington, A.F., 1958, Iron-titanium oxide minerals, rocks, and aeromagnetic anomalies of the Adirondack area, New York: Economic Geology, v. 53, no. 7, pp. 777-805.

Barker, Fred, 1969, Precambrian geology of the Needle Mountains, southwestern Colorado: U.S. Geological Survey Professional Paper, 644-A, p. A1-A35.

Bejnar, Waldemere, 1957, Lithologic control of ore deposits in the southwestern San Juan Mountains, *in* Kottlowski, F. E., and Baldwin, Brewster, eds., Guidebook of southwestern San Juan Mountains, Colorado: New Mexico Geological Society 8th Annual Field Conference Guidebook, p. 162-173.

Blair, R.W., Jr., Yager, D.B., and Church, S.E., 2002, Surficial geologic maps along the riparian zone of the Animas River and its headwater tributaries, Silverton to Durango, Colorado, with upper Animas River watershed gradient profiles: U.S. Geological Survey Digital Data Series 071.

Blowes, D.W., Ptacek, C.J., and Jurjovic, Jasna, 2003, Mill tailings: hydrogeology and geochemistry: *in* Mineralogical Association of Canada Short Course Series, v. 31, p. 95-116.

Bove, D.J., Mast, M.A., Dalton, J.B., Wright, W.G., and Yager, D.B., (in press), Major styles of mineralization and hydrothermal alteration and related solid and aqueous-phase geochemical signatures, Chapter E3: U.S. Geological Survey Professional Paper 1651, Church, S.E., and Vonguerard, Paul, eds.

Bove, D.J., Hon, Ken, Budding, K.E., Slack, J.F., Snee, L.W., and Yeoman, R.A., 2001, Geochronology and geology of late Oligocene through Miocene volcanism and mineralization in the Western San Juan Mountains, Colorado: U.S. Geological Survey Professional Paper 1642, 30 p.

Burbank, W.S., 1960, Pre-ore propylization, Silverton Caldera, Colorado, *in* Geological Survey Research 1960: U.S. Geological Survey Professional Paper 400-B, article 6, p. B12-B13.

Burbank, W.S., and Luedke, R.G., 1969, Geology and ore deposits of the Eureka and adjoining districts, San Juan Mountains, Colorado: U.S. Geological Survey Professional Paper 535, 73 p.

Casadevall, Thomas, and Ohmoto, H., 1977, Sunnyside mine, Eureka mining district, San Juan County, Colorado— Geochemistry of gold and base metal ore deposition in a volcanic environment: Economic Geology, v. 92, p. 1285-1320.

Chapin, C.E., and Cather, S.M., 1994, Tectonic setting of the axial basins of the northern and central Rio Grande rift: Geological Society of America Special Paper 291, p. 5-25.

Davis, J.A., and Kent, D.B., 1990, Surface complexation modeling in aqueous geochemistry: *in* Mineral-Water Interface Geochemistry, Hochella, M.F., Jr., and White, A.F., eds., Mineralogical Society of America Reviews in Mineralogy, v. 23, p.177-260.

Desborough, G.A., and Driscoll, R.L., 1998, Mineralogical characteristics and acid-neutralizing potential of drill core samples from eight sites considered from metal-mine related waste repositories in northern Jefferson, Powell, and Lewis and Clark counties, Montana: U.S. Geological Survey Open-File Report 98-0790, 6 p.

Desborough, G.A., and Yager, D.B., 2000, Acid-neutralizing potential of igneous bedrocks in the Animas River headwaters, San Juan County, Colorado: U.S. Geological Survey Open-File Report 00-0165, 14 p.

Dobrin, M.B., and Savit, C.H., 1988, Introduction to geophysical prospecting, Fourth Edition, New York, McGraw Hill, 867 p.

Gill, J.B., 1981, Orogenic andesites and plate tectonics: Berlin, Springer, 389 p.

Gillam, M.E., 1998, Late Cenozoic geology and soils of the lower Animas River valley, Colorado and New Mexico: Boulder, Colo., University of Colorado Ph. D. dissertation, 477 p., 3 plates.

Hoch, A.R., Reddy, M.M., and Drever, J.I., 1999, Importance of mechanical disaggregation in chemical weathering in a cold alpine environment, San Juan Mountains, Colorado: Geological Society of America Bulletin, v. 111, p. 304-314.

Hutchison, I.P.G., and Ellison, R.D., eds., 1992, Mine waste management: a resource for mining industry professionals, regulators and consulting engineers: Lewis Publishers, Inc., 672 p.

Jambor, J.L., 2003, Mine-waste mineralogy and mineralogical perspectives of acid-base accounting: *in* Environmental Aspects of Mine Wastes, Jambor, J.L., Blowes, D.W., and Ritchie, A.I.M., eds.: Mineralogical Association of Canada Short Course Series, v. 31, p. 117-145.

Jambor, J.L., and Blowes, 1998, Theory and applications of mineralogy, in environmental studies of sulfide-bearing mine wastes: *in* Modern Approaches to Ore and Environmental Mineralogy, Cabri, J.L., and Vaughan, D.J., eds.: Mineralogical Association of Canada Short Course Series, v. 27, p. 367-401.

Jambor, J.L., Dutrizac, J.E., Groat, L.A., and Raudsepp, Mati, 2002, Static tests of neutralization potentials of silicate and aluminosilicate minerals: Environmental Geology, v. 43, p. 1-17.

Kottlowski, F.E., 1957, Mesozoic strata flanking the southwestern San Juan Mountains Colorado and New Mexico, *in* Kottlowski, F. E., and Baldwin, Brewster, eds., Guidebook of southwestern San Juan Mountains, Colorado: New Mexico Geological Society 8th Annual Field Conference Guidebook, p. 138-153.

Kwong, J.Y.T., and Furgeson, K.D., 1997, Mineralogical changes during NP determinations and their implications: Proceedings of the Fourth International Conference on Acid Rock Drainage, Volume 1: Society for Mining, Metallurgy, and Exploration, Inc., p. 435-447.

LeBas, M.J., LeMaitre, R.W., Streckeisen, A., and Zanettin, B., 1986, A chemical classification of volcanic rocks based on the total alkali silica diagram: Journal of Petrology, v. 27, p. 745-750.

Lanphere, M.A., 1988, High resolution $^{40}Ar/^{39}Ar$ chronology of Oligocene volcanic rocks, San Juan Mountains, Colorado: Geochimica et Cosmochimica Acta, v. 52, p. 1425-1434.

Lapakko, Kim, and Lawrence, R.W., 1993, Modification of the net acid production (NAP) test: *in* Proceedings of the Seventeenth Annual British Columbia Mine Reclamation Symposium, Port Hardy, British Columbia, 1993, p. 145-159.

Leonard, Eric, Merritts, Dorothy, and Carson, Robert, 1993, Quaternary geology, upper Rio Grande drainage, San Juan Mountains, Colorado, *in* Wilson, M.A., compiler: Beloit Wisconsin, Beloit College, The Sixth Keck research symposium in geology, v. 6, p. 170-172.

Lipman, P.W., 1976, Geologic map of the Lake City caldera area, western San Juan Mountains, southwestern Colorado: U.S. Geological Survey Miscellaneous Investigation Series Map I-962, scale 1:48,000.

Lipman, P.W., Dungan, Michael, Bachmann, Olivier, 1997, Comagmatic granophyric granite in the Fish Canyon Tuff, Colorado— Implications for magma-chamber processes during a large ash-flow eruption: Geology, v. 25, p. 915-918.

Lipman, P.W., Steven, T.A., Luedke, R.G., and Burbank, W.S., 1973, Revised volcanic history of the San Juan, Uncompahgre, Silverton, and Lake City calderas in the western San Juan Mountains, Colorado: U.S. Geological Survey Journal of Research, v. 1, p. 627-642.

Lister, D., 1994, An assessment of acid rock drainage potential of waste rock and implications for long term weathering of the north dump at Island Cooper mine, Port

Hardy, B.C., Masters of Science Thesis, Vancouver, The University of British Columbia, 217 pp.
Luedke, R.G., and Burbank, W.S., 2000, Geologic map of the Silverton and Howardsville quadrangles, southwestern Colorado: U.S. Geological Survey Geologic Investigation Series Map I-2681, scale 1:24,000.
Hutchison, I.P.G., and Ellison, R.D., eds., 1992, Mine waste management: a resource for mining industry professionals, regulators and consulting engineers: Lewis Publishers, Inc., 672 p.
Nash, J.T., 2000, Geochemical studies of mines, dumps, and tailings, as sources of contamination, upper Animas River watershed, Colorado: U.S. Geological Survey Open-File Report 00-104. [1 CDROM]
Raudsepp, Mati, and Pani, Elisabetta, 2003, Application of Rietveld analysis to environmental mineralogy: *in* Mineralogical Association of Canada Short Course Series, v. 31, p. 165-180.
Raudsepp, Mati, Pani, Elisabetta, and Dipple, G.M., 1999, Measuring mineral abundance in skarn I: the Rietveld method using X-ray Powder diffraction data: Canadian Mineralogist, v. 37, p. 1-15.
Ringrose, C.R., 1982, Geology, geochemistry, and stable isotope studies of a porphyry-style hydrothermal system, west Silverton district, San Juan Mountains, Colorado: Aberdeen, Scotland, University of Aberdeen Ph. D. dissertation, 257 p., 19 plates.
Salmon, U.S., and Malmström, M.E., 2004, Geochemical processes in mill tailings deposits: modeling of groundwater composition: Applied Geochemistry, v. 19, p. 1-17.
Shaw, Shannon, Wels, Christoph, Robertson, Andy, and Lorinczi, Geyza, 2002, Physical and Geochemical Characterization of Mine Rock Piles at the Questa mine, New Mexico: *in* Tailings and Mine Waste 2002, proceedings of the Ninth International Conference on Tailings and Mine Waste, Fort Collins, Colorado, USA, 27-30 January 2002, pp. 447-458.
Sherlock, E.J., Lawrence, R.W., and Poulin, R., 1995, On the neutralization of acid rock drainage by carbonate and silicate minerals: Environmental Geology, v. 25, p. 43-54.
Smith, B.D., McDougal, R.R., Deszcz-Pan, Maryla, and Yager, D.B.., in press, Helicopter electromagnetic and magnetic surveys, Chapter E4 *in* Church, S.E., von Guerard, Paul, and Finger, S.E., eds., Integrated investigations of environmental effects of historical mining in the Animas River watershed, San Juan County, Colorado: U.S. Geological Survey Professional Paper 1651.
Steven, T.A., Hon, Ken, and Lanphere, M.A., 1995, Neogene geomorphic evolution of central San Juan Mountains near Creede, Colorado: Miscellaneous Investigation Series Map I-2504, scale 1:100,000.
Steven, T.A., Lipman, P.W., 1976, Calderas of the San Juan volcanic field, southwestern Colorado: U.S. Geological Survey Professional Paper, 958, 35 p.
Steven, T.A., Schmitt, L.J., Jr., Sheridan, M.J., Williams, F.E., Gair, J.E., and Klemic, H., 1969, Mineral resources of the San Juan primitive area, Colorado: U.S. Geological Survey Bulletin 1261-F, 187 p.
Wirt and others, in press

Yager, D.B., and Bove, D.J., in press, Geologic Framework, Chapter E1: U.S. Geological Survey Professional Paper 1651, Church, S.E., and Vonguerard, Paul, eds.

Bove, D.J., Generalized Geologic Map of Part of the Upper Animas River Watershed and Vicinity, Silverton, Colorado: U.S. Geological Survey Miscellaneous Field Studies Map, MF-2377.

Yager, D.B., Mast, M.A., Verplanck, P.L., Bove, D.J., Wright, W.G., and Hageman, P.L., 2000, Natural versus mining-related water quality degradation to tributaries draining Mount Moly, Silverton, Colorado, *in* ICARD 2000; Proceedings of the Fifth International Conference on Acid Rock Drainage, Volume 1: Society for Mining, Metallurgy, and Exploration, Inc., p. 535-547.

Yager, D.B., and Bove, D.J., 2002, Generalized Geologic Map of Part of the Upper Animas River Watershed and Vicinity, Silverton, Colorado: U.S. Geological Survey Professional Paper, Miscellaneous Field Studies Map MF-2377.

Young, R.A., 1993, The Rietveld Method: International Union Crystallography, Oxford University Press, New York, 298 p.